https://doi.org/10.5194/essd-2020-342
Preprint. Discussion started: 21 November 2020

Open Access Earth System Science Data Discussions

Overview and update of the SPARC Data Initiative: Comparison of stratospheric composition measurements from satellite limb sounders

Michaela I. Hegglin[1], Susann Tegtmeier[2], John Anderson[3], Adam E. Bourassa[4], Samuel Brohede[5], Doug Degenstein[4], Lucien Froidevaux[6], Bernd Funke[7], John Gille[8], Yasuko Kasai[9], Erkki Kyrölä[10], Jerry Lumpe[11], Donal Murtagh[12], Jessica L. Neu[6], Kristell Pérot[12], Ellis Remsberg[13], Alexey Rozanov[14], Matthew Toohey[2], Joachim Urban[12, deceased], Thomas von Clarmann[15], Kaley A. Walker[16], Hsiang-Jiu Wang[17], Carlo Arosio[14], Robert Damadeo[13], Ryan Fuller[6], Gretchen Lingenfelser[13], Christopher McLinden[18], Diane Pendlebury[18], Chris Roth[4], Niall J. Ryan[16], Christopher Sioris[18], Lesley Smith[19], and Katja Weigel[14]

[1]Department of Meteorology, University of Reading, Reading, United Kingdom
[2]GEOMAR Helmholtz Centre for Ocean Research Kiel, Kiel, Germany
[3]Atmospheric Science, Hampton University, Hampton, VA, United States
[4]University of Saskatchewan, Saskatoon, SK, Canada
[5]FluxSense AB, Gothenburg, Sweden
[6]Jet Propulsion Laboratory, California Institute of Technology, Pasadena, CA, United States
[7]Instituto de Astrofísica de Andalucía, CSIC, Granada, Spain
[8]National Center for Atmospheric Research, Boulder, CO, United States
[9]National Institute of Information and Communications Technology, Tokyo, Japan
[10]Earth observation, Finnish Meteorological Institute, Helsinki, Finland
[11]Computational Physics, Inc., Boulder, CO, United States
[12]Department of Space, Earth, and Environment , Chalmers University of Technology, Gothenburg Sweden
[13]NASA Langley Research Center, Hampton, VA, United States
[14]Institute of Environmental Physics (IUP), University of Bremen, Bremen, Germany
[15]Karlsruhe Institute of Technology, IMK, Karlsruhe, Germany
[16]Department of Physics, University of Toronto, Toronto, Canada
[17]School of Earth and Atmospheric Sciences, Georgia Institute of Technology, Atlanta, GA, United States
[18]Environment and Climate Change Canada, Toronto, Canada
[19]Cooperative Institute for Research in Environmental Sciences, University of Colorado, Boulder, CO, United States

Correspondence: M. I. Hegglin (m.i.hegglin@reading.ac.uk)

Abstract.

The SPARC Data Initiative (SPARC, 2017) performed the first comprehensive assessment of currently available stratospheric composition measurements obtained from an international suite of space-based limb sounders. The initiative‘s main objectives were (1) to assess the state of data availability, (2) to compile vertically resolved, monthly zonal mean trace gas and aerosol climatologies, and (3) to perform a detailed inter-comparison of these climatologies, summarising useful information and highlighting differences among datasets. The vertically-resolved climatologies of 26 different atmospheric constituents extending over the region from the upper troposphere to the lower mesosphere (300-0.1 hPa) are provided on a common latitude-pressure grid and include most major long-lived trace gases (O_3, H_2O, N_2O, CH_4, CCl_3F, and CCl_2F_2), transport

https://doi.org/10.5194/essd-2020-342
Preprint. Discussion started: 21 November 2020

Open Access Earth System Science Data Discussions

tracers (HF, SF_6, HCl, CO, HNO_3, NO_y), and shorter-lived trace gases important to stratospheric chemistry including nitrogens (NO, NO_2, NO_x, N_2O_5,and HNO_4), halogens (BrO, ClO, $ClONO_2$ and HOCl), and other minor species (OH, HO_2, CH_2O, CH_3CN), and aerosol. This overview of the SPARC Data Initiative introduces the updated versions of the SPARC Data Initiative climatologies for the extended time period 1979-2018 and provides information on the satellite instruments included in the assessment: LIMS, SAGE I/II/III, HALOE, UARS-MLS, POAM II/III, OSIRIS, SMR, MIPAS, GOMOS, SCIAMACHY, ACE-FTS, ACE-MAESTRO, Aura-MLS, HIRDLS, SMILES, OMPS-LP, and TES. It describes the Data Initiative's top-down approach to comparing stratospheric composition measurements based on zonal monthly mean climatologies which provides upper bounds to relative inter-instrument biases and an assessment of how well the instruments are able to capture geophysical features of the stratosphere. An update to previously published evaluations of ozone and water vapour monthly mean climatologies is provided. In addition, example trace gas evaluations of methane (CH_4), carbon monoxide (CO), a set of nitrogen species (NO, NO_2, and HNO_3), the reactive nitrogen family (NO_y), and hydroperoxyl (HO_2) are presented. The results highlight the quality, strengths and weaknesses, and representativeness of the different datasets. As intended summary, the current state of our knowledge of stratospheric composition and variability is provided based on the overall consistency between the datasets. The updated SPARC Data Initiative monthly zonal mean climatologies are publicly available and accessible via the Zenodo data archive (Hegglin et al., 2020, doi:10.5281/zenodo.4265393).

1 Introduction

The past four decades starting in the late 1970s represent a 'golden age' of stratospheric composition measurements from satellite limb sounders, which capture the vertical structure of stratospheric composition with a vertical resolution of approximately 1 to 4 km. These limb observations have been used extensively to monitor the state of the stratospheric ozone layer that protects human and ecosystem health (e.g., Randel et al., 1999; Harris et al., 2015; WMO, 2011, 2014, 2018) and to study the processes leading to anthropogenic ozone depletion (e.g., Manney et al., 1994; Dessler et al., 1995; Santee et al., 2008). Such research provided the crucial science basis that underpinned actions taken under the Montreal Protocol and its Amendments for the protection of the ozone layer, which is considered to be the most successful international treaty on an environmental issue to date. Limb observations, and merged products thereof, are also becoming increasingly important for the detection and attribution of climate change and potential feedback mechanisms, including the role of stratospheric water vapour and aerosol trends and variability in radiative forcing of climate (e.g., Solomon et al., 2010, 2011; Gilford et al., 2016; IPCC, 2014; Schmidt et al., 2018). More generally, limb observations are used for the study of stratospheric dynamics and transport (Gray and Pyle, 1986; Solomon et al., 1986; Holton and Choi, 1988), empirical studies of stratospheric climate and variability (Randel et al., 2006, 2010, 2011; Manney et al., 2008; Hegglin et al., 2009; Bourassa et al., 2010; Stiller et al., 2012; Gille et al., 2014), data merging and trend evaluation activities (e.g., Randel and Wu, 1998; Hegglin et al., 2014; Shepherd et al., 2014; Froidevaux et al., 2015;

https://doi.org/10.5194/essd-2020-342
Preprint. Discussion started: 21 November 2020

Open Access Earth System Science Data Discussions

Harris et al., 2015; Davis et al., 2016; Arosio et al., 2019; SPARC LOTUS report, 2019), with merged datasets also being used as forcing databases in climate models (e.g., Cionni et al. (2011) for ozone; Thomason et al. (2018) for aerosol), and for the validation of the representation of transport and chemistry in numerical models (e.g., Eyring et al., 2006; Gettelman et al., 2010; Hegglin et al., 2010; Strahan et al., 2011; Kolonjari et al., 2018; Froidevaux et al., 2019; Tegtmeier et al., in preparation).

The validity of any data and trend analysis, however, strongly depends on the understanding of the observational uncertainty and overall quality of the datasets used, which hitherto was deemed unsatisfactory (SPARC CCMVal, 2010). Uncertainty and bias estimates are particularly important to inform chemical data assimilation systems (Inness et al., 2013; Errera et al., 2016) and to develop observational metrics for the evaluation of model performance (Douglass et al., 1999; Waugh and Eyring, 2009). In response to this need, the Stratosphere-troposphere Processes and their Role in Climate (SPARC) core project of the World Climate Research Programme (WCRP) initiated the SPARC Data Initiative with the aim to coordinate a comprehensive assessment of available vertically-resolved chemical trace gas and aerosol observations obtained from an international suite of satellite limb-sounders. The SPARC Data Initiative's main objectives were (1) to assess the availability of datasets, (2) to compile vertically resolved trace gas and aerosol climatologies, and (3) to perform a detailed inter-comparison of these climatologies, summarizing useful information and highlighting differences among datasets. The SPARC Data Initiative thereby complements other SPARC activities that have focused on the assessment of stratospheric ozone (e.g., Harris et al., 2015; SPARC, 2019), water vapour (SPARC, 2000; Khosrawi et al., 2018; Lossow et al., 2019), and aerosol (SPARC, 2006; Kremser et al., 2016). The provision of error estimates for atmospheric temperature and composition measurements from space following a unified methodological approach, which was highlighted by the SPARC Data Initiative (SPARC, 2017) to be a missing component of its analysis, is now the focus of the SPARC Towards Unified Error Reporting (TUNER) Initiative (von Clarmann et al., 2019).

Here we present an update of the SPARC Data Initiative (SPARC, 2017), which focused on composition measurements from 1979-2010, extending its evaluation of trace gas climatologies out to 2018 (see Figure 1). The update features climatologies based on more recent retrieval versions and adds the climatologies of OMPS-LP (on SUOMI NPP) and SAGE III/ISS to the original list of satellite limb sounders presented in SPARC (2017) (LIMS, SAGE I/II/III, HALOE, UARS-MLS, POAM II/III, OSIRIS, SMR, MIPAS, GOMOS, SCIAMACHY, ACE-FTS, ACE-MAESTRO, Aura-MLS, HIRDLS, SMILES; see Section 2 for the full meaning of these acronyms). The climatologies include most major long-lived trace gases (O_3, H_2O, N_2O, CH_4, CCl_3F, and CCl_2F_2), transport tracers (HF, SF_6, HCl, CO, HNO_3, NO_y), and shorter-lived trace gases important to stratospheric chemistry including nitrogens (NO, NO_2, NO_x, N_2O_5,and HNO_4), halogens (BrO, ClO, $ClONO_2$ and HOCl), and other minor species (OH, HO_2, CH_2O, CH_3CN), as well as aerosol. The observations considered have been compiled on a common latitude-pressure grid, covering the region from the upper troposphere to the lower mesosphere (300-0.1 hPa) with a latitudinal resolution of 5°. A summary of the available climatologies from each instrument is given in Figure 2. Almost half of the trace gas climatologies are based on newer data versions than those used in SPARC (2017) (highlighted in Figure 2 and with details provided in Appendix Tables A2). The data is published via Zenodo (doi:10.5281/zenodo.4265393). Note that early data versions of chemical trace gases (i.e., research products) are not included (except for the SAGE III/ISS H_2O product) and many more species could be made available. Also, there are a handful of early limb satellite sounders such as SAMS on

https://doi.org/10.5194/essd-2020-342
Preprint. Discussion started: 21 November 2020

Nimbus 7 (Jones et al., 1986), ISAMS (Taylor et al., 1993) and CLAES (Roche et al., 1993) on UARS, ATMOS (Gunson et al., 1996) and MAS (Hartmann et al., 1996) on the ATLAS Space Shuttle missions, and ILAS on ADEOS (Sasano et al., 1999) that could not be evaluated in this assessment due to a lack of resources and generally shorter time series than those from other datasets.

The paper is organised as follows. Section 2 provides information on the participating satellite instruments, which vary in terms of measurement method, geographical coverage, spatial and temporal sampling and resolution, time period, and retrieval algorithm. The methodology used to create and compare the trace gas and aerosol climatologies is described in Section 3. The SPARC Data Initiative introduced a top-down approach to the evaluation of stratospheric composition measurements (Hegglin et al., 2013; Tegtmeier et al., 2013; SPARC, 2017), based on the comparison of zonal monthly mean trace gas and aerosol climatologies. This top-down approach complements (but does not replace) the more traditional validation approach that uses coincident profile measurements and sometimes focuses on bottom-up error budgets to characterise measurement uncertainty. The top-down climatological validation approach has the advantages that it is consistent between all instruments, avoids sensitivity to arbitrary coincidence criteria, and generally produces larger sample sizes, which minimises the random sampling error (or in other words cancels any kind of random fluctuations).

The information gained from the SPARC Data Initiative approach allows us to obtain upper bounds of systematic biases between instruments by reducing the noise from single measurements through averaging. This work also provides unique information on how well the different instruments are capable of capturing geophysical features in the stratosphere, with the consistency among the instruments constraining our current knowledge of the state of the stratosphere.

As highlighted in the sampling study by Toohey et al. (2013) as an integral part of the SPARC Data Initiative, sampling biases in the climatologies may contribute to the derived biases; this requires careful consideration in the interpretation of the results, as was attempted throughout SPARC (2017) and also in this update and extension. Another important aspect of our approach is that trace gas climatologies are compared without any modification to account for different vertical resolutions due to application of the averaging kernels. We consider our simplified approach as justified, because in most cases the vertical resolutions of the limb sounders are quite similar, and the degree to which a priori information influences the retrieved profiles is usually limited. Exceptions are discussed where they appear. Furthermore, highly structured and transient features that may not be resolved by some instruments will most likely average out in the monthly climatologies. All evaluations presented here are based on the use of the multi-instrument mean (MIM) as a reference. This choice is not based on the assumption that the MIM is the best climatology available, but is motivated by the need for a reference that does not favour a certain instrument. The climatological validation approach is applied to all evaluations and the above advantages and disadvantages will be discussed where appropriate.

Section 4 includes example trace gas evaluations of the longer-lived trace gases ozone (Section 4.1), water vapour (Section 4.2), and methane (CH_4; Section 4.3); the medium- to shorter-lived trace gases carbon monoxide (CO; Section 4.4); several nitrogen-containing species (NO, NO_2, NO_x, HNO_3, and NO_y; Section 4.5); as well as hydroperoxyl (HO_2; Section 4.6). These evaluations all use updated versions of the climatologies used in SPARC (2017), with differences to the old versions highlighted. A summary and conclusions of the updated and evaluated SPARC Data Initiative climatologies, including

https://doi.org/10.5194/essd-2020-342
Preprint. Discussion started: 21 November 2020

an overview of our knowledge of the mean state of atmospheric trace gas distributions, are given in Section 5. Note that, due to the complicating factor that aerosol extinction measurements are wavelength-dependent, the aerosol evaluations are based on a modified comparison approach, which will be presented in a follow-on publication (Hegglin et al., in preparation). In addition to this paper, a special issue in the Journal of Geophysical Research (JGR) - Atmosphere on the SPARC Data Initiative has presented the evaluations of water vapour (Hegglin et al., 2013), ozone (Tegtmeier et al., 2013), the comparison of ozone from limb sounders with the nadir-viewing Aura-TES instrument (Neu et al., 2014), an assessment of the impact of instrument-specific sampling patterns on measurement bias (Toohey et al., 2013), the dependence of the standard error of the mean on the sample size for profiles obtained with a non-random sampling pattern (Toohey and von Clarmann, 2013), and a single instrument study on SMILES observations (Kreyling et al., 2013). The reader is also referred to the WCRP SPARC Data Initiative Report (SPARC, 2017) which offers the complete assessment of all the different original atmospheric constituent climatologies and is accessible via dx.doi.org/10.3929/ethz-a-010863911.

2 Satellite Instruments

The SPARC Data Initiative (SPARC, 2017) originally evaluated observations from 18 different satellite limb sounders and additionally, the nadir sounder Aura-TES. The latter instrument was used for comparisons in the upper troposphere and lower stratosphere (UTLS) only, focusing on the comparability between limb (with high vertical resolution measurements) and nadir sounders (with high horizontal resolution measurements) applying observation operators (Neu et al., 2014). In this update, the instruments SAGE III on the ISS (hereafter SAGE III/ISS) and OMPS-LP on SUOMI NPP are added for evaluations including trace gas climatologies between 2011 and 2018.

The instruments considered here all use passive remote sensing techniques, which are based on the detection of natural radiation emitted from the Sun or stars, or from the atmosphere itself (unlike active sounders such as LIDARs). The different instruments can be classified according to their observation geometry (limb emission, solar or stellar occultation, limb scattering or nadir) and the wavelengths they are measuring at, as compiled in Appendix Table A4. In the following, we provide a short description of each instrument, with the most important instrument characteristics summarized in Tables 1 and 2, and the representative sampling patterns summarized in Figure 3. Note that the vertical range observed can depend on the retrieved species. Further information on the instrument and retrieval algorithms can be found in the SPARC Data Initiative report (SPARC, 2017).

2.1 LIMS on Nimbus 7

The Limb Infrared Monitor of the Stratosphere (LIMS) on Nimbus 7 was a limb infrared emission sounder and was launched into space on 24 October 1978 in order to measure the state of the stratosphere by observing temperature, ozone, and species that affect ozone. Nimbus 7 was in a sun-synchronous orbit with a noon and midnight equator crossing time. However, LIMS was designed to look off-plane, so measurements were made near 1 pm and 11 pm local time. The resulting sampling pattern

https://doi.org/10.5194/essd-2020-342
Preprint. Discussion started: 21 November 2020


Open Access Earth System Science Data Discussions

can be found in Gille and Russell (1984). The mission lifetime of 7 months (see Table 1) was limited by the availability of the cooling agent for the detectors.

2.2 SAGE I on AEM-2, SAGE II on ERBS, SAGE III on Meteor-3M, and SAGE III on the ISS

The Stratospheric Aerosol and Gas Experiment (SAGE) series of instruments consists of five instruments including the Stratospheric Aerosol Measurement (SAM II) on Nimbus 7 that span the period from 1978 through 2005 (McCormick, 1989). Note that SAM II has not been included in the SPARC Data Initiative evaluations. All of the instruments used solar occultation to measure attenuated solar radiation through the Earth's limb during satellite sunrise and sunset. Both SAGE I and II instruments were in inclined orbits (∼57°) that permitted near-global coverage over the course of 30 to 40 days (McCormick et al., 1989; Wang et al, 2002). There are 15 sunrise and 15 sunset measurements each day that covered a narrow latitude band and are separated by ∼24° in longitude. Unlike SAGE I and II, where sunrise and sunset measurements alternatively observed the Northern and Southern Hemispheres, all SAGE III on Meteor-3M (hereafter SAGE III/M3M) sunrise measurements occurred in the Southern Hemisphere (30°S to 60°S) while all sunset measurements occurred in the Northern Hemisphere (40°N to 80°N) due to its Sun-synchronous orbit (see Figure 3) (Thomason et al, 2010). Note that SAGE III/M3M additionally operated in lunar occultation and limb scattering mode retrieving O_3, NO_2, NO_3, and OClO, however, these measurements are not included in the SPARC Data Initiative climatologies. (see also https://ntrs.nasa.gov/archive/nasa/casi.ntrs.nasa.gov/20150001521.pdf). The SAGE III on the International Space Station (hereafter SAGE III/ISS) is in a mid-inclination orbit (51.6°) and began routine operations in June 2017. The solar measurements can provide near global observations (70°S to 70°N) on a monthly basis with coverages similar to that of SAGE II. The sampling pattern and resulting monthly and annual sampling density of SAGE III/ISS is shown in Appendix Figure A1.

2.3 HALOE on UARS

The Halogen Occultation Experiment (HALOE; see Russell et al., 1993) was launched on board the Upper Atmosphere Research Satellite (UARS) on 12 September 1991. UARS was in a 600-km near-circular orbit with a 57° inclination. HALOE used the solar occultation technique and achieved a vertical resolution of approximately 2.3 km. Note that the altitude coverage of HALOE is species-dependent, but limited to within the 10-150 km range. HALOE measured 15 sunrise and 15 sunset events per day and achieved near-global coverage in approximately a month. The daily measurement spacing was equal in longitude and varied seasonally in latitude (see Figure 3).

2.4 MLS on UARS

UARS-MLS was a Microwave Limb Sounder (MLS) instrument and one of ten instruments on the UARS platform, launched on 12 September 1991 (Reber et al., 1993). UARS-MLS (a predecessor to Aura-MLS) pioneered microwave limb sounding of the Earth's stratosphere and mesosphere from space. Aside from the stratospheric species, it measured stratospheric and mesospheric temperature and upper tropospheric humidity, which are not used in this study. UARS-MLS measured millimeter-

https://doi.org/10.5194/essd-2020-342
Preprint. Discussion started: 21 November 2020

wavelength thermal emission from about 1 to 90 km through the atmospheric limb (Barath et al., 1993; Waters et al., 1999; Livesey et al., 2003). The vertical resolution in the stratosphere (for O_3 and H_2O) was about 3 to 5 km. The UARS orbit was inclined at 57° and the satellite performed a 180° yaw maneuver 10 times per year, at approximately 36 day intervals. The resulting sampling pattern (see Figure 3) covers 34° on one side of the equator to 80° on the other side, with hemispheric coverage switching with each yaw maneuver. Profiles were spaced 3-4° along the orbit track and the average daily sampling in longitude was 12°. In mid-April 1993 there was a failure of the 183-GHz radiometer, resulting in the loss of stratospheric H_2O (and 183-GHz O_3 observations). The frequency of UARS MLS operational days generally decreased over the mission, from close to 100% from late 1991 through 1993, down to about 50% in late 1994, and only several tens of measurement days per year from 1995 onward.

2.5 POAM II/III on SPOT-3/4

The Polar Ozone and Aerosol Measurement II (POAM II) instrument was launched aboard the French SPOT-3 satellite on 26 September 1993 into a 98.7° inclination, Sun-synchronous orbit at an altitude of 833 km (Glaccum et al., 1996). The instrument operated between October 1993 and November 1996 when the SPOT-3 satellite suffered a malfunction and contact with the instrument was terminated. POAM III was launched on the French SPOT-4 spacecraft on 24 March 1998 into an orbit identical to the one of SPOT-3 (Lucke et al., 1999). The instrument began taking data on 22 April 1998 and operated until 5 December 2005. POAM III was functionally very similar to its predecessor, although it contained a number of design changes that improved sensitivity and accuracy. POAM II and III both used the solar occultation technique and made 14 measurements per day in each hemisphere, equally spaced in longitude around a circle of approximately constant latitude. Satellite sunrise measurements were made in the Northern Hemisphere (55°N-71°N) and sunsets in the Southern Hemisphere (63°S-88°S). The latitude coverage changes slowly with season and is exactly periodic from year to year (see Figure 3).

2.6 OSIRIS on Odin

The Odin satellite was launched on 20 February 2001 into a 600-km circular Sun-synchronous near-terminator orbit with a 97.8° inclination (Murtagh et al., 2002). Odin carries two instruments: the Optical Spectrograph and Infra-Red Imager System (OSIRIS) (Llewellyn et al., 2004) and the Sub-Millimetre Radiometer (SMR, see next section) (Frisk et al., 2003). Due to Odin's orbit, the data from both instruments are generally limited to between 82°S and 82°N except for occasional short periods of off-plane pointing at high latitudes during early polar spring. OSIRIS is a grating spectrometer that measures limb-scattered sunlight spectra in the spectral range from 280 nm to 810 nm at a resolution of about 1 nm. The scattered sunlight measurements are used to provide vertical profiles of the stratospheric constituents listed in Figure 2 and Table A2. In addition to these products used within the Data Initiative, there are several more research products of other constituents available. Since OSIRIS observations are dependent on sunlight, the full latitude range is only covered around the equinoxes and hemispheric coverage is provided at other times.

https://doi.org/10.5194/essd-2020-342
Preprint. Discussion started: 21 November 2020

2.7 SMR on Odin

The Sub-Millimetre Radiometer (SMR) on board the Odin satellite (for details, see Section 2.6) uses four sub-mm and one mm wave radiometers to measure thermal emission from the atmospheric limb in the 486-581 GHz spectral range and around 119 GHz (Murtagh et al., 2002; Frisk et al., 2003). SMR was used for both atmospheric and astronomical observations until April 2007, when the astronomical part of the mission ended. It provided middle atmospheric trace gas profiles every third day before this date, and has been observing the atmosphere daily since then. The altitude range and resolution varies for each species depending on the signal-to-noise ratio, the frequency band, and the retrieval mode employed. The sampling pattern and resulting measurement density from SMR for the stratospheric mode can be seen in Figure 3.

2.8 GOMOS on Envisat

GOMOS (Global Ozone Monitoring by Occultation of Stars) was a stellar occultation instrument on board the European Space Agency‘s Environmental satellite, Envisat (Bertaux et al., 2010). Envisat was launched into its Sun-synchronous polar orbit of 98.55°S inclination at about 800 km altitude on 1 March 2002 and remained operational up to April 2012. Its equator crossing time was 10 am. In every occultation, GOMOS first measured a star‘s reference spectrum when the star is seen above the atmosphere. This reference spectrum and the spectra measured through the atmosphere are then used to calculate the horizontal transmission spectra through the atmosphere. Transmissions are the basis for spectral and vertical retrieval of species profiles. GOMOS performed 100-200 night occultations per day. The measurement coverage of night occultations used in this study was global, except for the summer-time polar regions. Measurements started at 150 km and extend down to 5 km in cloudless conditions. The altitude sampling resolution is 0.5-1.7 km and depends on the azimuth of the line-of-sight (LOS) with respect to the orbital plane.

2.9 MIPAS on Envisat

The Michelson Interferometer for Passive Atmospheric Sounding (MIPAS) was a mid-infrared Fourier transform limb emission spectrometer (Fischer et al., 2008) on board of Envisat (for details see Section 2.8). MIPAS observed the atmosphere during day and night with global coverage from pole to pole. The instrument‘s field of view was 30 km in the horizontal and ∼3 km in the vertical direction. MIPAS covered the 4.3-15 μm region in five spectral bands: band A (685-970 cm^{-1}), AB (1020-1170 cm^{-1}), B (1215-1500 cm^{-1}), C (1570-1750 cm^{-1}), and D (1820-2410 cm^{-1}).

MIPAS operated during July 2002-March 2004 at full spectral resolution of 0.035 cm^{-1}. During this period, MIPAS recorded a rear-viewing limb sequence of 17 spectra each 90 seconds, corresponding to an along track sampling of ∼500 km and providing about 1000 vertical profiles per day in its standard observation mode. Tangent heights covered the altitude range from 68 down to 6 km with tangent altitudes at 68, 60, 52, 47, and then at 3 km steps from 42 to 6 km. Due to problems with the interferometer mirror slide system, MIPAS was put on hold in April 2004, but resumed operation in January 2005 with a reduced duty cycle and spectral resolution of 0.0625 cm^{-1}. Tangent heights after January 2005 covered the range from 70 down to 6 km with tangent altitudes at 70, 66, 62, 58, 54, 50, 46, 43, 40, 37, 34, 31, 29, 27, 25, 23, and then at 1.5 km steps

https://doi.org/10.5194/essd-2020-342
Preprint. Discussion started: 21 November 2020


Open Access Earth System Science Data Discussions

from 21 to 6 km. Due to the 'low'-spectral resolution mode, the number of measured profiles increased by about 20%. Note that for the SPARC Data Initiative, MIPAS data generated with the IMK/IAA data processor (von Clarmann et al. 2003; von Clarmann et al. 2009) have been provided.

2.10 SCIAMACHY on Envisat

The Scanning Imaging Absorption spectroMeter for Atmospheric CHartographY (SCIAMACHY) (Burrows et al., 1995; Bovensmann et al., 1999) was a payload on Envisat launched in March 2002 (for details see Section 2.8). SCIAMACHY was one of the new-generation space-borne instruments capable of performing spectrally resolved measurements in several different modes: alternate nadir and limb observations of the solar radiation scattered by the atmosphere or reflected by the Earth's surface, as well as observations of the light transmitted through the atmosphere during solar or lunar occultation when feasible. Only limb-viewing profiles are used here. SCIAMACHY was a passive imaging spectrometer comprising eight spectral channels covering a wide spectral range from 214 to 2386 nm. In the limb geometry, SCIAMACHY observed the atmosphere between about 10 and 100 km. Horizontal scans of 1.5 s duration were performed followed by an elevation step of about 3.3 km. No measurements were performed during the vertical step. This results in a vertical sampling of 3.3 km. The vertical instantaneous field-of-view of SCIAMACHY is about 2.6 km at the tangent point. Up to 1456 observation points are obtained per day.

2.11 ACE-FTS on SCISAT-1

The Atmospheric Chemistry Experiment-Fourier Transform Spectrometer (ACE-FTS), on board the SCISAT-1 satellite, uses mid-infrared solar occultation to investigate the chemical composition of the atmosphere (Bernath, 2006). SCISAT-1 was launched on 12 August 2003 and routine measurements began on 21 February 2004. The ACE-FTS instrument is a high-resolution (0.02 cm^{-1}) FTS measuring the full spectral range between 750 and 4400 cm^{-1} (Bernath et al., 2005). The ACE-FTS measures approximately 15 sunrise and 15 sunset occultations per day and achieves global latitude coverage over a period of three months (i.e., one season). The latitude scanning (see Figure 3) is the same each year. The spectral measurements extend from the cloud tops to 150 km with a vertical spacing varying between 1.5 and 6 km depending on the satellite's orbit geometry. Because of the high inclination of the SCISAT-1 orbit (74°), almost 50% of the occultation measurements made by the ACE-FTS are at latitudes of 60° and higher.

Note that the methodology for the calculation of the ACE-FTS climatologies has changed since SPARC (2017). While for the older climatologies, data were binned for each midpoint between the Data Initiative pressures levels, interpolation to these levels is now used (matching what has been done in Koo et al. (2017)).

2.12 ACE-MAESTRO on SCISAT-1

The Measurement of Aerosol Extinction in the Stratosphere and Troposphere Retrieved by Occultation (MAESTRO) is a dual UV/VIS/Near-IR spectrophotometer that is part of the Atmospheric Chemistry Experiment (ACE) mission onboard the

https://doi.org/10.5194/essd-2020-342
Preprint. Discussion started: 21 November 2020

SCISAT-1 satellite (see Section 2.11)(McElroy et al., 2007). ACE-MAESTRO was designed to extend the ACE wavelength coverage to the 280-1030 nm spectral region using two spectrometers with overlapping coverage (280-550 nm, 500-1030 nm) to reduce stray light. Currently, it makes measurements of solar radiation between 450-1030 nm during each sunrise and sunset with a spectral resolution of 1-2 nm (depending on spectral region). The two ACE instruments take simultaneous measurements of the same air mass using a common Sun-tracking mirror that is located within the ACE-FTS. During each occultation (sunrise or sunset measurement), approximately 60 spectra are measured by ACE-MAESTRO between the cloud tops and 100 km. The vertical spacing of these measurements varies from 300 m to 2 km at altitudes below 50 km and the spacing increases to 5 km for altitudes above 50 km. The methodology for the calculation of ACE-MAESTRO climatologies is done in the same way as for ACE-FTS.

2.13 MLS on Aura

Aura-MLS is also a microwave limb sounder, launched on the NASA Earth Observing System (EOS) Aura satellite on 15 July 2004. Aura has a 705 km Sun-synchronous polar orbit with an inclination of 98.21°, which provides global coverage from 82°S to 82°N with equator crossing times of 1:43 pm (ascending node) and 1:43 am (descending node) and a 16 day repeat cycle. Aura-MLS, like its UARS predecessor version (see Section 2.4), measures microwave thermal emission day and night, using an antenna that scans the Earth‘s atmospheric limb, in this case every 24.7 s. Aura-MLS measures in five broad spectral regions between 118 GHz and 2.5 THz. Aura-MLS views the atmosphere ahead of the Aura satellite, with 240 limb scans per orbit providing almost 3500 profiles every day. For further instrument details, see Waters et al. (2006).

2.14 HIRDLS on Aura

The High Resolution Dynamics Limb Sounder (HIRDLS) instrument was a 21-channel limb-scanning infrared radiometer, designed to scan from the upper troposphere into the mesosphere and provide data with 1-km vertical resolution (Gille and Barnett, 1992). Its channels cover the wavelength range from 6.12 to 17.76 μm, or 563 -1634 cm^{-1}. HIRDLS was launched on the Aura satellite (for details see Section 2.13). Unfortunately it was damaged during launch, such that most of the aperture was obstructed. However, the impact of the blockage can be accounted for in the retrieval of the different species (Gille et al., 2012; see also SPARC Data Initiative report for a brief summary). Data coverage is from 63°S to 80°N, with 5600 profiles per day spaced every 100 km along the scan track.

2.15 SMILES on the ISS

SMILES (Superconducting Submillimeter-Wave Limb Emission Sounder) was the first Earth observation mission selected for the Exposed Facility (EF) of the Japanese Experiment Module (JEM) on the International Space Station (ISS), where it was installed on 25 September 2009. The purpose of SMILES was the demonstration of the ultra sensitive sub-mm limb emission observation with a 4-K cooled receiver system (Kikuchi et al., 2010). The ISS orbit is circular, with an inclination of 51.6°. With the SMILES antenna mounted so that its field-of-view is 45° to the left of the orbital plane, the observed latitude region

https://doi.org/10.5194/essd-2020-342
Preprint. Discussion started: 21 November 2020

was increased to between 38°S and 65°N (nominal). 1630 observation points were obtained per day. The non-Sun-synchronous orbit of the ISS allowed the instrument to observe the diurnal variation of minor short-lived species.

2.16 OMPS-LP on Suomi NPP

The advanced Ozone Mapping and Profiler Suite (OMPS) currently flying on board the Suomi National Polar-orbiting Partnership (NPP) spacecraft consists of three spectrometers: a downward-looking nadir mapper (OMPS-NM), nadir profiler (OMPS-NP), and limb profiler (OMPS-LP). Here, we use data from the limb profiler only. The OMPS-LP instrument is equipped with a prism spectrometer and a CCD detector collecting images of the atmosphere within a vertical range of about 112 km though three entrance slits. Due to technical issues only images from the central slit are used for the retrievals so far. The instantaneous vertical field of view of each detector pixel is about 1.5 km and the vertical sampling is 1 km. The spectral range covered by the OMPS-LP instrument spans from 280 to 1000 nm with the spectral resolution degrading with increasing wavelength from 1 nm in the UV to 40 nm in the NIR spectral range. Detailed discussion of the OMPS-LP instrument is provided by Jaross et al. (2014). The sampling pattern and resulting monthly and annual sampling density of OMPS-LP is shown in Appendix Figure A1.

2.17 TES on Aura

The Tropospheric Emission Spectrometer (TES) is a Fourier Transform Spectrometer that (along with Aura-MLS and HIRDLS) was launched on Aura in 2004 (Beer, 2006; Beer et al., 2001). TES measures spectrally-resolved thermal infrared radiation (650-3050 cm^{-1}) with a spectral resolution of 0.06 cm^{-1} (unapodized) in the nadir mode. TES is a pointable instrument and can access any target within 45° of the local vertical, allowing for more tightly spaced measurements during Special Observations modes. Here we use only the standard nadir-viewing Global Survey O_3 measurements, with near-global coverage in 16 orbits (∼26 hours) (see Figure 2). In cloud-free conditions, TES nadir profiles have approximately 4 degrees of freedom for signal, with ∼2 in the troposphere and ∼2 in the stratosphere (below ∼5 hPa). This is equivalent to a vertical resolution of ∼6-7 km. TES sampling has changed over the mission lifetime in response to instrument ageing as indicated in Table 2.

3 Climatology Construction and Evaluation Methodology

The SPARC Data Initiative introduces a complementary approach of testing data quality using zonal mean monthly mean climatologies of trace gas observations for comparison, rather than using profile-to-profile evaluations based on measurement coincidences, which has been done extensively in the literature. The term climatology in this context is not used to refer to a time-averaged climate state (which should be reproduced by free-running models, averaged over many years) but to refer to year-by-year values (which free-running models would not be expected to match). The climatological approach was chosen because multiple measurements can in principle be averaged to reduce the random errors, leaving the systematic error (or bias, although it needs to be noted that here this bias is defined as relative to the multi-instrument mean and not an absolute truth). Comparing these quasi-climatologies has the advantage of removing much of the natural variability inherent to trace

https://doi.org/10.5194/essd-2020-342
Preprint. Discussion started: 21 November 2020

gas observations from both in-situ sensors and measurements from space (e.g., Hegglin et al., 2008) and yields information on the behaviour of the retrievals resolved in latitude and height. In addition, monthly mean comparisons allow for testing how well the instruments' measurement characteristics are capable of resolving geophysical features (e.g., interannual variability, seasonality, or periodicities). Note that within the SPARC Data Initiative, agreement between instruments is defined using the terminology specified in Table 3. All these numbers are with respect to the multi-instrument mean (MIM, see Section 3.2.1), so that where two instruments show excellent agreement of $\pm 2.5\%$, the two instruments could show a maximum difference of 5% between them. The definition of different altitude regions in the atmosphere as used throughout this study is given in Table 4.

In the following, a short summary of the methods used to compile and evaluate the SPARC Data Initiative zonal monthly mean time series is provided. More detailed information on the evaluation approach or instrument-specific data preparation and handling can be found in the *SPARC Data Initiative* report (SPARC, 2017).

3.1 Climatology Construction and Uncertainty

Zonal monthly mean time series of each trace gas species (in volume mixing ratio, *VMR*) and aerosol (as extinction ratio) have been calculated for each instrument on the SPARC Data Initiative climatology grid, using 5-degree latitude bins (with mid-points at 87.5°S, 82.5°S, 77.5°S, ..., 87.5°N) and 28 pressure levels (300, 250, 200, 170, 150, 130, 115, 100, 90, 80, 70, 50, 30, 20, 15, 10, 7, 5, 3, 2, 1.5, 1, 0.7, 0.5, 0.3, 0.2, 0.15, and 0.1 hPa). To this end, profile data have been carefully screened before binning and a hybrid log-linear interpolation in the vertical has been performed. For instruments that provide data on an altitude grid, a conversion from altitude to pressure levels is performed using retrieved temperature/pressure profiles (as is the case for MIPAS, ACE-FTS, and ACE-MAESTRO) or meteorological analyses (ECMWF for OSIRIS, GOMOS, and SCIAMACHY, NCEP for SAGE I and III/M3M, MERRA for SAGE II, MERRA-2 for SAGE III/ISS, UKMO for POAM II/III, and GMAO/GEOS-5 for OMPS-LP). Similarly, this information is used to convert retrieved number densities into *VMR*, where needed. Along with the monthly zonal mean value, the standard deviation and the number of averaged data values are given for each grid point, as well as the average day of month, and the minimum, mean, and maximum local solar times for these values (see Figure 4 and Table A1 for an illustration and summary of the variables included in each SPARC Data Initiative climatology file).

Interpretation of the differences between the individual trace gas and aerosol climatologies will need to take into account several sources of uncertainty, including systematic errors of both the measurements and the climatology construction. Random measurement errors have little impact on the climatological means, however measurement biases (e.g., related to retrieval errors) will introduce systematic differences between an individual instrument's climatology and the truth. Differences in the climatologies from the truth arise also from sampling biases (*Toohey et al.*, 2013) and differences in the averaging technique used to produce the climatologies (*Funke and von Clarmann*, 2012). Since the overall uncertainty of the climatology is not accessible in a consistent way from bottom-up estimates for all of the datasets included in the SPARC Data Initiative (a task

https://doi.org/10.5194/essd-2020-342
Preprint. Discussion started: 21 November 2020


Open Access Earth System Science Data Discussions

now being addressed by SPARC TUNER), we use here as an approximate measure of the uncertainty in each monthly mean climatology, the standard error of the mean (*SEM*):

$$SEM = \sigma/\sqrt{n}, \tag{1}$$

where σ is the standard deviation of the measurements and n the number of measurements at each grid point. The range of twice the *SEM* can be roughly interpreted as the 95% confidence interval of the monthly mean under the assumption of Gaussian statistics and independent errors. Although sampling patterns and densities differ greatly between different instruments, the *SEM* has been shown to generally produce a conservative estimate of the true random error in the mean for both solar occultation and dense sampling patterns (*Toohey and von Clarmann*, 2013). This is due to the fact that sampling by satellite instruments is generally roughly-uniform with respect to longitude. It should be noted, however, that the *SEM* does not reflect the potential influence of irregular or incomplete sampling of the month and latitude band, which can produce sampling biases in the climatologies (*Toohey et al.*, 2013).

3.2 Evaluation Diagnostics

A set of standard diagnostics is used to investigate the differences between the time series obtained from the different instruments. The diagnostics include comparisons of annual or monthly zonal mean climatologies, vertical and meridional mean profiles, seasonal cycles for a single year or averaged over multiple years, and multi-annual averages of latitude-month evolution. Additional evaluations of inter-annual variability and known tracer-specific features (such as the tape-recorder signal in water vapour or the Quasi-Biennial Oscillation signal in ozone) which test the physical consistency of the datasets, were also carried out and those not presented here an be found in SPARC (2017). The evaluation methods for the trace gas species time series and more examples are more thoroughly described in Hegglin et al. (2013), Tegtmeier et al. (2013), and SPARC (2017).

3.2.1 Multi-Instrument Mean (MIM) Reference

The SPARC Data Initiative‘s approach is to use the multi-instrument mean (*MIM*) as a reference to which all instruments are compared. The *MIM* is calculated by taking the mean of all available instrument climatologies within a given time period of interest, aiming at maximum spatial and temporal data coverage for each instrument in order to limit the impact of sampling bias. Note, that the *MIM* does not represent the best estimate of the atmospheric state, since most datasets are included in its calculation regardless of their quality and without any weighting applied to them. In particular, the climatologies from instruments with sparse sampling have the same weight as climatologies from instruments with much higher sampling in the calculation of the *MIM*. Only if measurements from a particular instrument are deemed unrealistic, or if another version of a specific trace gas data product is available from the same instrument, are they not included. The relative percentage differences between the trace gas mixing ratios of an instrument (χ_i) and the *MIM* (χ_{MIM}) are then given by:

$$100 * (\chi_i - \chi_{MIM})/\chi_{MIM}. \tag{2}$$

https://doi.org/10.5194/essd-2020-342
Preprint. Discussion started: 21 November 2020

One always has to keep in mind when interpreting relative differences with respect to the *MIM* that the composition of instruments from which the *MIM* was calculated may have changed between time periods. Hence, changes in derived differences are not to be interpreted as changes in the performance (or drifts) of an individual instrument. Also, if there is an unphysical behaviour in one instrument, the *MIM* and thus the differences with respect to the *MIM* of the other instruments will most certainly reflect this unphysical behaviour as well, although we have tried to eliminate the largest outliers. Finally, if one instrument does not have global coverage for every month some sampling biases may be introduced into the *MIM*. A detailed assessment of the uncertainty introduced due to inhomogeneous temporal or spatial sampling in the SPARC Data Initiative climatologies is provided by Toohey et al. (2013). This study found sampling biases of up to 10% for O_3 monthly means, and up to 20% for annual means for some instruments, generally in atmospheric regions with high natural variability such as the high-latitude stratosphere or the the UTLS. Longer-lived species with lower variability such as H_2O show smaller sampling biases (except in the UTLS). Non-uniform sampling in both space and time thereby contribute to these sampling biases.

3.2.2 Summary Evaluations

Finally, the SPARC Data Initiative uses two different summary evaluations in order to present an overview of the findings on instrument performance. The first summary evaluation (seen in Figures 14-16 and discussed in Section 5) provides the uncertainty estimate in our knowledge of the atmospheric mean state using the relative standard deviation over all instruments to give information on the spread around the *MIM*.

The second summary evaluation (not shown here) highlights in addition specific inter-instrument differences in selected regions of the atmosphere, emphasizing those datasets that are consistent with one another and those that are not. To this end, the differences are plotted for each instrument and region in the form of the median deviation from the MIM, calculated over all the differences at each individual grid point within the selected region. In addition, the median absolute deviation (*MAD*) is provided for each instrument and region, which represents the interval around the median that contains 50% of the data (Rousseeuw and Croux, 1993).

4 Examples of SPARC Data Initiative Trace Gas Evaluations

The approach of the SPARC Data Initiative for evaluating chemical trace gas climatologies from stratospheric limb sounders is illustrated in the following providing updates to the ozone (Tegtmeier et al.,. 2013) and water vapour evaluations (Hegglin et al., 2013) and presenting additional examples based on CH_4, CO, different nitrogen-containing species like NO, NO_2, HNO_3, and NO_y, and HO_2 measurements. These species were chosen to highlight particular differences in the evaluation approach that were necessary to account for the wide range of average stratospheric lifetimes valid for the lower stratosphere among the species considered (e.g., 8 years for CH_4, 3 months for CO, seconds for HO_2).

https://doi.org/10.5194/essd-2020-342
Preprint. Discussion started: 21 November 2020

4.1 Ozone (O_3)

Ozone is one of the most important trace species in the stratosphere due to its absorption of biologically harmful ultraviolet radiation and its role in determining the temperature structure of the atmosphere. A systematic comparison of the SPARC Data Initiative ozone climatologies has been provided in Tegtmeier et al. (2013) and SPARC (2017), revealing that the uncertainty in our knowledge of the O_3 mean state is smallest in the tropical middle and midlatitude lower/middle stratosphere. Notable differences between the datasets, on the other hand, exist in the tropical lower stratosphere and at high latitudes. Here, the multi-instrument spread increases to $\pm 30\%$ at the tropical tropopause and $\pm 15\%$ at polar latitudes, which is partially related to inter-instrumental differences in vertical resolution and geographical sampling.

An update of Figure 2 from Tegtmeier et al. (2013) is given in Figure 5 including new versions of SAGE II, SMR, OSIRIS, MIPAS, GOMOS, SCIAMACHY, ACE-FTS, ACE-MAESTRO, Aura-MLS, and HIRDLS ozone datasets. Note, MIPAS measured in a high-spectral measurement mode between 2002 and 2004 (hereafter called MIPAS(1)), which switched to a low-spectral measurement mode after 2004 (hereafter called MIPAS(2)). In addition, new climatologies obtained from OMPS-LP and SAGE III/ISS have been added. Appendix Tables A2 and A5 provide detailed information on time period, vertical range, vertical resolution and other information on the different data versions evaluated here. Overall the updated climatologies agree better with notably smaller differences found for SMR, SCIAMACHY, ACE-FTS, GOMOS and MIPAS.

For SAGE II, the updated data version (v7.0) shows very similar structures in the relative differences to the MIM as version v6.2 used in Tegtmeier et al. (2013), albeit tending to more negative values throughout the atmosphere. Some of the rapid transitions between positive and negative values is a result of the combination of seasonal and diurnal sampling biases during the last few years of the mission (as evaluated here), when sampling became more sparse.

For SMR, a new data product (v3.1) is evaluated here, based on the frequency mode 2 that monitors the band 544.102-544.902 GHz. This product has been improved from earlier versions (not included in SPARC, 2017) by adjusting the line broadening constant and removing the pointing offset (Murtagh et al., 2018). Compared to the SMR frequency mode 1, version 2.1 ozone product (included in SPARC, 2017), the negative bias of 10-20% in the upper stratosphere has been reduced to values of 2.5-10% (Figure 5). The updated MIPAS(2) ozone (v224) benefits from better temperature data in the mesosphere and optimization of spectroscopical data for some spectral regions. In comparison to the old MIPAS(2) ozone (v220), differences in the upper stratosphere are now reduced to 2.5-5%, which is about half of their original amount. SCIAMACHY provides an updated data version (V3-5) based on a new retrieval algorithm (Jia et al., 2015), which improved the retrievals considerably compared to the previously evaluated version (V2.5; Tegtmeier et al., 2013), with a positive bias in the middle and upper stratosphere now reduced from 10-20% to 2.5-10%.

Updated ACE-FTS ozone (v3.6) in the MS and US shows considerable smaller differences to the MIM (mostly up to 5%, Figure 5) than the old climatology (v2.2), which had a low bias in the MS of up to 10% and a high bias in the US of up to 10-20% (Tegtmeier et al., 2013). Interpolation of mixing ratios to the SPARC Data Initiative grid in log-pressure, data filtering based on quality flag information (Sheese et al., 2015) and reduced nonphysical oscillations in the updated pressure and temperature retrievals all contribute to the improved performance (Koo et al., 2017; Waymark et al., 2013). The ACE-

https://doi.org/10.5194/essd-2020-342
Preprint. Discussion started: 21 November 2020

MAESTRO climatology (v3.13), on the other hand, has larger biases than the previously evaluated version (v2.1; Tegtmeier et al., 2013). In particular, the low bias in the LS and the high bias in the US increased from 2.5-5% to 10-20% (Figure 5, see also Bognar et al., 2019). Both MAESTRO versions use ACE-FTS temperature profiles in the retrieval, which requires information on the relative time difference between the measurements. For v3.13, this time difference is determined from MAESTRO O_2 slant column and ACE-FTS air mass slant column instead of using a constant value based on the best match between the ozone profiles. However, it is not clear if these changes cause the larger biases or if they are related to other issues of the v3.13 processing. This is under investigation.

GOMOS O_3 climatologies (v5.0) used previously have shown a substantial positive bias in the LS (30%) and UT (80%) (Tegtmeier et al., 2013) due to the high sensitivity of the retrieval algorithms to the aerosol extinction model. The new GOMOS climatologies (ALGOM2s; Sofieva et al., 2017), whilst similar to additionally available v6.01 data (not used here) at higher altitudes, are based on a new O_3 profile inversion algorithm, which is optimized by enhancing the spectral inversion at visible wavelengths for the UTLS, thus decreasing the impact of the aerosol model. As a result, GOMOS performs much better with excellent agreement in the LS (Figure 5). In the UT, GOMOS retrieves lower ozone values than the other instruments, with differences to the MIM of 20 to 50%.

New O_3 data products from IUP-OMPS (Arosio et al., 2018) and USask-OMPS (based on a 2D retrieval) agree very well with the other datasets in the middle and upper stratosphere (Figure 5). The two data products are based on different retrieval algorithms, but show very similar structure with positive differences of 2.5-5% in the MS and US increasing up to 10-20% at the SH high latitudes and higher deviations of up to 50% in the tropical UTLS. The new O_3 data product from SAGE III/ISS (v5.1) agrees also very well with the other datasets. While the US shows even excellent agreement, differences in the LS down to 100 hPa are mostly below 5-10% and thus considerably smaller than for most other instruments. For this work, the 'AO3' product was used because it has reduced noise compared to the 'MLR' product, particularly in the UT and US (see Wang et al. (in preparation) for details). It should also be noted that the auxiliary temperature and pressure data (interpolated from MERRA-2) profiles used in SAGE III/ISS (v5.1) retrievals have a small altitude registration problem, which could affect O_3 data particularly in the tropical upper stratosphere by around 1-2%.

In summary, the updated O_3 climatologies show improved agreement in most regions of the atmosphere (Figure 14). In particular, the 1-σ multi-instrument spread in the UT decreased significantly at all latitudes from $\pm$45% on average to $\pm$25%, among other things due to improved GOMOS performance. The region of very good agreement (1-σ of $\pm$5%), previously restricted to below 3 hPa, extends now further up into the US reaching the level of 1 hPa. In the LM, agreement also improves, with maximum deviations of $\pm$30% due to POAM III being not included in the updated evaluations. At polar latitudes, however, deviations are still large with maximum values of $\pm$30% found in the Antarctic LS.

4.2 Water Vapor (H_2O)

H_2O is the single most important natural greenhouse gas and provides a positive feedback to man-made climate change due to the emission of carbon dioxide. H_2O is also a key constituent in atmospheric chemistry. It is the source gas of the hydroxyl radical, which controls the lifetime of atmospheric pollutants, ozone (also in the stratosphere), and greenhouse gases.

https://doi.org/10.5194/essd-2020-342
Preprint. Discussion started: 21 November 2020

Open Access Earth System Science Data Discussions

A comprehensive assessment of the SPARC Data Initiative H_2O climatologies has been provided by Hegglin et al. (2013) and SPARC (2017). While substantial biases exist between the instruments particularly in the troposphere (±30-50%), the lower mesosphere (±15%), and the polar regions (±10-15%), our knowledge of the mean state is best in the tropical and mid-latitude LS and MS with a relative uncertainty of only ±2-6%. Also, once these biases are removed, the instruments showed very good agreement in the magnitude and structure of interannual variability.

Figure 6 shows an update of Figure 5 from Hegglin et al. (2013) including new data versions for ACE-FTS, Aura-MLS, MIPAS(1) and MIPAS(2), SAGE II and SCIAMACHY, and adding new climatologies obtained from HIRDLS, ACE-MAESTRO, and SAGE III/ISS. Appendix Tables A2 and A6 provide detailed information on data versions, time period, vertical range, vertical resolution and other information on the different data versions evaluated here. LIMS and UARS-MLS (although having measured during an earlier period) are also added for comparison. All other climatologies remain the same. Overall, the differences between instruments have not changed by much relative to each other using the updated data versions, although notably smaller differences are found for SAGE II.

SAGE II (v7.0) has much improved over SAGE II (v6.2) used in Hegglin et al. (2013) and SPARC (2017). In the MS, the differences to the MIM have decreased from between -5% and -10% (v6.2) to values mostly within ±2.5% (v7.0) (Figure 6). Smaller differences to the MIM between ±5% are also found in the UTLS, where large negative biases (>10-20%) existed in the previous version (v6.2) (Hegglin et al., 2013). This overall improvement is a consequence of modifying a spectral filter channel correction in the SAGE II retrieval (Thomason, 2004) using SAGE III/M3M as the basis for comparison in v7.0 instead of HALOE in v6.2 (Damadeo et al., 2013; see also Hegglin et al., 2014).

The new MIPAS(1) (V3o_H2O_21) and MIPAS(2) (V5r_H2O_224) data versions show generally very similar features in the differences to the MIM as the earlier data versions V3o_H2O_13 and V5r_H2O_220 used in Hegglin et al. (2013), respectively. MIPAS(2) exhibits some improvements in the tropical US, where differences to the MIM decreased from around 10% to 5% in the newer version. MIPAS(1) improved in the LM, where differences to the MIM decreased from >10% in V3o_H2O_13 evaluated in Hegglin et al. (2013) to smaller or even slightly negative values (between 2.5% to -5%). As a consequence, the new data versions of MIPAS(1) and MIPAS(2) seem more similar in character throughout the stratosphere and lower mesosphere, except in the UTLS where MIPAS(2) generally shows positive differences to the MIM (>10%), while MIPAS(1) shows both positive (>5%) and negative differences to the MIM (>-5%) depending on the region. Note, that in this comparison, the MIPAS averaging kernels have not been considered. Since MIPAS H_2O is retrieved in the log space, the H_2O averaging kernels are concentration-dependent and thus highly variable, in particular in the UTLS where H_2O exhibits strong gradients. Thus the mean differences should be interpreted with care.

The new ACE-FTS (v3.6) and Aura-MLS (v4.2) data versions show both slight improvements in the UTLS, and Aura-MLS also slightly smaller positive differences to the MIM in the US. The negative bias seen in Aura MLS around 200 hPa in the evaluation of Hegglin et al. (2013), which extended the findings by Vömel et al. (2007) based on balloon soundings to all latitudes, is, however, still apparent. ACE-MAESTRO (v31), a new instrument in the comparison, shows rather large positive differences to the MIM (mostly >10-20%) across its measurement range in the UTLS. The wet bias in the tropical LS is a known issue for this version of ACE-MAESTRO (Lossow et al., 2019).

https://doi.org/10.5194/essd-2020-342
Preprint. Discussion started: 21 November 2020

SCIAMACHY's negative bias to the MIM of around 10% found for data version v3.0 by Hegglin et al. (2013) in the NH LS slightly improved in the version evaluated here (v4.0) to 5%, and also the positive bias when compared to the MIM in the tropical UTLS (from 20% to 10%). HIRDLS (v7.0) exhibits a negative bias of >10% with respect to the MIM extending across the MS, and SMR (v2.0) an even larger negative bias of >20%.

While LIMS (v6.0) and UARS-MLS (v6) are not directly comparable to the other instruments due to the time period they measured in, the very different character in the differences still highlights that trends in H_2O are of minor importance when compared to inter-instrument differences. UARS-MLS shows a very uniform negative bias with respect to the MIM of -10% whereas LIMS exhibits a positive bias in the extratropical LS and MS, and a more negative bias across the US and in the tropical LS. A part of the negative H_2O bias for the US in LIMS may be due to the increases in CH_4 and its conversion to H_2O during the intervening years.

The new instrument SAGE III/ISS (v5.1) shows excellent agreement with the MIM across the MS and US (with relative differences of $\pm$ 2.5% only), while a strong positive relative difference from the MIM (up to $\pm$ 50%) is found in the LM. This feature persists even when comparing climatologies from instruments available during the same years (2017-2018) (including ACE-FTS and Aura MLS) (not shown) and is likely due to some reminiscent profiles that 'keel over' to very high values in the USLM, potentially biasing the climatology high. These profiles will be filtered out and/or corrected in future versions. In the UT and LS, SAGE III/ISS (v5.1) shows largely positive (up to 20%) and negative (up to -5%) differences to the MIM, respectively.

Overall, the update in the H_2O climatologies has led to only some small improvements and only in some regions of the atmosphere (see Figure 14). In the NH lower stratosphere, the 1-σ multi-instrument spread decreased from $\pm$10% to $\pm$5% and in the tropical UTLS from $\pm$20% to $\pm$10%, among other reasons due to improved performance of SCIAMACHY. However, in the US, the multi-instrument spread increased slightly from $\pm$10% to $\pm$12.5%.

4.3 Methane (CH_4)

CH_4 is the most abundant hydrocarbon in the atmosphere and with a lifetime of around 8 years (Lelieveld et al., 1998) is considered long-lived. It is a very effective greenhouse gas and the second-largest contributor to anthropogenic radiative forcing since preindustrial times after CO_2. CH_4 is a source gas for stratospheric water vapour (resulting in a positive climate feedback), affects stratospheric ozone chemistry, and in the troposphere acts to reduce the atmosphere's oxidizing capacity.

The earliest CH_4 measurements from space were obtained from SAMS on Nimbus-7 between 1979 and 1981 (Taylor, 1987), followed by measurements from ATMOS since the mid-1980s (Gunson et al., 1996), and from ISAMS (Taylor et al., 1993) and CLAES (Roche et al., 1993) on UARS (along with HALOE). As mentioned above, these climatologies were not considered in the SPARC Data Initiative. The first vertically resolved satellite climatologies of CH_4 available to the SPARC Data Initiative were made by HALOE in 1991. MIPAS started measuring CH_4 in 2002 providing about 4 years of overlap (although with a major gap in 2004). From 2004 onwards there are also ACE-FTS measurements available for comparison. Table A7 provides information on the availability of CH_4 measurements, including data version, time period, height range, vertical resolution, and references relevant for the data product.

https://doi.org/10.5194/essd-2020-342
Preprint. Discussion started: 21 November 2020


Open Access Earth System Science Data Discussions

Figure 7 shows meridional profiles of CH_4 at different pressure levels for August averaged over 1998-2008. These comparisons provide information on the latitudinal distribution of CH_4 and latitude-height dependency of the differences between the instruments. At 50 hPa, the instruments tend to agree very well with each other mostly within $\pm 5\%$. The same is largely true for the 10 hPa level. In both cases, ACE-FTS (v3.6) and HALOE (v19) agree best with each other, while MIPAS(2) (v224) seems to have somewhat higher discrepancies from the MIM than the other instruments and also exhibits differences that vary more with latitude. At 5 hPa, however, the differences of the instruments with respect to the MIM increase to $\pm 20\%$. Here, HALOE is closest to the MIM, ACE-FTS shows largest negative values and MIPAS(1) (v21) largest positive values. The deterioration in the agreement between the instruments with height is qualitatively consistent with the results of SPARC (2017). However, the new data versions used here agree quantitatively much better with each other, particularly at the 50 hPa and 10 hPa levels.

We now turn to an example which can be used to test the physical consistency of the available datasets. To this end, the latitude-time evolution of CH_4 for the different instruments at 2 hPa is shown in Figure 8. ACE-FTS and HALOE fields have been constructed using linear interpolation to fill in data gaps that arise from their sparse latitude-time sampling patterns. Figure 8 reveals local maxima located in the tropics just off the equator in the respective summer hemisphere, distinct features that were found in earlier studies (e.g., Jones and Pyle, 1984; Ruth et al., 1997) and attributed to the equatorial semiannual oscillation (Choi and Holton, 1991). The maxima in the trace gas thereby coincide with maxima in upwelling, which brings younger air (less depleted in CH_4) to higher altitudes. Tropical CH_4 thus should show a semi-annual cycle. Photochemistry, on the other hand, causes minima at high latitudes during summer and autumn, with CH_4 lifetimes decreasing to 4 months at these altitudes (Solomon et al., 1986; Randel et al., 1998).

HALOE captures the tropical semiannual oscillation well and also indicates the high-latitude minima during the summer months. MIPAS shows very similar features, but due to its better spatio-temporal sampling extends further into the polar regions, revealing the full extent and timing of these features. The tropical maxima in both MIPAS(1) and MIPAS(2) are stronger than in HALOE. ACE-FTS exhibits a much noisier field due to its limited sampling and hence exhibits sharp maxima and edges especially in the tropics, where the instrument scans through only once a season. While climatologies in equivalent latitude would help to reduce the noise, this quantity was not available to the SPARC Data Initiative. Knowledge of the representativeness of ACE-FTS in geographical latitude is however still valuable for model-measurement comparisons.

The difference plots indicate a low bias in HALOE and ACE-FTS versus a known high bias in MIPAS(1). MIPAS(2) exhibits a somewhat patchier difference field, however, provides supporting evidence for the high bias in MIPAS(1) rather than a low bias in the other two instruments at this pressure level. Compared to the data versions used in SPARC (2017), the new data versions used here agree generally somewhat better even at this level. While HALOE‘s difference field to the MIM remains the same (no new data version available), ACE-FTS has somewhat less noise, now tending to more negative values, MIPAS(1) shows smaller differences especially in the tropical and mid-latitude regions, and MIPAS(2) shows slightly increased differences across the time-latitude domain. It is important to note that CH_4 showed only small trends in the troposphere over the time period 1998-2008, and an evaluation focusing on the overlap year 2005 largely confirms the here described results (not shown).

https://doi.org/10.5194/essd-2020-342
Preprint. Discussion started: 21 November 2020

The overall impact of updated data versions on our knowledge of the mean-state of the atmosphere in terms of CH_4 is shown in Figure 14. Compared to SPARC (2017), the new data versions have led to decreases in the 1-σ multi-instrument spread across the UTLS and MS from $\pm$10% to $\pm$5%. A decrease of around 5% in the 1-σ multi-instrument spread is also found across the USLM in comparison with SPARC (2017), although the values are much more variable in this region.

4.4 Carbon monoxide (CO) comparisons

Carbon monoxide (CO) has a lifetime of approximately three months in the UT and LS. In the troposphere, CO impacts air quality and has an indirect radiative forcing effect, since it scavenges OH that would otherwise react with (and deplete) the greenhouse gases methane and ozone (Daniel and Solomon, 1998). Due to its intermediate lifetime, it is often used as tracer to identify troposphere-stratosphere exchange (e.g., Hoor et al., 2004; Hegglin et al., 2009). In the lower stratosphere, CO reaches a background value ranging between 8 and 15 ppbv (Flocke et al., 1999) as determined by the equilibrium between its production (from methane oxidation) and loss (from CO oxidation).

Only a few limb-sounders provide CO measurements, with climatologies from SMR, MIPAS, ACE-FTS, and Aura-MLS contributing to the SPARC Data Initiative. The earliest dataset that would offer CO, but which is not included in the comparisons here, can be obtained from SAMS on Nimbus 7 (although with a very high noise level; Taylor, 1987). Other useful CO measurements were obtained by ATMOS on the Space Shuttle (Gunson et al., 1996), and from ISAMS on UARS (Taylor et al., 1993). Table A8 compiles information on the availability of CO measurements, including time period, height range, vertical resolution, and references relevant for the data product used in this report.

For CO, we focus first on the zonal annual mean evaluation as shown in Figure 9, which is one of the standard evaluations in the SPARC Data Initiative (as also shown in Figures 5 and 6). ACE-FTS and Aura-MLS are averaged over the period 2004-2009, while MIPAS(2) is averaged over 2005-2009, MIPAS(1) over 2002-2004, and SMR over 2003-2004. The figure reveals large differences in the structure and values of CO as measured by the different instruments. Nevertheless, common features are minimum values around 15 ppbv in the LS and MS, and strongly increasing values towards the USLM with maxima in the polar regions. These large values stem from the photodissociation of CO_2 in the mesosphere and subsequent downward transport (Solomon et al., 1985). Increasing values can also be seen when moving towards the UT (with tropospheric CO coming mostly from anthropogenic sources). The mid-infrared sensors MIPAS(1) (v20), MIPAS(2) (v222), and ACE-FTS (v3.6) agree best. SMR (v2.1) CO exhibits a fair amount of noise, which stems from the fact that the CO was retrieved about 2 days per month and during a limited time period from October 2003 to October 2004 only. SMR does not reproduce the low background values of 8-15 ppbv expected in the LS to MS. Aura-MLS (v4.2), on the other hand, shows stratospheric CO values of smaller than 10 ppbv that are somewhat lower than those observed by MIPAS and ACE-FTS (see also Pumphrey et al., 2007). Aura-MLS also shows a local minimum in CO in the tropical LM (around 0.2 hPa), which is not seen in other datasets. Aura-MLS and also SMR do not reproduce the same downward and poleward sloping trace gas isopleths in the LS as seen by MIPAS and ACE-FTS, a typical feature observed for long-lived trace gases as a result of transport and mixing within the Brewer-Dobson circulation (Tung, 1982).

https://doi.org/10.5194/essd-2020-342
Preprint. Discussion started: 21 November 2020


Open Access Earth System Science Data Discussions

In comparison with the CO evaluations in SPARC (2017), significant improvements are found for the new data versions of MIPAS(1) and ACE-FTS. For these instruments, the relative biases with respect to the MIM in the tropical MS have decreased from 10-20% to ±5%. While the shortcomings in Aura-MLS were already pointed out in SPARC (2017), the relative biases with respect to the MIM in the LM (around ±10%) are now much closer to ACE-FTS and MIPAS(2). Positive biases of more than 50% in Aura-MLS (v3) in the UTLS have also decreased to 20%, although the isopleths are still relatively flat compared to those found by the other instruments.

In addition, Figure 10 shows deseasonalized anomalies for CO at three different pressure levels in either the tropics or extra-tropics. The instruments all capture the interannual variability well. Despite its limited tropical sampling, ACE-FTS seems to capture the interannual variability in the tropical UT at 200 hPa well, and notably better than data version 2.6 used for SPARC (2017). It is also noteworthy that the shortcomings of Aura-MLS in reproducing the zonal annual mean are not hampering the ability of the retrieval to observe the correct interannual variability in these time series, hence still pointing out the usefulness of the Aura-MLS product for such evaluations.

Overall, our knowledge of the mean state for CO as expressed by the 1-σ multi-instrument spread (see Figure 14) has improved across the USLM by about 5%. In the UTLS and MS, however, the 1-σ spread remains similar, at above ±30%. At least in the LS, this is largely due to the persisting problems in the CO distribution obtained from Aura-MLS. Note that SMR and MIPAS(1) were not included in Figure 14 due to differences in the time period for which they provided data for.

4.5 Nitrogen species (NO, $\mathrm{NO_2}$, $\mathrm{NO_x}$, $\mathrm{HNO_3}$ and $\mathrm{NO_y}$) comparisons

Total reactive nitrogen ($\mathrm{NO_y}$) is the sum of all atmospheric reactive nitrogen species with largest contributions from nitric oxide (NO), nitrogen dioxide ($\mathrm{NO_2}$) and nitric acid ($\mathrm{HNO_3}$). Tropospheric $\mathrm{NO_y}$ originates mostly from sources of NO and $\mathrm{NO_2}$ (together known as the nitrogen oxide family, $\mathrm{NO_x}$) released from fossil fuel burning, lightning, chemical processes in soils, and biomass burning. In the stratosphere, $\mathrm{NO_y}$ is primarily produced from the oxidation of $\mathrm{N_2O}$, which originates from soil and ocean emissions, biomass and fossil fuel burning, livestock manure and fertilization in agriculture. Another important source is the enhancement of upper atmospheric $\mathrm{NO_x}$ through ionizing energetic particle precipitation (Solomon et al., 1982) and the $\mathrm{NO_x}$ downward transport inside the polar vortex (Funke et al., 2005a). Reactive nitrogen species play an important role in stratospheric ozone chemistry through different mechanism including the catalytic $\mathrm{NO_x}$ cycle (Crutzen, 1970), the role of $\mathrm{HNO_3}$ in polar stratospheric cloud formation (Fahey et al., 2001) and $\mathrm{NO_2}$-driven conversion of halogens into reservoir substances. Stratospheric nitrogen will remain a future research focus as unregulated $\mathrm{N_2O}$ emissions are expected to become the most important ozone-depleting emission during the 21st century (Ravishankara et al., 2009).

Sunlight-driven exchange between stratospheric NO and $\mathrm{NO_2}$ causes a strong diurnal cycle in both species with large NO abundances during daytime, large $\mathrm{NO_2}$ abundances during nighttime and steep gradients at sunrise and sunset in both species. A direct comparison of satellite-based NO and $\mathrm{NO_2}$ measurements (which correspond to different local solar times, LST) is not possible, unless the dependence on the solar zenith angle (SZA) is being taken into account. Solar occultation measurements made at SZA = 90° (NO from HALOE and ACE-FTS, $\mathrm{NO_2}$ from SAGE II, HALOE, POAM II, POAM III, SAGE III/M3M and ACE-FTS) can be compared amongst each other if separated into local sunrise and sunset. Limb scattering

https://doi.org/10.5194/essd-2020-342
Preprint. Discussion started: 21 November 2020

and emission measurements (NO from MIPAS and SMR, NO_2 from LIMS, OSIRIS, SCIAMACHY, MIPAS, and HIRDLS) and stellar occultation measurements (NO_2 from GOMOS) correspond to different SZAs and need to be scaled to a common LST. We follow the approach to scale the NO measurements from ACE-FTS and SMR as well as the NO_2 measurements from OSIRIS, SCIAMACHY, and ACE-FTS with a chemical box model (McLinden et al., 2010) to the LST of the MIPAS measurements 10am/pm. NO_2 date from HIRDLS (June 2005 to May 2006) has been scaled to 10am/pm with the SD-WACCM Version 3 (Garcia et al., 2007). Appendix Tables A9-A11 summarise information on the availability of NO, NO_2, and HNO_3 measurements, including data version, time period, height range, vertical resolution, and references relevant for the data product used in this study. For these species, updated data versions are available from ACE-FTS (v3.6), GOMOS (v6.01), HIRDLS (v7.0), MIPAS(1) (v20), SAGE II (v7.0), and SCIAMACHY (v4-0).

NO_x shows only a weak diurnal cycle in the LS to MS and is available from HALOE, ACE-FTS and MIPAS based on the sum of NO and NO_2. OSIRIS and SCIAMACHY measure NO_2 but not NO and their NO_x climatologies are compiled with the help of a chemical box model (McLinden et al., 2010). In the following evaluations the NO_x datasets from ACE-FTS, HIRDLS, OSIRIS, and SCIAMACHY are scaled to 10am and 10pm, respectively.

The nitrogen species HNO_3 (from LIMS, UARS-MLS, SMR, MIPAS, ACE-FTS, Aura-MLS, and HIRDLS) and also the reactive nitrogen family NO_y (from ACE-FTS, MIPAS, and a combination of the Odin measurements of OSIRIS and SMR) are long lived, except for some diurnal variations of HNO_3 in the LM. The NO_y climatologies from ACE-FTS (based on the methodology of Jones et al. (2011), except for the vertical binning) and MIPAS (Funke et al., 2014) are compiled from NO, NO_2, HNO_3, HNO_4, 2 x N_2O_5 and $ClONO_2$ (six-species climatologies) all directly measured by the instruments. The NO_y Odin climatology (Brohede et al., 2008) is based on NO_2 from OSIRIS, HNO_3 from SMR and NO, 2 x N_2O_5 and $ClONO_2$ taken from scan-based chemical box model simulations (McLinden et al., 2010), while HNO_4 is not included (five-species climatology). In all figures the instrument names will be completed by lower indices giving the number of species used to compile the climatology, e.g., Odin5 for the Odin five-species climatology. Note that the ACE-FTS and Odin NO_y products are daytime climatologies and do not include polar night data as opposed to MIPAS.

We present here the evaluation of the seasonal cycle of the nitrogen species NO, NO_2, NO_x, HNO_3 and NO_y in the mid-latitudes (30°S-60°S and 30°N-60°N) and tropics (10 hPa 20°S-20°N) at 10 hPa (Figure 11). The latitude band and pressure level have been chosen to include as many species and instruments as possible. While the NO maximum can be found around 1 hPa, the HNO_3 maximum is situated much lower in the atmosphere at around 30 hPa. The choice of evaluations at the 10 hPa level in the MS thereby ensures that both species are abundant. For NO, ACE-FTS shows good agreement with MIPAS except for NH mid-latitudes during boreal winter when ACE-FTS can be up to 25% lower. In particular in the SH midlatitudes, the new data version of ACE-FTS (v3.6) has led to clear improvements and the consistently too low NO values (ACE-FTS v2.2) are now much closer to MIPAS. Scaled SMR data agrees well with the other two datasets in the US to LM, but shows large deviations in the MS and is thus omitted from the comparison in Figure 11.

The NO_2 comparison (Figure 11, 2nd row) in the mid-latitudes shows a very good agreement of all datasets except for ACE-FTS and HIRDLS during boreal winter. The seasonal cycle of NO_2 from ACE-FTS and HIRDLS in the NH, and to some degree also in the SH, has a larger amplitude than the one derived from the other three instruments. In the tropics, all

https://doi.org/10.5194/essd-2020-342
Preprint. Discussion started: 21 November 2020


Open Access Earth System Science Data Discussions

instruments agree on a very weak seasonal signal except for HIRDLS, which displays an annual cycle with an amplitude of 50%. Over the whole measurement range (LS to US), the datasets from MIPAS, OSIRIS and SCIAMACHY agree better with each other than with ACE-FTS or HIRDLS. Compared to the old data versions (SPARC, 2017), largest improvement is found for the updated ACE-FTS (v3.6) in the SH mid-latitudes, where the negative bias has been removed, consistent with NO evaluations.

The NO_x seasonal cycles of all datasets agree well on the phase, but show some deviations in the amplitude of the signal (Figure 11, 3rd row). For the mid-latitudes, absolute values of ACE-FTS NO_x are considerably lower than the other instruments during the respective winter season confirming the findings of the NO and NO_2 evaluations. The latter characteristic also causes a larger amplitude of the ACE-FTS seasonal cycle in the both mid-latitude bands. In the tropics, datasets agree well with a relatively weak seasonal cycle that is most pronounced in MIPAS. Again, largest improvement is found for ACE-FTS (v3.6) in the SH mid-latitudes and NH mid-latitudes during winter.

The comparison of the HNO_3 seasonal cycle (Figure 11, 4th row) includes in addition to ACE-FTS, HIRDLS and MIPAS, also the SMR and Aura-MLS datasets. All climatologies can be evaluated without chemical scaling and show mostly a very good agreement of the mean values except for higher ACE-FTS values in the SH mid-latitudes during austral winter. The updated HIRDLS climatology (v7.0) shows an improved performance compared to the old data version (v6.0, SPARC, 2017), since the too low HNO_3 values during boreal autumn and the resulting semiannual signal are now removed. For all regions above 30 hPa, Aura-MLS and HIRDLS are on the low side while ACE-FTS, MIPAS and SMR are on the high side. Below 30 hPa, the situation is reversed.

Finally, evaluations of the NO_y seasonal cycle (Figure 11, 5th row) show some severe differences (although not necessarily in the mean value, just the amplitude), most notably in the SH mid-latitudes where the seasonal cycle from Odin is completely opposite to the one from ACE-FTS and MIPAS. These deviations can be understood from the OSIRIS NO_2 and NO_x as well as the SMR HNO_3 seasonal cycles in the SH, which show a smaller amplitude than the respective MIPAS and ACE-FTS datasets. In general, we expect increasing NO_y values during the dynamically quiescent spring and summer time as observed by ACE-FTS and MIPAS. For the NH, the same is true with the NO_y maximum observed in boreal autumn by all three instruments. Similar to the SH, Odin shows a secondary maximum in spring, which is however, less pronounced allowing for a better agreement with the other two datasets. For ACE-FTS, the too low NO_x values in the SH and NH boreal winter cancel out with the too high HNO_3 values resulting in an overall good agreement with MIPAS. The overall annual mean state of NO_y is well known and the three datasets show excellent agreement (Figure 15) with differences smaller than $\pm 5\%$. However, deviations can be larger for individual months (up to $\pm 10\%$, Figure 11) and cancel out in the annual mean.

Apart from the climatological and seasonal differences between the datasets, it is of interest to evaluate how well the instruments detect signals of interannual variability. Figure 12 shows the time series of NO_2 mean values (upper panels) and deseasonalized anomalies (lower panels) for the tropical latitude band 20°S-20°N at 10 hPa. We focus on the evaluation of the NO_2 interannual anomalies of the longer time series SAGE II and HALOE in comparison with interannual variability of ACE-FTS, MIPAS, OSIRIS, SCIAMACHY, GOMOS and HIRDLS. Anomalies calculated in an additive sense by subtracting monthly multi-year mean values for each month might also display a diurnal cycle and are therefore not suitable evaluation

https://doi.org/10.5194/essd-2020-342
Preprint. Discussion started: 21 November 2020

tools for unscaled datasets. However, anomalies calculated in a multiplicative sense as percentage deviations from the monthly multi-year mean values are less affected by the diurnal variations. Since no scaled versions of SAGE II and HALOE data are available the comparison focuses on multiplicative anomalies of the sunset/nighttime NO_2 climatologies including SAGE II, HALOE, ACE-FTS local sunset datasets and MIPAS, OSIRIS, SCIAMACHY, GOMOS 10pm and HIRDLS night datasets.

The comparison of the mean values (upper panel) shows a very good agreement of MIPAS, GOMOS and scaled SCIAMACHY measurements. Scaled OSIRIS data are somewhat lower than the other three datasets. Diurnal NO_2 variations between 10pm and local sunset at the 10 hPa level are so small, that SAGE II, HALOE and ACE-FTS data taken at local sunset mostly agree with the other datasets for the overlap period 2003-2005. From 2003 onwards the multiplicative anomalies of all datasets display the expected QBO signal with the best agreement between MIPAS, OSIRIS, GOMOS and SCIAMACHY. The three years of HIRDLS measurements display a larger amplitude of the QBO signal and also larger month-to-month fluctuations, possibly due its higher vertical resolution. Interannual anomalies from ACE-FTS agree for some months with the other datasets, but show large deviations for other months. Due to the sparse sampling it is not possible to diagnose a QBO signal in the ACE-FTS time series. Local sunset evaluations from SAGE II and HALOE show also large month-to-month variations but agree reasonably well on their interannual variability and display the QBO signal over the whole time period. The same is not true, however, for the local sunrise evaluations of the two instruments where HALOE shows only a weak and SAGE II no clear indication of a QBO signal (SPARC, 2017).

The overall knowledge on the atmospheric mean state of the different trace gases treated in this section as expressed by the 1-σ multi-instrument spread is shown in Figure 15.

4.6 Hydroperoxyl (HO_2) comparisons

Hydroperoxyl (HO_2) together with the hydrogen atom (H) and hydroxyl (OH) form the HO_x -family. HO_2 is formed in the reaction between a hydrogen atom (H) and molecular oxygen (O_2), or between ozone (O_3) and OH. OH affects stratospheric ozone chemistry through its role in the HO_x catalytic reaction cycle that destroys ozone. The HO_x cycle was the first catalytic reaction cycle to be identified (Bates and Nicolet, 1950). HO_x chemistry dominates ozone destruction above 40 km, while NO_x dominates ozone destruction in the middle stratosphere (Salawitch et al., 2005). In the troposphere, HO_2 is generated as an intermediate product of the oxidation of many hydrocarbons.

Measurements of HO_2 are available from instruments that measure in the sub-mm/microwave wavelength bands, namely SMILES, SMR, and Aura-MLS. Other available HO_2 datasets are restricted to balloon campaigns, such as from the Far Infrared Spectrometer (FIRS-2) (Johnson et al., 1995; Jucks et al., 1998). There is no temporal overlap between the three satellite instruments, since SMR currently only provides HO_2 data as research product during one year (October 2003-2004). SMILES on the other hand operated between October 2009 to April 2010 only. While SMILES measures the full diurnal cycle, Aura-MLS measures at 1:30am/pm, and SMR at 6:30am/pm. Since HO_2 does not exhibit very strong variations during the day, daytime climatologies are compared only (using SMR am data, which are deemed closer to the daytime values than the pm data). Table A12 compiles information on the availability of HO_x measurements, including data version, time period, height range, vertical resolution, and references relevant for the data product used in this study.

https://doi.org/10.5194/essd-2020-342
Preprint. Discussion started: 21 November 2020


Open Access Earth System Science Data Discussions

Figure 13 shows the zonal monthly mean evaluation between Aura-MLS and SMILES for November 2009 and February 2010. As seen in the MIM, mixing ratios are similar in both months in the tropics (where SZAs do not vary much with season), indicating only a weak seasonal cycle in the daytime monthly mean climatologies. Lowest mixing ratios are found in the polar region of the winter hemisphere (during high SZA conditions), indicating a somewhat more pronounced seasonal cycle in these regions of the atmosphere. The differences to the MIM indicate very good (up to $\pm 5\%$) to excellent (up to $\pm 2.5\%$) agreement between SMILES and Aura-MLS, except in the lower part of the measurement range (around 20 hPa) where differences to the MIM increase to $\pm 10\%$ and more. The results presented here are comparable to (if not somewhat better than) what was found in SPARC (2017), where multi-year monthly mean climatologies were used for the comparison.

5 Summary Evaluations

The SPARC Data Initiative provides an estimate of the systematic uncertainty in our knowledge of the measured fields' mean state derived from the inter-instrument spread defined as $\pm 1\sigma$. Figure 14 shows these fields for the long-lived trace gases. For CH_4, the uncertainty is smallest in the tropical and mid-latitude MS and LS and larger towards the UTLS, the US and LM. The same has been found for other long-lived trace gases such as O_3, H_2O, N_2O, and HF. In contrast, the trace gases CFC-11 (or CCl_3F), CFC-12 (or CCl_2F_2), and SF_6 show the best agreement in the UTLS and larger deviations in the MS. Nearly all trace gases show larger deviations in the polar regions than at lower latitudes. Climatologies of CO, which is a trace gas with an intermediate lifetime, are characterized by large relative differences throughout most of the measurement range. The large CO differences in the annual zonal mean structure ($\pm 30\%$ in the LS) should be further addressed in forthcoming retrieval revisions. Overall, the $\pm 1\sigma$ multi-instrument spread has decreased for all long-lived trace gas species by up to 10% since SPARC (2017), except possibly CO, indicating an improved knowledge of the state of the atmosphere resulting from improvements in the retrievals of these species.

The agreement of the nitrogen species NO, NO_2, and HNO_3, as derived from the relative deviations between the climatologies, depends strongly on the atmospheric distribution of the respective gas with larger relative differences in regions of smaller mixing ratios (Figure 15). While NO and NO_x agree very well in the tropical and subtropical MS and US, NO_2 and HNO_3 have larger deviations in the US and show the best agreement in the tropical and mid-latitude MS and for HNO_3 also in the LS. All climatologies (except for HNO_3 and NO_y in the Northern Hemisphere) have considerably larger deviations in the polar regions, at least in part because of sampling issues and the large atmospheric variability that is less well sampled by the measurements going into the monthly mean climatologies (cf. Toohey et al, 2013). Finally, the NO_y climatologies show excellent agreement throughout most of the measurement range except for the polar latitude LM. Overall, the $\pm 1\sigma$ multi-instrument spread in the nitrogen species has decreased only slightly (by 5%) when compared to SPARC (2017).

The agreement between climatologies of chlorine compounds (Figure 16) and shorter-lived species depends strongly on the lifetime of the trace gas considered. HCl, which is longer-lived, exhibits very good agreement and the day-time climatologies of the shorter-lived ClO show good to reasonable agreement in the MS and US where mixing ratios are highest. HOCl, which is short-lived, shows mostly reasonable agreement in the US during night-time. HO_2 is available from a small number of

https://doi.org/10.5194/essd-2020-342
Preprint. Discussion started: 21 November 2020


Open Access Earth System Science Data Discussions

instruments only and is thus not included in the synopsis plots, although the HO_2 comparisons show promising results with mostly good agreement throughout the MS, US, and LM. The large deviations between the datasets of shorter-lived species stem partially from the difficulty of accounting for the strong diurnal cycles these trace gases exhibit. Scaling of the data to a common day- or nighttime using a chemical box model helped improve the comparisons in some cases. However, it remains a challenge to estimate how much these deviations are related to errors introduced by the scaling procedures and how much of the deviations correspond to direct measurement differences. Overall, the $\pm 1\sigma$ multi-instrument spread in the chlorine-containing species has improved for HCl, but has remained very similar for ClO and HOCl when compared to SPARC (2017).

6 Conclusions

This paper presents an overview and update of the evaluations performed within the WCRP SPARC Data Initiative as published in the SPARC Data Initiative Report (SPARC, 2017). To date, the SPARC Data Initiative represents the most comprehensive assessment of stratospheric composition measurements obtained from an international suite of limb sounders from the CSA, ESA, JAXA, NASA, SNSB and other national institutions. The SPARC Data Initiative thereby offers the first systematic assessment of the availability of chemical trace gas and aerosol observations from satellite limb sounders; provides these observations in a common and easy-to-handle data format (monthly zonal means); and presents a detailed comparison between these climatologies, importantly covering different generations of satellite limb instruments and contrasting the products of different agencies around the world. Here we extended the SPARC (2017) evaluations, which covered the period 1978-2010, out to the end of 2018, and used the most recent data versions that have become available in the meantime. New observations from OMPS-LP (on SUOMI NPP) and SAGE III/ISS are also added to the original list presented in SPARC (2017), which included LIMS, SAGE I/II, SAGE III/M3M, HALOE, UARS-MLS, POAM II/III, OSIRIS, SMR, MIPAS, GOMOS, SCIAMACHY, ACE-FTS, ACE-MAESTRO, Aura-MLS, HIRDLS, and SMILES.

The SPARC Data Initiative comparisons are based on vertically-resolved zonal monthly mean climatologies of 26 different atmospheric constituents, including most major long-lived trace gases (e.g., O_3, H_2O, N_2O, CH_4), medium-lived trace gases considered transport tracers (e.g., CO, HNO_3), shorter-lived trace gases important to stratospheric chemistry (e.g., BrO, ClO, NO_2), and aerosol. The observations considered have been compiled on a common latitude-pressure grid, covering the region from the upper troposphere to the lower mesosphere (300-0.1 hPa) with a latitudinal resolution of 5°. The monthly zonal mean time series are available from the Zenodo data archive (doi:10.5281/zenodo.4265393). A consistent file format was designed and is being used across the different composition measurements and instruments, so as to allow for easy handling by the user (see Popp et al. (submitted) for a discussion of the importance of a consistent data format in the provision of observational datasets).

The trace gas time series have then been evaluated by a common approach, comparing (single- or multiyear) annual or monthly mean climatologies derived from the monthly zonal mean fields, allowing for maximum overlap between different instruments. By evaluating monthly zonal mean averages, the SPARC Data Initiative has taken a 'climatological' approach to data validation (Hegglin et al., 2008; Hegglin et al., 2013; Tegtmeier et al., 2013; SPARC, 2017) in contrast to the more common

https://doi.org/10.5194/essd-2020-342
Preprint. Discussion started: 21 November 2020

approach of using coincident profile measurements. The climatological comparison method averages over multiple measurements, thereby reducing both instrument noise and geophysical variability from single profile comparisons, and offering a top-down instead of a bottom-up assessment of the (systematic) biases between different measurements. The climatological validation method has therewith the advantage that it is consistent for all instrument comparisons, avoids sensitivity to chosen limits defining coincident measurements, and produces generally larger sample sizes, which should in theory minimise the random sampling error. This climatological approach, however, has the disadvantage that climatological means can be biased due to non-uniformity of sampling. The extent to which the monthly and annual zonal mean climatologies are representative of the true mean has therefore been evaluated as part of the SPARC Data Initiative by investigating the impact of each instrument's sampling patterns on the climatologies as published in a separate paper by Toohey et al. (2013). This yields information on the potential sampling bias of each instrument's climatology and is particularly useful to users examining variability and trends, or comparisons with free-running models, though extra care should be taken when using data sets with sparse sampling as sampling biases can sometimes have a significant impact on the results of these analyses (Damadeo et al., 2018).

The findings of the trace gas climatology comparisons presented here are generally consistent with the results of previous validation efforts based on the classical validation approach using profile coincidences (where available). Instruments with sparser sampling show noisier zonal means. Profiles with wide averaging kernels do not resolve sharp structures such as those found across the tropopause region. However, the climatological approach yields generally more comprehensive information on measurement uncertainty in terms of latitude-pressure range covered. The comparisons of the climatologies have in many cases improved our knowledge of the systematic biases between the available data products. Although not shown here, the comparison results generally do not change substantially when changing the number of years going into a climatology or, in case of the longer-lived species, when calculating instrument differences for a month instead of a year. From this, it follows that the comparisons shown yield relatively robust conclusions on instrument/retrieval performance (see SPARC (2017) for detailed examples).

The conclusions from the SPARC Data Initiative highlight the use (or necessity) of observations from multiple instruments in order to characterize retrieval behaviour and overall observation quality as a function of latitude and pressure (or altitude). The small number of stratospheric limb sounders currently remaining in space (with most of them being long past their expected lifetime) and the even smaller number of planned future missions will likely have serious implications. These may impact not only our ability to perform a robust assessment of the quality of stratospheric composition measurements, but more importantly to derive stratospheric composition changes from these measurements, which are needed to better understand the state of the ozone layer that protects life on Earth and its response to climate change.

7 Data availability

All SPARC Data Initiative zonal monthly mean climatologies can be found in the Zenodo data archive (Hegglin et al., 2020, doi:10.5281/zenodo.4265393).

https://doi.org/10.5194/essd-2020-342
Preprint. Discussion started: 21 November 2020

Open Access Earth System Science Data Discussions

Author contributions. MIH and ST have designed and co-led the SPARC Data Initiative, performed all the evaluations, and written the text. The instrument PIs and their research staff have compiled the SPARC Data Initiative climatologies to their best current knowledge and contributed to the writing and interpretation of the evaluation results.

Competing interests. The authors declare no competing interests.

Acknowledgements. While the SPARC Data Initiative has been driven from a user perspective, the measurement partners have been critical to its success. These partners to whom the SPARC Data Initiative extends its thanks include the relevant instrument teams, the various space agencies (CSA, ESA, NASA, JAXA, SNSA, and other national agencies), and organizations such as CEOS-ACC and IGACO. We thank the World's Climate Research Programme (WCRP) for travel funding through the SPARC office to support our activity. The SPARC Data Initiative also thanks the International Space Science Institute in Bern (ISSI) who supported the activity through their ISSI International Team activity program and facilitated two successful team meetings in Bern. The work of MIH within the SPARC Data Initiative was funded by the CSA SSEP (9SCIGRA-29), the ESA STSE-SPIN (4000105291/12/I-NB), and more recently for water vapour evaluations the ESA (Contract No. 4000123554) via the Water_Vapour_cci project of ESA's Climate Change Initiative (CCI). The work from ST was funded from the WGL project TransBrom and the EU project SHIVA (FP7-ENV-2007-1-226224). Work at the Jet Propulsion Laboratory, California Institute of Technology, was funded by the National Aeronautics and Space Administration (NASA). The Atmospheric Chemistry Experiment is a Canadian-led mission mainly supported by the CSA. Development of the ACE-FTS climatologies was supported by grants from the Canadian Foundation for Climate and Atmospheric Sciences and the CSA. MIPAS data analysis and validation was supported by the German Federal Ministry for Economic Affairs and Energy under project number 50EE1547 and by the ESA CCI-O3 project. BF acknowledges support by the Spanish MCINN (ESP2017-87143-R) and EC FEDER funds. Development of SCIAMACHY and IUP-OMPS climatologies at the University of Bremen was supported by the German Research Foundation (GFD), the German Aerospace Agency (DLR), ESA, and the University and Municipality of Bremen. Work on HIRDLS was supported in the US by the National Aeronautics and Space Administration (NASA) and in the UK by the National Environmental Research Council (NERC). Development of Odin/SMR climatologies was supported by the Swedish National Space Agency (SNSA).

https://doi.org/10.5194/essd-2020-342
Preprint. Discussion started: 21 November 2020

References

Arosio, C., Rozanov, A., Malinina, E., Weber, M., and Burrows, J. P.: Merging of ozone profiles from SCIAMACHY, OMPS and SAGE II observations to study stratospheric ozone changes, Atmos. Meas. Tech., 12, 2423-2444, https://doi.org/10.5194/amt-12-2423-2019, 2019.

Arosio, C., Rozanov, A., Malinina, E., Eichmann, K.-U., von Clarmann, T., and Burrows, J. P.: Retrieval of ozone profiles from OMPS limb scattering observations, Atmos. Meas. Tech., 11, 2135-2149, https://doi.org/10.5194/amt-11-2135-2018, 2018.

Barath, F.T., Chavez, M.C., Cofield, R.E., Flower, D.A., Frerking, M.A., Gram, M.B., Harris, W.M., Holden, J.R., Jarnot, R.F., Kloezeman, W.G. and Klose, G.J.: The upper atmosphere research satellite microwave limb sounder instrument, J. Geophys. Res., 98(D6), pp.10751-10762, 1993.

Bates, D.R. and Nicolet, M.: The photochemistry of atmospheric water vapor, J. Geophys. Res., 55(3), pp.301-327, 1950.

Beer, R., Glavich, T. A., and Rider, D. M.: Tropospheric Emission Spectrometer for the Earth Observing System's Aura satellite, Appl. Opt., 40, 2356–2367, doi:10.1364/AO.40.002356, 2001.

Beer, R.: TES on the Aura mission: scientific objectives, measurements, and analysis overview, JIEEE Trans. Geosci. Remote Sens., 44(5), 1102–1105, doi:10.1109/TGRS.2005.863716, 2006.

Belmont Rivas, M., Veefkind, P., Boersma, F., Levelt, P., Eskes, H., and Gille, J.: Intercomparison of daytime stratospheric NO_2 satellite retrievals and model simulations, Atmos. Meas. Tech., 7, 2203-2225, doi 10.5194/amt-7-2203-2014, 2014.

Bernath, P.F., McElroy, C.T., Abrams, M.C., Boone, C.D., Butler, M., Camy-Peyret, C., Carleer, M., Clerbaux, C., Coheur, P.F., Colin, R. and DeCola, P.: Atmospheric chemistry experiment (ACE): mission overview, Geophys. Res. Lett., 32(15), 2005.

Bernath, P.F.: Atmospheric chemistry experiment (ACE): Analytical chemistry from orbit. TrAC Trends in Analytical Chemistry, 25(7), 647-654, 2006.

Bertaux, J.L., Kyrölä, E., Fussen, D., Hauchecorne, A., Dalaudier, F., Sofieva, V., Tamminen, J., Vanhellemont, F., Fanton d'Andon, O., Barrot, G. and Mangin, A., Blanot, L., Lebrun, J. C., Pérot, K., Fehr, T., Saavedra, L., Leppelmeier, G. W., and Fraisse, R.: Global ozone monitoring by occultation of stars: an overview of GOMOS measurements on ENVISAT, Atmos. Chem. Phys., 10(24), 12091-12148, 2010.

Bognar, K., Zhao, X., Strong, K., Boone, C.D., Bourassa, A.E., Degenstein, D.A., Drummond, J.R., Duff, A., Goutail, F., Griffin, D., Jeffery, P.S., Lutsch, E., Manney, G.L., McElroy, C.T., McLinden, C.A., Millán, L.F., Pazmino, A., Sioris, C.E., Walker, K.A., and Zou, J.: Updated validation of ACE and OSIRIS ozone and NO_2 measurements in the Arctic using ground-based instruments at Eureka, Canada, Journal of Quantitative Spectroscopy and Radiative Transfer, ISSN 0022-4073, https://doi.org/10.1016/j.jqsrt.2019.07.014, 2019.

Bourassa, A. E., D. A. Degenstein, B. J. Elash, and E. J. Llewellyn: Evolution of the stratospheric aerosol enhancement following the eruptions of Okmok and Kasatochi: Odin/OSIRIS measurements, J. Geophys. Res., 115, D00L03, doi:10.1029/2009JD013274, 2010.

Bourassa, A. E., Roth, C. Z., Zawada, D. J., Rieger, L. A., McLinden, C. A., and Degenstein, D.A., Drift-corrected Odin-OSIRIS ozone product: algorithm and updated stratospheric ozone trends, Atmos. Meas. Tech., 11, 1, 489-498, DOI: 10.5194/amt-11-489-2018, 2018.

Bovensmann, H., Burrows, J.P., Buchwitz, M., Frerick, J., Noël, S., Rozanov, V.V., Chance, K.V. and Goede, A.P.H.: SCIAMACHY: Mission objectives and measurement modes. J. Atmos. Sci., 56(2), 127-150, 1999.

Brohede, S., McLinden, C.A., Urban, J., Haley, C.S., Jonsson, A.I. and Murtagh, D.: Odin stratospheric proxy NO y measurements and climatology, Atmos. Chem. Phys., 8(19), 5731-5754, 2008.

Burrows, J.P., Hölzle, E., Goede, A.P.H., Visser, H. and Fricke, W.: SCIAMACHY–Scanning imaging absorption spectrometer for atmospheric chartography, Acta Astronautica, 35(7), 445-451, 1995.

https://doi.org/10.5194/essd-2020-342
Preprint. Discussion started: 21 November 2020

Choi, W.K. and Holton, J.R.: Transport of N_2O in the stratosphere related to the equatorial semiannual oscillation, J. Geophys. Res., 96(D12), 22543-22557, 1991.

Cionni, I., Eyring, V., Lamarque, J.F., Randel, W.J., Stevenson, D.S., Wu, F., Bodeker, G.E., Shepherd, T.G., Shindell, D.T. and Waugh, D.W.: Ozone database in support of CMIP5 simulations: results and corresponding radiative forcing, Atmos. Chem. Phys., 11(21), 11267-11292, 2011.

Conway, R.R., Stevens, M.H., Brown, C.M., Cardon, J.G., Zasadil, S.E. and Mount, G.H.: Middle atmosphere high resolution spectrograph investigation, J. Geophys. Res., 104(D13), 16327-16348, 1999.

Conway, R.R., Summers, M.E., Stevens, M.H., Cardon, J.G., Preusse, P. and Offermann, D.: Satellite observations of upper stratospheric and mesospheric OH: The HO_x dilemma, Geophys. Res. Lett., 27(17), 2613-2616, 2000.

Crutzen, P.J.: The influence of nitrogen oxides on the atmospheric ozone content, QJRMS, 96(408), 320-325, 1970.

Damadeo, R. P., Zawodny, J. M., Thomason, L. W., and Iyer, N.: SAGE version 7.0 algorithm: application to SAGE II, Atmos. Meas. Tech., 6, 3539-3561, https://doi.org/10.5194/amt-6-3539-2013, 2013.

Damadeo, R., Zawodny, J., Remsberg, E. and Walker, K., Pitfalls in Trend Analysis: Sampling, Drifts, and Orthogonality. EGUGA, 9978, 2018.

Daniel, J.S. and Solomon, S.: On the climate forcing of carbon monoxide, J. Geophys. Res., 103(D11), 13249-13260, 1998.

Davis, S.M., Rosenlof, K.H., Hassler, B., Hurst, D.F., Read, W.G., Vömel, H., Selkirk, H., Fujiwara, M. and Damadeo, R.: The Stratospheric Water and Ozone Satellite Homogenized (SWOOSH) database: A long-term database for climate studies, Earth system science data, 8(2), p.461, 2016.

Degenstein, D. A., Roth, C.Z., Bourassa, A.E., and Llewellyn, E.J., Limb scatter ozone retrieval from 10 to 60 km using a multiplicative algebraic reconstruction technique, Atmos. Chem. Phys., 9, 17, 6521-6529, 2009.

Dessler, A.E., Considine, D.B., Morris, G.A., Schoeberl, M.R., Russell, J.M., Roche, A.E., Kumer, J.B., Mergenthaler, J.L., Waters, J.W., Gille, J.C. and Yue, G.K.: Correlated observations of HCl and $ClONO_2$ from UARS and implications for stratospheric chlorine partitioning, Geophys. Res. Lett., 22(13), pp.1721-1724, 1995.

Douglass, A. R., Prather, M. J., Hall, T. M., Strahan, S. E., Rasch, P. J., Sparling, L. C., Coy, L., and Rodriguez, J. M.: Choosing meteorological input for the global modeling initiative assessment of high-speed aircraft, J. Geophys. Res., 104, 27 545-27 564, 1999.

Errera, Q., Ceccherini, S., Christophe, Y., Chabrillat, S., Hegglin, M.I., Lambert, A., Ménard, R., Raspollini, P., Skachko, S., van Weele, M. and Walker, K.A.: Harmonisation and diagnostics of MIPAS ESA CH_4 and N_2O profiles using data assimilation. Atmospheric Measurement Techniques, 9(12), pp.5895-5909. 2016.

Eyring, V., N. Butchart, D. W. Waugh, et al.: Assessment of temperature, trace species and ozone in chemistry-climate model simulations of the recent past, J. Geophys. Res., 111, D22308, doi:10.1029/2006JD007327, 2006.

Fahey, D.W., Gao, R.S., Carslaw, K.S., Kettleborough, J., Popp, P.J., Northway, M.J., Holecek, J.C., Ciciora, S.C., McLaughlin, R.J., Thompson, T.L. and Winkler, R.H.: The detection of large HNO3-containing particles in the winter Arctic stratosphere, Science, 291(5506), 1026-1031, 2001.

Fischer, H., Birk, M., Blom, C., Carli, B., Carlotti, M., Clarmann, T.V., Delbouille, L., Dudhia, A., Ehhalt, D., Endemann, M. and Flaud, J.M.: MIPAS: an instrument for atmospheric and climate research. Atmospheric Chemistry and Physics, 8(8), 2151-2188, 2008.

Fiorucci, I., Muscari, G., Froidevaux, L., and Santee, M. L.: Ground-based stratospheric O_3 and HNO_3 measurements at Thule, Greenland: an intercomparison with Aura MLS observations, Atmos. Meas. Tech., 6, 2441-2453, doi:10.5194/amt-6-2441-2013, 2013.

https://doi.org/10.5194/essd-2020-342
Preprint. Discussion started: 21 November 2020

Frisk, U., Hagström, M., Ala-Laurinaho, J., Andersson, S., Berges, J.C., Chabaud, J.P., Dahlgren, M., Emrich, A., Florén, H.G., Florin, G. and Fredrixon, M.: The Odin satellite-I. Radiometer design and test. Astronomy and Astrophysics, 402(3), L27-L34, 2003.

Froidevaux, L., Anderson, J., Wang, H.J., Fuller, R.A., Schwartz, M.J., Santee, M.L., Livesey, N.J., Pumphrey, H.C., Bernath, P.F., Russell III, J.M. and McCormick, M.P.: Global OZone Chemistry And Related trace gas Data records for the Stratosphere (GOZCARDS): methodology and sample results with a focus on HCl, H_2O, and O_3, Atmos. Chem. Phys., 15(18), pp.10471-10507, 2015.

Froidevaux, L., Kinnison, D.E., Wang, R., Anderson, J. and Fuller, R.A.: Evaluation of CESM1 (WACCM) free-running and specified dynamics atmospheric composition simulations using global multispecies satellite data records. Atmospheric Chemistry and Physics, 19(7), pp.4783-4821, 2019.

Funke, B., López-Puertas, M., Gil-López, S., von Clarmann, T., Stiller, G.P., Fischer, H. and Kellmann, S.: Downward transport of upper atmospheric NO_x into the polar stratosphere and lower mesosphere during the Antarctic 2003 and Arctic 2002/2003 winters, J. Geophys. Res., 110(D24), 2005a.

Funke, B., López-Puertas, M., Von Clarmann, T., Stiller, G.P., Fischer, H., Glatthor, N., Grabowski, U., Höpfner, M., Kellmann, S., Kiefer, M. and Linden, A., Retrieval of stratospheric NO_x from 5.3 and 6.2 mm nonlocal thermodynamic equilibrium emissions measured by Michelson Interferometer for Passive Atmospheric Sounding (MIPAS) on Envisat, J. Geophys. Res., 110, D09302, doi:10.1029/2004JD005225, 2005b.

Funke, B. and v. Clarmann, T.: How to average logarithmic retrievals?, Atmos. Meas. Techn., 5(4), 831-841, 2012.

Funke, B., López?Puertas, M., Stiller, G.P. and Von Clarmann, T.: Mesospheric and stratospheric NO_y produced by energetic particle precipitation during 2002-2012, J. Geophys. Res., 119(7), 4429-4446, 2014.

Garcia, R.R., Marsh, D.R., Kinnison, D.E., Boville, B.A. and Sassi, F.: Simulation of secular trends in the middle atmosphere, 1950-2003, J. Geophys. Res., 112(D9), 2007.

Gettelman, A., Hegglin, M.I., Son, S.W., Kim, J., Fujiwara, M., Birner, T., Kremser, S., Rex, M., Añel, J.A., Akiyoshi, H. and Austin, J.: Multi-model assessment of the upper troposphere and lower stratosphere: Tropics and trends, J. Geophys. Res., 115 (D00M08), doi:10.1029/2009JD013638, 2010.

Gilford, D. M., Solomon, S., and Portmann, R. W.: Radiative impacts of the 2011 abrupt drops in water vapor and ozone in the tropical tropopause layer. J. Climate, 29, 595-612, 2016.

Gille, J., and, Russell III, J.M.: The Limb Infrared Monitor of the Stratosphere (LIMS) experiment: Experiment description, performance, and results. J. Geophys. Res., 88, 5125-5140, 1984.

Gille, J., and Barnett, J.: The High-Resolution Dynamics Limb Sounder (HIRDLS), An instrument for the study of global change, The Use of EOS for Studies of Atmospheric Physics, J. Gille and G. Visconti (Eds.), North-Holland, 433- 450, 1992.

Gille, J., Grey, L., Cavanaugh, C., Coffey, M., Dean, V., Halvorson, C., Karol, S., Khosravi, R., Kinnison, D., Massie, S., Nardi, B., Rivas, M. B., , Smith, L., Torpy, B., Waterfall, A., and Wright, C.: HIRDLS data description and quality version 7, http://docserver.gesdisc.eosdis.nasa.gov/repository/Mission/HIRDLS/3.3_Product_Documentation/3.3.5_Product_Quality/HIRDLS-DQD_V7.pdf, 2012.

Gille, J., Karol,S., Kinnison, D., .Lamarque, J.-F, and Yudin, V: The role of midlatitude mixing barriers in creating the annual variation of total ozone in high northern latitudes, J. Geophys. Res. Atmos.,119, 9578-9595, doi:10.1002/2013JD021416, 2014.

Glaccum, W., Lucke, R.L., Bevilacqua, R.M., Shettle, E.P., Hornstein, J.S., Chen, D.T., Lumpe, J.D., Krigman, S.S., Debrestian, D.J., Fromm, M.D. and Dalaudier, F.: The polar ozone and aerosol measurement instrument. Journal of Geophysical Research: Atmospheres, 101(D9), pp.14479-14487, 1996.

https://doi.org/10.5194/essd-2020-342
Preprint. Discussion started: 21 November 2020

Gray, L.J. and J.A. Pyle: The semi-annual oscillation and equatorial tracer distributions, Q.J. Roy. Met. Soc., 112, 387-407, 1986.

Gunson, M.R., Abbas, M.M., Abrams, M.C., Allen, M., Brown, L.R., Brown, T.L., Chang, A.Y., Goldman, A., Irion, F.W., Lowes, L.L. and Mahieu, E.: The Atmospheric Trace Molecule Spectroscopy (ATMOS) experiment: Deployment on the ATLAS space shuttle missions, Geophysical Research Letters, 23(17), pp.2333-2336, 1996.

Harris, N. R. P., Hassler, B., Tummon, F., Bodeker, G. E., Hubert, D., Petropavlovskikh, I., Steinbrecht, W., Anderson, J., Bhartia, P. K., Boone, C. D., Bourassa, A., Davis, S. M., Degenstein, D., Delcloo, A., Frith, S. M., Froidevaux, L., Godin-Beekmann, S., Jones, N., Kurylo, M. J., Kyrölä, E., Laine, M., Leblanc, S. T., Lambert, J.-C., Liley, B., Mahieu, E., Maycock, A., de Maziére, M., Parrish, A., Querel, R., Rosenlof, K. H., Roth, C., Sioris, C., Staehelin, J., Stolarski, R. S., Stübi, R., Tamminen, J., Vigouroux, C., Walker, K. A., Wang, H. J., Wild, J., and Zawodny, J. M.: Past changes in the vertical distribution of ozone – Part 3: Analysis and interpretation of trends, Atmos. Chem. Phys., 15, 9965-9982, https://doi.org/10.5194/acp-15-9965-2015, 2015. acp-15-9965-2015, 2015.

Hartmann, G.K., Bevilacqua, R.M., Schwartz, P.R., Kämpfer, N., Künzi, K.F., Aellig, C.P., Berg, A., Boogaerts, W., Connor, B.J., Croskey, C.L. and Daehler, M.: Measurements of O_3, H_2O and ClO in the middle atmosphere using the millimeter?wave atmospheric sounder (MAS). Geophysical research letters, 23(17), pp.2313-2316, 1996.

Hegglin, M. I., Boone, C. D., Manney, G. L., Shepherd, T. G., Walker, K. A., Bernath, P. F., Daffer, W. H., Hoor, P., and Schiller, C.: Validation of ACE-FTS satellite data in the upper troposphere/lower stratosphere (UTLS) using non-coincident measurements, Atmos. Chem. Phys., 8, 1483-1499, https://doi.org/10.5194/acp-8-1483-2008, 2008.

Hegglin, M. I., Boone, C. D., Manney, G. L. , and Walker, K. A.: A global view of the extratropical tropopause transition layer from Atmospheric Chemistry Experiment Fourier Transform Spectrometer O_3, H_2O, and CO, J. Geophys. Res., 114, D00B11, doi:10.1029/2008JD009984, 2009.

Hegglin, M.I., Gettelman, A., Hoor, P., Krichevsky, R., Manney, G.L., Pan, L.L., Son, S.W., Stiller, G., Tilmes, S., Walker, K.A. and Eyring, V.: Multimodel assessment of the upper troposphere and lower stratosphere: Extratropics, J. Geophys. Res., 115 (D00M09), doi:10.1029/2009JD013884, 2010.

Hegglin, M.I., Tegtmeier, S., Anderson, J., Froidevaux, L., Fuller, R., Funke, B., Jones, A., Lingenfelser, G., Lumpe, J., Pendlebury, D. and Remsberg, E.: SPARC Data Initiative: Comparison of water vapor climatologies from international satellite limb sounders. Journal of Geophysical Research: Atmospheres, 118(20), pp.11-824, 2013.

Hegglin, M.I., Plummer, D.A., Shepherd, T.G., Scinocca, J.F., Anderson, J., Froidevaux, L., Funke, B., Hurst, D., Rozanov, A., Urban, J. and Von Clarmann, T., Vertical structure of stratospheric water vapour trends derived from merged satellite data, Nature Geoscience, 7(10), p.768, 2014.

Hegglin, M. I., Tegtmeier S., and the SPARC Data Initiative: The SPARC Data Initiative: Comparison of aerosol measurements from satellite limb sounders, in preparation.

Hegglin, M.I., Tegtmeier, S., Anderson, J., Bourassa, A.E., Brohede, S., Degenstein, D., Froidevaux, L., Funke, B., Gille, J., Kasai, Y., Kyrölä, E., Lumpe, J., Murtagh, D., Neu, J.L., Pérot, K., Remsberg, E., Rozanov, A., Toohey, M., von Clarmann, T., Walker, K.A., Wang, H.-J., Damadeo, R., Fuller, R., Lingenfelser, G., Roth, C., Ryan, N.J., Sioris, C., Smith, L., and Weigel, K.: SPARC Data Initiative monthly zonal mean composition measurements from stratospheric limb sounders (1978-2018). Zenodo, doi:10.5281/zenodo.4265393, 2020.

Holl, G., Walker, K. A., Conway, S., Saitoh, N., Boone, C. D., Strong, K., and Drummond, J. R.: Methane cross-validation between three Fourier transform spectrometers: SCISAT ACE-FTS, GOSAT TANSO-FTS, and ground-based FTS measurements in the Canadian high Arctic, Atmos. Meas. Tech., 9, 1961-1980, https://doi.org/10.5194/amt-9-1961-2016, 2016.

Holton, J. R., and W.-K. Choi, Transport circulation deduced from SAMS trace species data, J. Atmos. Sci. 45, 1929-1939, 1988.

https://doi.org/10.5194/essd-2020-342
Preprint. Discussion started: 21 November 2020

Hoor, P., Gurk, C., Brunner, D., Hegglin, M.I., Wernli, H. and Fischer, H.: Seasonality and extent of extratropical TST derived from in-situ CO measurements during SPURT. Atmospheric Chemistry and Physics, 4(5), 1427-1442, 2004.

Hubert, D., Lambert, J.-C., Verhoelst, T., Granville, J., Keppens, A., Baray, J.-L., Cortesi, U., Degenstein, D. A., Froidevaux, L., Godin-Beekmann, S., Hoppel, K. W., Kyrölä, E., Leblanc, T., Lichtenberg, G., McElroy, C. T., Murtagh, D., Nakane, H., Russell III, J. M., Salvador, J., Smit, H. G. J., Stebel, K., Steinbrecht, W., Strawbridge, K. B., Stübi, R., Swart, D. P. J., Taha, G., Thompson, A. M., Urban, J., van Gijsel, J. A. E., von der Gathen, P., Walker, K. A., Wolfram, E., and Zawodny, J. M.: Ground-based assessment of the bias and long-term stability of fourteen limb and occultation ozone profile data records, Atmos. Meas. Tech. Discuss., 8, 6661-6757, doi:10.5194/amtd-8-6661-2015, 2015.

Inness, A., et al.: The MACC reanalysis: an 8 yr dataset of atmospheric composition, Atmos. Chem. Phys., 13, 4073-4109, doi:10.5194/acp-13-4073-2013, 2013.

IPCC, Climate change 2013: the physical science basis: Working Group I contribution to the Fifth assessment report of the Intergovernmental Panel on Climate Change, Ed.: Stocker, T., Cambridge University Press, 2014.

Jaross, G., Bhartia, P. K., Chen, G., Kowitt, M., Haken, M., Chen,Z., Xu, P., Warner, J., and Kelly, T.: OMPS Limb Profiler instrument performance assessment, J. Geophys. Res.-Atmos., 119,4399-4412, 2014.

Jia, J., Rozanov, A., Ladstätter-Weissenmayer, A., and Burrows, J. P.: Global validation of SCIAMACHY limb ozone data (versions 2.9 and 3.0, IUP Bremen) using ozonesonde measurements, Atmos. Meas. Tech., 8, 3369-3383, 2015.

Johnson, D. G., K. W. Jucks, W. A. Traub, and K. V. Chance: Smithsonian stratospheric far-infrared Spectrometer and data reduction system, J. Geophys. Res., 100, 3091, 1995.

Jones, R.L., and Pyle, J.A.: Observations of CH_4 and N_2O by the Nimbus 7 SAMS: A comparison with in situ data and two?dimensional numerical model calculations, J. Geophys. Res., 89(D4), 5263-5279, 1984.

Jones, R.L., Pyle, J.A., Harries, J.E., Zavody, A.M., Russell III, J.M., and Gille, J.C.: The water vapour budget of the stratosphere studied using LIMS and SAMS satellite data, QJRMS, 112, doi:10.1256/smsqj.47411, 1986.

Jones, A., Qin, G., Strong, K., Walker, K.A., McLinden, C.A., Toohey, M., Kerzenmacher, T., Bernath, P.F. and Boone, C.D.: A global inventory of stratospheric NO_y from ACE?FTS, J. Geophys. Res., 116(D17), 2011.

Jucks, K.W., Johnson, D.G., Chance, K.V., Traub, W.A., Margitan, J.J., Osterman, G.B., Salawitch, R.J. and Sasano, Y.: Observations of OH, HO_2, H_2O, and O_3 in the upper stratosphere: Implications for HO_x photochemistry, Geophys. Res. Lett., 25(21), pp.3935-3938, 1998.

Kolonjari, F., Plummer, D. A., Walker, K. A., Bernath, P. F., Boone, C. D., Elkins, J. W., Hegglin, M. I. Manney, G. L. Montzka, S. A. Moore, F. L., Pendlebury, D., Ray, E.A., Rosenlof, K.H., and Stiller, G. P.: Assessing stratospheric transport in the CMAM30 simulations using ACE-FTS measurements, Atmos. Chem. Phys., 18, 6801-6828, https://doi.org/10.5194/acp-18-6801-2018, 2018.

Koo J.-H., Walker, K.A., Jones, A., Sheese P.E., Boone C.D., Bernath P.F., Manney, G.L.: Global climatology based on the ACE-FTS version 3.5 dataset: Addition of mesospheric levels and carbon-containing species in the UTLS, JQSRT, Volume 186, 2017, Pages 52-62, ISSN 0022-4073, https://doi.org/10.1016/j.jqsrt.2016.07.003, 2017.

Khosravi, M., Baron, P., Urban, J., Froidevaux, L., Jonsson, A. I., Kasai, Y., Kuribayashi, K., Mitsuda, C., Murtagh, D. P., Sagawa, H., Santee, M. L., Sato, T. O., Shiotani, M., Suzuki, M., von Clarmann, T., Walker, K. A., and Wang, S.: Diurnal variation of stratospheric and lower mesospheric HOCl, ClO and HO2 at the equator: comparison of 1-D model calculations with measurements by satellite instruments, Atmos. Chem. Phys., 13, 7587-7606, doi:10.5194/acp-13-7587-2013, 2013.

Khosrawi, F., Lossow, S., Stiller, G. P., Rosenlof, K. H., Urban, J., Burrows, J. P., Damadeo, R. P., Eriksson, P., García-Comas, M., Gille, J. C., Kasai, Y., Kiefer, M., Nedoluha, G. E., Noël, S., Raspollini, P., Read, W. G., Rozanov, A., Sioris, C. E., Walker, K. A., and Weigel,

https://doi.org/10.5194/essd-2020-342
Preprint. Discussion started: 21 November 2020

K.: The SPARC water vapour assessment II: comparison of stratospheric and lower mesospheric water vapour time series observed from satellites, Atmos. Meas. Tech., 11, 4435-4463, https://doi.org/10.5194/amt-11-4435-2018, 2018.

Kikuchi, K.I., Nishibori, T., Ochiai, S., Ozeki, H., Irimajiri, Y., Kasai, Y., Koike, M., Manabe, T., Mizukoshi, K., Murayama, Y. and Nagahama, T.: Overview and early results of the Superconducting Submillimeter-Wave Limb-Emission Sounder (SMILES). J. Geophys. Res., 115(D23), 2010.

Kremser, S., et al.: Stratospheric aerosol–Observations, processes, and impact on climate, Rev. Geophys., 54,doi:10.1002/2015RG000511, 2016.

Kreyling, D., Sagawa, H., Wohltmann, I., Lehmann, R., and Kasai, Y.: SMILES zonal and diurnal variation climatology of stratospheric and mesospheric trace gasses: O_3, HCl, HNO_3, ClO, BrO, HOCl, HO_2, and temperature, J. Geophys. Res., 118, 11,888-11,903, doi:10.1002/2012JD019420, 2013.

Kyrölä, E., Tamminen, J., Sofieva, V., Bertaux, J. L., Hauchecorne, A., Dalaudier, F., Fussen, D., Vanhellemont, F., Fanton d'Andon, O., Barrot, G., Guirlet, M., Fehr, T., and Saavedra de Miguel, L., GOMOS O_3, NO_2, and NO_3 observations in 2002-2008, Atmos. Chem. Phys., 10, 7723-7738, https://doi.org/10.5194/acp-10-7723-2010, 2010.

Lambert, A., Read, W. G., Livesey, N. J., Santee, M. L., Manney, G. L., Froidevaux, L., Wu, D. L., Schwartz, M. J., Pumphrey, H. C., Jimenez, C., Nedoluha, G. E., Cofield, R. E., Cuddy, D. T., Daffer, W. H., Drouin, B. J., Fuller, R. A., Jarnot, R. F., Knosp, B. W., Pickett, H. M., Perun, V. S., Snyder, W. V., Stek, P. C., Thurstans, R. P.,Wagner, P. A.,Waters, J.W., Jucks, K.W., Toon, G. C., Stachnik, R. A., Bernath, P. F., Boone, C. D., Walker, K. A., Urban, J., Murtagh, D., Elkins, J.W., and Atlas, E.: Validation of the Aura Microwave Limb Sounder stratospheric water vapour and nitrous oxide measurements, J. Geophys. Res., 112, D24S36, doi:10.1029/2007JD008724, 2007.

Laeng, A., Grabowski, U., Von Clarmann, T., Stiller, G., Glatthor, N., Höpfner, M., Kellmann, S., Kiefer, M., Linden, A., Lossow, S. and Sofieva, V., Petropavlovskikh, I., Hubert, D., Bathgate, T., Bernath, P., Boone, C. D., Clerbaux, C., Coheur, P., Damadeo, R., Degenstein, D., Fritz, S., Froideveaux, L., Gille, J., Hoppel, J., McHugh, M., Kasai, Y., Lumpe, J., Rapoe, N., Toon, G., Sano, T., Suzuki, M., Tamminen, J., Urban, J., Walker, K., Weber, M. and Zawodny, J., Validation of MIPAS IMK/IAA V5R_O3_224 ozone profiles, Atmos. Meas. Tech., 8(11), 4657-4670, doi:10.5194/amt-8-4657-2015, 2015.

Lelieveld, J.O.S., Crutzen, P.J. and Dentener, F.J.: Changing concentration, lifetime and climate forcing of atmospheric methane. Tellus B, 50(2), pp.128-150, 1998.

Livesey, N. J., Read, W. G., Froidevaux, L., Lambert, A., Manney, G. L., Pumphrey, H. C., Santee, M. L., Schwartz, M. J., Wang, S., Cofield, R. E., Cuddy, D. T., Fuller, R. A., Jarnot, R. F., Jiang, J. H., Knosp, B. W., Stek, P. C., Wagner, P. A., and Wu, D. L.: EOS MLS Version 3.3/3.4 Level 2 data quality and description document, Tech. rep., Jet Propulsion Laboratory, available at: http://mls.jpl.nasa.gov/ (last access: 15 December 2013), 2013.

Livesey, N. J., Read, W. G., Froidevaux, L., Lambert, A., Manney, G. L., Pumphrey, H. C., Santee, M. L., Schwartz, M. J., Wang, S., Cofield, R. E., Cuddy, D. T., Fuller, R. A., Jarnot, R. F., Jiang, J. H., Knosp, B. W., Stek, P. C., Wagner, P. A., and Wu, D. L.: EOS MLS Version 4.2x Level 2 data quality and description document, Tech. rep., Jet Propulsion Laboratory D-33509 Rev. D, available at: http://mls.jpl.nasa.gov/ (last access: 4 April 2019), 2018.

Lossow, S., Khosrawi, F., Kiefer, M., Walker, K. A., Bertaux, J.-L., Blanot, L., Russell, J. M., Remsberg, E. E., Gille, J. C., Sugita, T., Sioris, C. E., Dinelli, B. M., Papandrea, E., Raspollini, P., Garcia-Comas, M., Stiller, G. P., von Clarmann, T., Dudhia, A., Read, W. G., Nedoluha, G. E., Damadeo, R. P., Zawodny, J. M., Weigel, K., Rozanov, A., Azam, F., Bramstedt, K., Noël, S., Burrows, J. P., Sagawa, H., Kasai, Y., Urban, J., Eriksson, P., Murtagh, D. P., Hervig, M. E., Högberg, C., Hurst, D. F., and Rosenlof, K. H.: The SPARC water vapour assessment

https://doi.org/10.5194/essd-2020-342
Preprint. Discussion started: 21 November 2020

II: profile-to-profile comparisons of stratospheric and lower mesospheric water vapour data sets obtained from satellites, Atmos. Meas. Tech., 12, 2693-2732, https://doi.org/10.5194/amt-12-2693-2019, 2019.

Lucke, R.L., Korwan, D.R., Bevilacqua, R.M., Hornstein, J.S., Shettle, E.P., Chen, D.T., Daehler, M., Lumpe, J.D., Fromm, M.D. and Debrestian, D.: The Polar Ozone and Aerosol Measurement (POAM) III instrument and early validation results (Paper 1999JD900235), J. Geophys. Res., 104, 18-785, 1999.

Manney, G. L., Froidevaux, L., Waters, J. W., et al.: Chemical depletion of ozone in the Arctic lower stratosphere during winter 1992-1993, Nature, 370, 429-434, doi:10.1038/370429a0, 1994.

Manney, G.L., Daffer, W.H., Strawbridge, K.B., et al.: The high Arctic in extreme winters: vortex, temperature, and MLS and ACE-FTS trace gas evolution, Atmos. Chem. Phys., 8, 505-522, doi:10.5194/acp-8-505-2008, 2008.

McCormick, M.P., Zawodny, J.M., Veiga, R.E., Larsen, J., and Wang, P.-H.: An overview of SAGE-I and II ozone measurements, Planetary and Space Science, 37, 1567-86, doi:10.1016/0032-0633(89)90146-3, 1989.

McElroy, C.T., Nowlan, C.R., Drummond, J.R., Bernath, P.F., Barton, D.V., Dufour, D.G., Midwinter, C., Hall, R.B., Ogyu, A., Ullberg, A. and Wardle, D.I.: The ACE-MAESTRO instrument on SCISAT: description, performance, and preliminary results, Applied Optics, 46(20), 4341-4356, 2007.

McLinden, C.A., Haley, C.S., Lloyd, N.D., Hendrick, F., Rozanov, A., Sinnhuber, B.M., Goutail, F., Degenstein, D.A., Llewellyn, E.J., Sioris, C.E. and Van Roozendael, M.: Odin/OSIRIS observations of stratospheric BrO: Retrieval methodology, climatology, and inferred Bry, J. Geophys. Res., 115(D15), 2010.

Murtagh, D., Frisk, U., Merino, F., Ridal, M., Jonsson, A., Stegman, J., Witt, G., Eriksson, P., Jiménez, C., Megie, G. and Noë, J.D.L.: An overview of the Odin atmospheric mission, Canadian Journal of Physics, 80(4), 309-319, 2002.

Murtagh et al., https://odin.rss.chalmers.se/static/documents/DDS.pdf, 2018.

Neu, J.L., Hegglin, M.I., Tegtmeier, S., Bourassa, A., Degenstein, D., Froidevaux, L., Fuller, R., Funke, B., Gille, J., Jones, A. and Rozanov, A.: The SPARC Data Initiative: Comparison of upper troposphere/lower stratosphere ozone climatologies from limb-viewing instruments and the nadir-viewing Tropospheric Emission Spectrometer, J. Geophys. Res., 119(11), 6971-6990, 2014.

Plieninger, J., Laeng, A., Lossow, S., von Clarmann, T., Stiller, G. P., Kellmann, S., Linden, A., Kiefer, M., Walker, K. A., Noël, S., Hervig, M. E., McHugh, M., Lambert, A., Urban, J., Elkins, J. W., and Murtagh, D.: Validation of revised methane and nitrous oxide profiles from MIPAS-ENVISAT, Atmos. Meas. Tech., 9, 765-779, https://doi.org/10.5194/amt-9-765-2016, 2016.

Popp, T., Hegglin, M.I., Hollmann R., et al., Consistency of satellite climate data records for Earth system monitoring, BAMS, submitted.

Pumphrey, H. C.: Validation of a new prototype water vapor retrieval for UARS MLS, J. Geophys. Res, 104, 9399-9412, doi:10.1029/1998JD200113, 1999.

Pumphrey, H.C., Filipiak, M.J., Livesey, N.J., Schwartz, M.J., Boone, C., Walker, K.A., Bernath, P., Ricaud, P., Barret, B., Clerbaux, C. and Jarnot, R.F.: Validation of middle-atmosphere carbon monoxide retrievals from the Microwave Limb Sounder on Aura, J. Geophys. Res., 112(D24), 2007.

Randel, W.J., Wu, F., Russell III, J.M., Roche, A. and Waters, J.W.: Seasonal cycles and QBO variations in stratospheric CH_4 and H_2O observed in UARS HALOE data, J. Atmos. Sci., 55(2), 163-185, 1998.

Randel, W.J., Stolarski, R.S., Cunnold, D.M., Logan, J.A., Newchurch, M.J., and Zawodny, J.M.: Trends in the vertical distribution of ozone, Science, 285, 1689-1692,1999.

Randel, W. J., F. Wu, G. Nedoluha, H. Vomel and P. Forster: Decreases in stratospheric water vapour since 2001: Links to changes in the tropical tropopause and the Brewer-Dobson circulation, J. Geophys. Res., 111, D12312, doi:10.1029/2005JD006744, 2006.

https://doi.org/10.5194/essd-2020-342
Preprint. Discussion started: 21 November 2020

Randel, W. J., Park, M., Emmons, L., Kinnison, D., Bernath, P., Walker, K., Boone, C., and Pumphrey, H.: Asian monsoon transport of pollution to the stratosphere,Science, 328, 611, doi:10.1126/science.1182274, 2010.

Randel, W. J., and Thompson, A.M.: Interannual variability and trends in tropical ozone derived from SAGE II satellite data and SHADOZ ozonesondes, J. Geophys. Res., 116, D07303, doi:10.1029/2010JD015195, 2011.

Ravishankara, A. R., John S. Daniel, and Robert W. Portmann, Nitrous oxide (N2O): the dominant ozone-depleting substance emitted in the 21st century, Science 326, 5949:123-125, 2009.

Read, W. G., Lambert, A., Bacmeister, J., Cofield, R. E., Christensen, L. E., Cuddy, D. T., Daffer, W. H., Drouin, B. J., Fetzer, E., Froidevaux, L., Fuller, R., Herman, R., Jarnot, R. F., Jiang, J. H., Jiang, Y. B., Kelly, K., Knosp, B. W., Kovalenko, L. J., Livesey, N. J., Liu, H.-C., Manney, G. L., Pickett, H. M., Pumphrey, H. C., Rosenlof, K. H., Sabounchi, X., Santee, M. L., Schwartz, M. J., Snyder, W. V., Stek, P. C., Su, H., Takacs, L. L., Thurstans, R. P., Voemel, H., Wagner, P. A., Waters, J. W., Webster, C. R., Weinstock, E. M., and Wu, D. L.: Aura Microwave Limb Sounder upper tropospheric and lower stratospheric H2O and relative humidity with respect to ice validation, J. Geophys. Res., 112, D24S35, doi:10.1029/2007JD008752, 2007.

Reber, C.A., Trevathan, C.E., McNeal, R.J. and Luther, M.R.: The upper atmosphere research satellite (UARS) mission, J. Geophys. Res., 98(D6), 10643-10647, 1993.

Roche, A. E., et al.: The Cryogenic Limb Array Etalon Spectrometer (CLAES) on UARS: Experiment description and performance, J. Geophys. Res., 98, 10763–10775, doi:10.1029/93JD00800, 1993.

Rousseeuw, P.J. and Croux, C.: Alternatives to the median absolute deviation. Journal of the American Statistical association, 88(424), 1273-1283, 1993.

Rong, P. P., Russell III, J. M., Marshall B. T., Siskind D. E., Hervig M. E., Gordley L. L., Bernath, P. F., and Walker, K. A.: Version 1.3 AIM SOFIE measured methane (CH4): Validation and seasonal climatology, J. Geophys. Res. Atmos.,121,13,158-13,179, doi:10.1002/2016JD025415, 2016.

Russell III, J.M., Gordley, L.L., Park, J.H., Drayson, S.R., Hesketh, W.D., Cicerone, R.J., Tuck, A.F., Frederick, J.E., Harries, J.E. and Crutzen, P.J.: The halogen occultation experiment, J. Geophys. Res., 98(D6), 10777-10797, 1993.

Ruth, S., Kennaugh, R., Gray, L.J. and Russell III, J.M.: Seasonal, semiannual, and interannual variability seen in measurements of methane made by the UARS Halogen Occultation Experiment, J. Geophys. Res., 102(D13), 16189-16199, 1997.

Salawitch, R. J., D. K. Weisenstein, L. J. Kovalenko, C. E. Sioris, P. O. Wennberg, K. Chance, M. K. W. Ko, and C. A. McLinden: Sensitivity of ozone to bromine in the lower stratosphere, Geophys. Res. Lett., 32, L05811, doi:10.1029/2004GL021504, 2005.

Santee, M. L., Lambert, A., Read, W. G., Livesey, N. J., Cofield, R. E., Cuddy, D. T., Daffer, W. H., Drouin, B. J., Froidevaux, L., Fuller, R. A., Jarnot, R. F., Knosp, B. W., Manney, G. L., Perun, V. S., Snyder, W. V., Stek, P. C., Thurstans, R. P., Wagner, P. A., Waters, J. W., Muscari, G., de Zafra, R. L., Dibb, J. E., Fahey, D. W., Popp, P. J., Marcy, T. P., Jucks, K. W., Toon, G. C., Stachnik, R. A., Bernath, P. F., Boone, C. D., Walker, K. A., Urban, J., and Murtagh, D.: Validation of the Aura Microwave Limb Sounder HNO_3 measurements, J. Geophys. Res., 112, D24S40, doi:10.1029/2007JD008, 2007.

Santee, M. L., I. A. MacKenzie, G. L. Manney, M. P. Chipperfield, P. F. Bernath, K. A. Walker, C. D. Boone, L. Froidevaux, N. J. Livesey, and J. W. Waters, A study of stratospheric chlorine partitioning based on new satellite measurements and modeling, J. Geophys. Res., 113, D12307, doi:10.1029/2007JD009057, 2008.

Sasano, Y., Suzuki, M., Yokota, T. and Kanzawa, H.: Improved Limb Atmospheric Spectrometer (ILAS) for stratospheric ozone layer measurements by solar occultation technique. Geophys. Res. Lett., 26(2), 197-200, 1999.

https://doi.org/10.5194/essd-2020-342
Preprint. Discussion started: 21 November 2020

Schmidt, A., Mills, M. J., Ghan, S., Gregory, J. M., Allan, R. P., Andrews, T., Bardeen, C. G., Conley, A., Forster, P. M., Gettelman, A. and Portmann, R. W.: Volcanic Radiative Forcing From 1979 to 2015, J. Geophys. Res. Atmos., 123(22), 12,491-12,508, doi:10.1029/2018JD028776, 2018.

Sheese PE, Boone CD, Walker KA, Detecting physically unrealistic outliers in ACE-FTS atmospheric measurements, Atmos. Meas. Tech., 8:741-50, http://dx.doi.org/10.5194/amt-8-741-2015, 2015.

Sheese, P. E., Walker, K. A., Boone, C. D., McLinden, C. A., Bernath, P. F., Bourassa, A. E., Burrows, J. P., Degenstein, D. A., Funke, B., Fussen, D., Manney, G. L., McElroy, C. T., Murtagh, D., Randall, C. E., Raspollini, P., Rozanov, A., Russell III, J. M., Suzuki, M., Shiotani, M., Urban, J., von Clarmann, T., and Zawodny, J. M.: Validation of ACE-FTS version 3.5 NOy species profiles using correlative satellite measurements, Atmos. Meas. Tech., 9, 5781-5810, https://doi.org/10.5194/amt-9-5781-2016, 2016.

Sheese, P. E., Walker, K. A., Boone, C. D., Bernath, P. F., Froidevaux, L., Funke, B., Raspollini, P., and von Clarmann, T.: ACE-FTS ozone, water vapour, nitrous oxide, nitric acid, and carbon monoxide profile comparisons with MIPAS and MLS, J. Quant. Spectrosc. Ra., 186, 63-80, https://doi.org/10.1016/j.jqsrt.2016.06.026, 2017.

Shepherd, T.G., Plummer, D.A., Scinocca, J.F., Hegglin, M.I., Fioletov, V.E., Reader, M.C., Remsberg, E., Von Clarmann, T. and Wang, H.J.: Reconciliation of halogen-induced ozone loss with the total-column ozone record, Nature Geoscience, 7(6), p.443, 2014.

Sofieva, V. F., Ialongo, I., Hakkarainen, J., Kyrölä, E., Tamminen, J., Laine, M., Hubert, D., Hauchecorne, A., Dalaudier, F., Bertaux, J.-L., Fussen, D., Blanot, L., Barrot, G., and Dehn, A.: Improved GOMOS/Envisat ozone retrievals in the upper troposphere and the lower stratosphere, Atmos. Meas. Tech., 10, 231-246, https://doi.org/10.5194/amt-10-231-2017, 2017.

Solomon, S., Crutzen, P.J. and Roble, R.G.: Photochemical coupling between the thermosphere and the lower atmosphere: 1. Odd nitrogen from 50 to 120 km, J. Geophys. Res., 87(C9), 7206-7220, 1982.

Solomon, S., Garcia, R.R., Olivero, J.J., Bevilacqua, R.M., Schwartz, P.R., Clancy, R.T. and Muhleman, D.O.: Photochemistry and transport of carbon monoxide in the middle atmosphere, J. Atmos. Sci., 42(10), 1072-1083, 1985.

Solomon, S., Kiehl, J.T., Garcia, R.R. and Grose, W.: Tracer transport by the diabatic circulation deduced from satellite observations. Journal of the atmospheric sciences, 43(15), pp.1603-1617, 1986.

Solomon, S., Rosenlof, K.H., Portmann, R.W., Daniel, J.S., Davis, S.M., Sanford, T.J. and Plattner, G.K., Contributions of stratospheric water vapor to decadal changes in the rate of global warming. Science, 327(5970), pp.1219-1223, 2010.

Solomon, S., Daniel, J.S., Neely, R.R., Vernier, J.P., Dutton, E.G. and Thomason, L.W.: The persistently variable 'background' stratospheric aerosol layer and global climate change. Science, 333(6044), pp.866-870, 2011.

SPARC: Upper Tropospheric and Stratospheric Water Vapour, D. Kley, J. M. Russell III, and C. Phillips (Eds.), *SPARC Report No. 2*, WCRP-113, WMO/TD - No. 1043, available at www.sparc-climate.org/publications/sparc-reports/, 2000.

SPARC: SPARC Assessment of Stratospheric Aerosol Properties (ASAP), L. Thomason and Th. Peter (Eds.), *SPARC Report No. 4*, WCRP-124, WMO/TD - No. 1295, available at www.sparc-climate.org/publications/sparc-reports/, 2006.

SPARC: SPARC CCMVal Report on the Evaluation of Chemistry-Climate Models, V. Eyring, T. Shepherd and D. Waugh (Eds.), *SPARC Report No. 5*, WCRP-30/2010, WMO/TD - No. 40, available at www.sparc-climate.org/publications/sparc-reports/, 2010.

SPARC: The SPARC Data Initiative: Assessment of stratospheric trace gas and aerosol climatologies from satellite limb sounders. By M. I. Hegglin and S. Tegtmeier (eds.), SPARC Report No. 8, WCRP-5/2017, available at www.sparc-climate.org/publications/sparc-reports/, 2017.

https://doi.org/10.5194/essd-2020-342
Preprint. Discussion started: 21 November 2020

SPARC: SPARC/IO3C/GAW Report on Long-term Ozone Trends and Uncertainties in the Stratosphere. I. Petropavlovskikh, S. Godin-Beekmann, D. Hubert, R. Damadeo, B. Hassler, V. Sofieva (Eds.), SPARC Report No. 9, GAW Report No. 241, WCRP-17/2018, doi: 10.17874/f899e57a20b, available at www.sparc-climate.org/publications/sparc-reports/, 2019.

Stiller, G.P., von Clarmann, T., Haenel, F., Funke, B., Glatthor, N., Grabowski, U., Kellmann, S., Kiefer, M., Linden, A., Lossow, S. and López-Puertas, M.: Observed temporal evolution of global mean age of stratospheric air for the 2002 to 2010 period, Atmos. Chem. Phys., 12(7), pp.3311-3331, 2012.

Strahan, S. E., et al.: Using transport diagnostics to understand chemistry climate model ozone simulations, J. Geophys. Res., 116, D17302, doi:10.1029/2010JD015360, 2011.

Taylor, F. W.: Infrared remote sensing of the middle atmosphere from satellites: The stratospheric and mesospheric sounder experiment 1978-1983, Surveys in Geophysics, 9, 123-148, doi:10.1007/BF01904119, 1987.

Taylor, F. W., et al.: Remote sensing of atmospheric structure and composition by pressure modulator radiometry from space: The ISAMS experiment on UARS, J. Geophys. Res., 98, 10799-10814, doi:10.1029/92JD03029, 1993.

Tegtmeier, S., Hegglin, M.I., Anderson, J., Bourassa, A., Brohede, S., Degenstein, D., Froidevaux, L., Fuller, R., Funke, B., Gille, J. and Jones, A.: SPARC Data Initiative: A comparison of ozone climatologies from international satellite limb sounders. J. Geophys. Res., 118(21), pp.12-229, 2013.

Tegtmeier, S., M.I. Hegglin, and the SPARC Data Initiative Team: Evaluation of chemistry-climate models using SPARC Data Initiative climatologies, in preparation.

Thomason, L.W. et al.: A revised water vapor product for the Stratospheric Aerosol and Gas Experiment (SAGE) II version 6.2 data set. J. Geophys. Res. 109, D06312, 2004.

Thomason, L.W., Moore, J.R., Pitts, M.C., Zawodny, J.M. and Chiou, E.W.: An evaluation of the SAGE III version 4 aerosol extinction coefficient and water vapor data products, *Atmos. Chem. Phys.*, 10(5), pp.2159-2173., 2010.

Thomason, L.W., Ernest, N., Millan, L., Rieger, L., Bourassa, A., Vernier, J.P., Manney, G., Luo, B., Arfeuille, F. and Peter, T.: A global space-based stratospheric aerosol climatology: 1979-2016, *Earth Syst. Sc. Data*, 10(1), pp.469-492, 2018.

Toohey, M., Hegglin, M.I., Tegtmeier, S., Anderson, J., Añel, J.A., Bourassa, A., Brohede, S., Degenstein, D., Froidevaux, L., Fuller, R. and Funke, B.: Characterizing sampling biases in the trace gas climatologies of the SPARC Data Initiative. J. Geophys. Res., 118(20), pp.11-847, 2013.

Toohey, M. and von Clarmann, T.: Climatologies from satellite measurements: the impact of orbital sampling on the standard error of the mean, Atmos. Meas. Techn., 6(4), 937-948, 2013.

Tung, K.K.: On the two-dimensional transport of stratospheric trace gases in isentropic coordinates, J. Atmos. Sci., 39(10), 2330-2355, 1982.

Vömel, H., David, D.E. and Smith, K.: Accuracy of tropospheric and stratospheric water vapor measurements by the cryogenic frost point hygrometer: Instrumental details and observations, J. Geophys. Res., 112(D8), 2007.

von Clarmann, T., Höpfner, M., Funke, B., López-Puertas, M., Dudhia, A., Jay, V., Schreier, F., Ridolfi, M., Ceccherini, S., Kerridge, B.J. and Reburn, J.: Modelling of atmospheric mid-infrared radiative transfer: the AMIL2DA algorithm intercomparison experiment, Journal of Quantitative Spectroscopy and Radiative Transfer, 78(3-4), 381-407, 2003.

von Clarmann, T., Höpfner, M., Kellmann, S., Linden, A., Chauhan, S., Funke, B., Grabowski, U., Glatthor, N., Kiefer, M., Schieferdecker, T. and Stiller, G.P.: Retrieval of temperature, H_2O, O_3, HNO_3, CH_4, N_2O, $ClONO_2$ and ClO from MIPAS reduced resolution nominal mode limb emission measurements, Atmos. Meas. Tech, 2(1), pp.159-175, 2009.

https://doi.org/10.5194/essd-2020-342
Preprint. Discussion started: 21 November 2020

von Clarmann, T., Degenstein, D. A., Livesey, N. J., Bender, S., Braverman, A., Butz, A., Compernolle, S., Damadeo, R., Dueck, S., Eriksson, P., Funke, B., Johnson, M. C., Kasai, Y., Keppens, Y., Kleinert, A., Kramarova, N. A., Laeng, A., Payne, V. H., Rozanov, A., Sato, T. O., Schneider, M., Sheese, P., Sofieva, V., Stiller, G. P., von Savigny, C., and Zawada, D., Estimating and Reporting Uncertainties in Remotely Sensed Atmospheric Composition and Temperature, Atmos. Meas. Tech., https://doi.org/10.5194/amt-2019-350, 2019.

Wang, H.J., Cunnold, D.M., Thomason, L.W., Zawodny, J.M., and Bodeker, G.E.: Assessment of SAGE version 6.1 ozone data quality, *J. Geophys. Res.*, 107(D23), doi: 10.1029/2002JD002418, 2002.

Wang, H.-J., Cunnold, D. M., Trepte, C., Thomason, L. W., Zawodny J. M.: SAGE III solar ozone measurements: Initial results, *Geophys. Res. Lett.*, 33, L03805, doi:10.1029/2005GL025099, 2006.

Wang, H.J., R. Damadeo, D. Flittner, N. Kramarova, G. Taha, S. Davis , A. M. Thompson, S. Strahan, Y. Wang, L. Froidevaux, D. Degenstein, A. Bourassa, W. Steinbrecht , K. A. Walker: Validation of SAGE III/ISS solar ozone data with correlative satellite and ground based measurements, in preparation.

Waters, J.W., Read, W. G., Froidevaux, L., Jarnot, R. F., Cofield, R. E., Flower, D. A., Lau, G. K., Pickett, H. M., Santee, M. L., Wu, D. L., Boyles, M. A., Burke, J. R., Lay, R. R., Loo, M. S., Livesey, N. J., Lungu, T. A., Manney, G. L., Nakamura, L., Perun, V. S., Ridenoure, B. P., Shippony, Z., Siegel, P. H., Thurstans, R. P., Harwood, R. S., and Filipiak,M. J.: The UARS and EOS Microwave Limb Sounder Experiments, J. Atmos. Sci., 56, 2, 194-218, doi:10.1175/1520-0469(1999), 1999.

Waters, J.W., Froidevaux, L., Harwood, R.S., Jarnot, R.F., Pickett, H.M., Read, W.G., Siegel, P.H., Cofield, R.E., Filipiak, M.J., Flower, D.A., Holden, J.R., et al.: The earth observing system microwave limb sounder (EOS MLS) on the Aura satellite, IEEE Transactions on Geoscience and Remote Sensing, 44(5), pp.1075-1092, 2006.

Waugh, D.W., and Eyring, V.: Quantitative performance metrics for stratospheric-resolving chemistry-climate models. Atmospheric Chemistry and Physics, 8(18), 5699-5713, 2008.

Waymark, C., Walker, K.A., Boone, C.D., and Bernath, P.F.: ACE-FTS version 3.0 data set: validation and data processing update. Ann Geophys, 56, http://dx.doi.org/10.4401/ag-6339, 2013.

Weigel, K., Rozanov, A., Azam, F., Bramstedt, K., Damadeo, R., Eichmann, K.-U., Gebhardt, C., Hurst, D., Kraemer, M., Lossow, S., Read, W., Spelten, N., Stiller, G. P., Walker, K. A., Weber, M., Bovensmann, H., and Burrows, J. P.: UTLS water vapour from SCIAMACHY limb measurementsV3.01 (2002-2012), Atmos. Meas. Tech., 9, 133-158, https://doi.org/10.5194/amt-9-133-2016, 2016.

Weaver, D., Strong, K., Walker, K. A., Sioris, C., Schneider, M., McElroy, C. T., Vömel, H., Sommer, M., Weigel, K., Rozanov, A., Burrows, J. P., Read, W. G., Fishbein, E., and Stiller, G.: Comparison of ground-based and satellite measurements of water vapour vertical profiles over Ellesmere Island, Nunavut, Atmos. Meas. Tech., 12, 4039-4063, https://doi.org/10.5194/amt-12-4039-2019, 2019.

WMO (World Meteorological Organization), Scientific Assessment of Ozone Depletion: 2010, Global Ozone Research and Monitoring Project-Report No. 52, 516 pp., Geneva, Switzerland, 2011.

WMO (World Meteorological Organization), Scientific Assessment of Ozone Depletion: 2014, Global Ozone Research and Monitoring Project-Report No. 55, 416 pp., Geneva, Switzerland, 2014.

WMO (World Meteorological Organization), Scientific Assessment of Ozone Depletion: 2018, Global Ozone Research and Monitoring Project-Report No. 58, 588 pp., Geneva, Switzerland, 2018.

Zawada, D. J., Rieger, L. A., Bourassa, A. E., and Degenstein, D. A.: Tomographic retrievals of ozone with the OMPS Limb Profiler: algorithm description and preliminary results, Atmos. Meas. Tech., 11, 2375-2393, https://doi.org/10.5194/amt-11-2375-2018, 2018.

https://doi.org/10.5194/essd-2020-342
Preprint. Discussion started: 21 November 2020

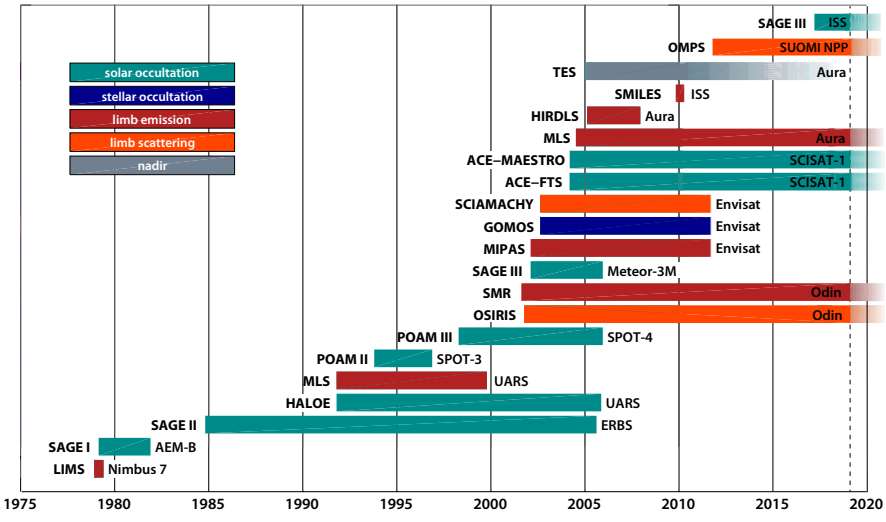

Figure 1. Mission lifetime of limb satellite instruments (left hand side of bars) evaluated within the SPARC Data Initiative. Also indicated are the mission platforms (right hand side of bars). The colors classify the instruments according to their observation geometry. Note that the SPARC Data Initiative Report (SPARC, 2017) only evaluated monthly zonal mean climatologies up to 2010. Here, we evaluate the climatologies out to 2018. Seven satellite limb sounders remain currently in space: Aura-MLS, ACE-FTS, ACE-MAESTRO, Odin/SMR, OSIRIS, OMPS, and SAGE III/ISS, of which the first five long passed their expected lifetimes.

https://doi.org/10.5194/essd-2020-342
Preprint. Discussion started: 21 November 2020

Open Access Earth System Science Data Discussions

SPARC Data Initiative	O_3	H_2O	CH_4	N_2O	CCl_3F	CCl_2F_2	CO	HF	SF_6	NO	NO_2	NO_x	HNO_3	HNO_4	N_2O_5	$ClONO_2$	NO_y	HCl	ClO	HOCl	BrO	OH	HO_2	CH_2O	CH_3CN	aerosol
ACE-FTS	x	x	x	x	x	x	x	x	x	x	x	x	x	x	x	x	x	x						x		
Aura-MLS	x	x		x			x						x					x	x	x		x	x			
GOMOS	x										x															x
HALOE	x	x	x					x		x	x	x						x								
HIRDLS	x	x			x	x					x		x													
LIMS	x	x									x		x													
MAESTRO	x	x																								
MIPAS	x	x	x	x	x	x	x		x	x	x	x	x	x	x	x	x		x	x				x		
OSIRIS	x										x	x_d					x_m				x					x
POAM II	x										x															x
POAM III	x	x									x															x
SAGE I	x																									
SAGE II	x	x									x															x
SAGE III	x	x									x															x
SCIAMACHY	x	x									x	x_d									x					x
SMILES	x												x					x	x	x	x		x		x	
Odin/SMR	x	x		x			x			x			x				x_m		x				x_{lc}			
UARS-MLS	x	x											x													
OMPS	x																									x
SAGE III ISS	x	x																								x
TES	x_t																									

x available climatology
x_t used in UTLS comparisons only
x_d derived with help of a chemical box model
x_m merged and derived from OSIRIS NO_2 and Odin/SMR HNO_3 data
x_{lc} with limited coverage

Figure 2. Monthly mean climatologies of atmospheric constituents available from Zenodo (doi:10.5281/zenodo.4265393), listed by instrument. Blue indicates the participating limb sounders, grey the nadir sounder Aura-TES, which was solely used for comparison in the UTLS applying TES averaging kernels to the limb sounders (see Neu et al. (2014)). Purple crosses indicate climatologies that are based on a newer data version than the ones used in SPARC (2017), pink crosses indicate climatologies newly added to the evaluations.

https://doi.org/10.5194/essd-2020-342
Preprint. Discussion started: 21 November 2020

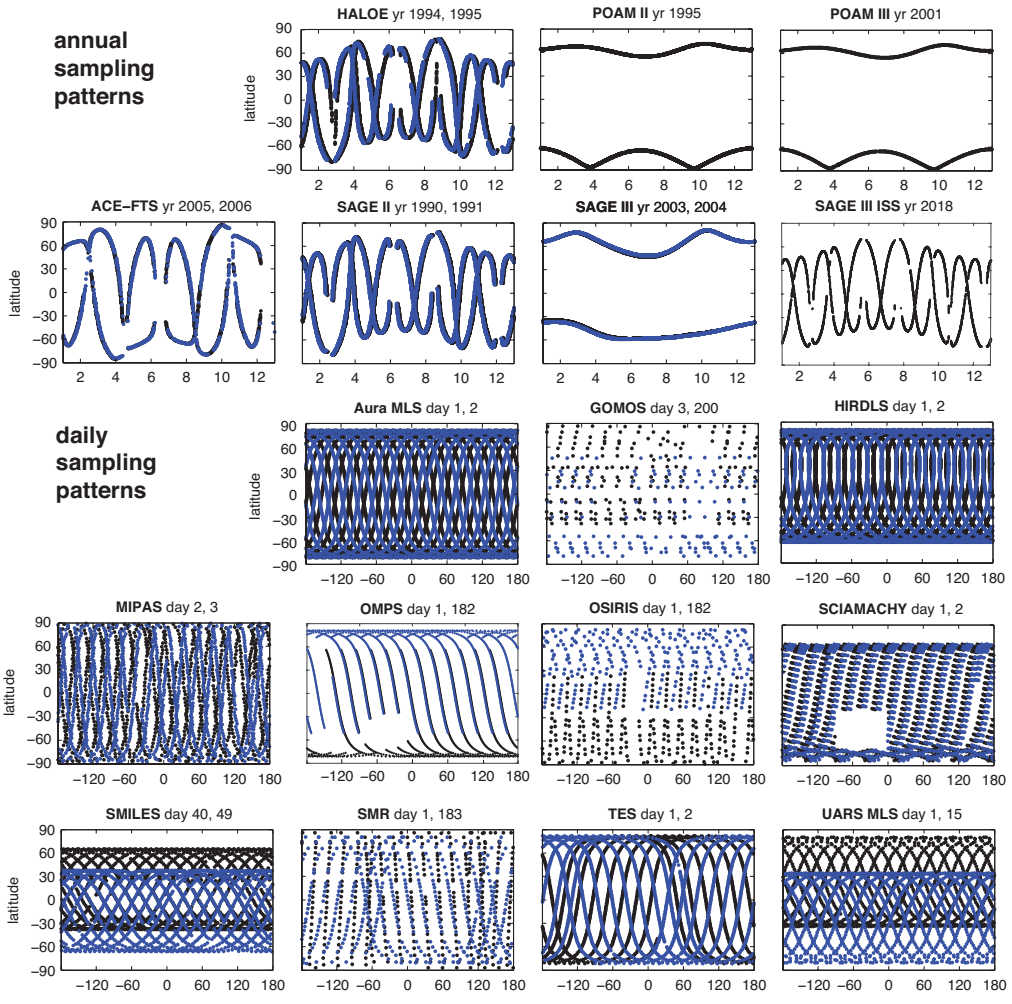

Figure 3. Representative sampling patterns for the instruments are shown in time-latitude space for solar occultation sounders (upper two rows) and in longitude-latitude space for emission/scattering and stellar occultation sounders (lower three rows). Different years or days are chosen to give a sense of change in the observed sampling patterns over time. See also Figure 1 in Toohey et al. (2013) for the resulting measurement density in latitude-time space for the original SPARC Data Initiative instruments.

https://doi.org/10.5194/essd-2020-342
Preprint. Discussion started: 21 November 2020

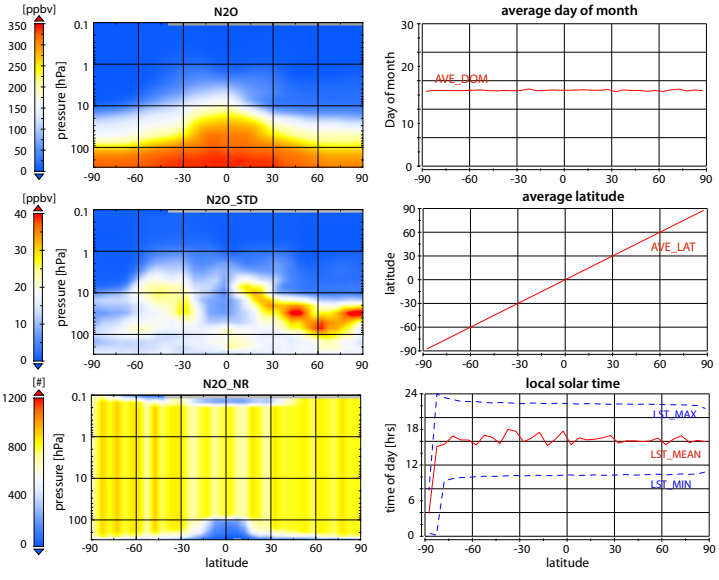

Figure 4. Variables in a typical climatology file that follows SPARC Data Initiative standards are N_2O, N_2O standard deviation (N_2O_STD), N_2O number, average day of month, average latitude, and minimum, mean, and maximum local solar time (LST_MIN, LST_MAX, andLST_MEAN). This example shows April data from the 2018 MIPAS climatology file.

https://doi.org/10.5194/essd-2020-342
Preprint. Discussion started: 21 November 2020

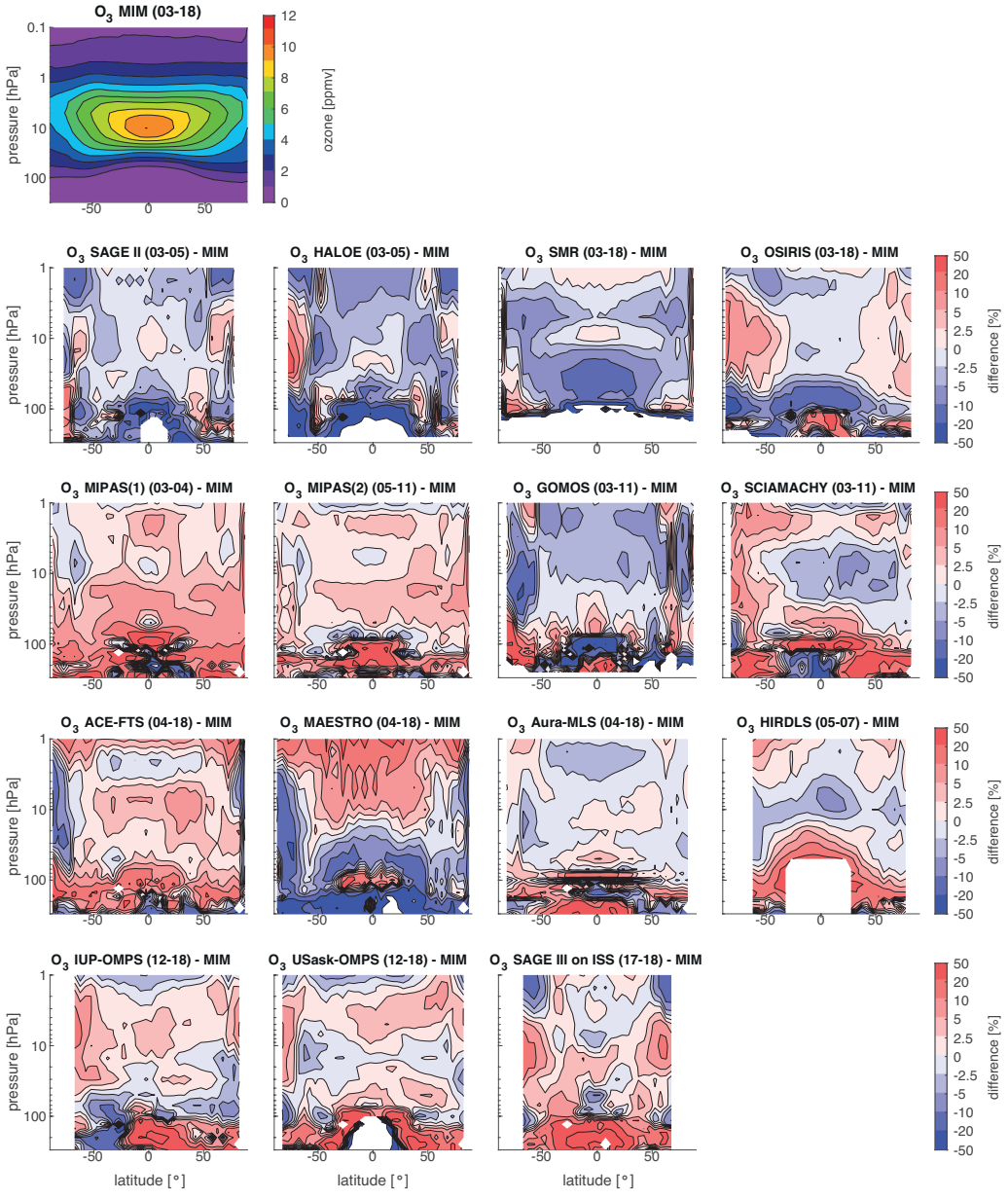

Figure 5. Cross-sections of the MIM annual zonal mean ozone for 2003-2018 and differences between the individual instruments and the MIM are shown. The MIM includes SAGE II, HALOE, SMR, OSIRIS, MIPAS(1) and MIPAS(2), GOMOS, SCIAMACHY, ACE-FTS, ACE-MAESTRO, Aura-MLS, HIRDLS, IUP-OMPS, USask-OMPS-LP and SAGE III/ISS. Note that while none of the instruments covers the full time period, detailed evaluations of shorter time periods (e.g., 2012-2018, 2005-2010) give very similar results.

https://doi.org/10.5194/essd-2020-342
Preprint. Discussion started: 21 November 2020

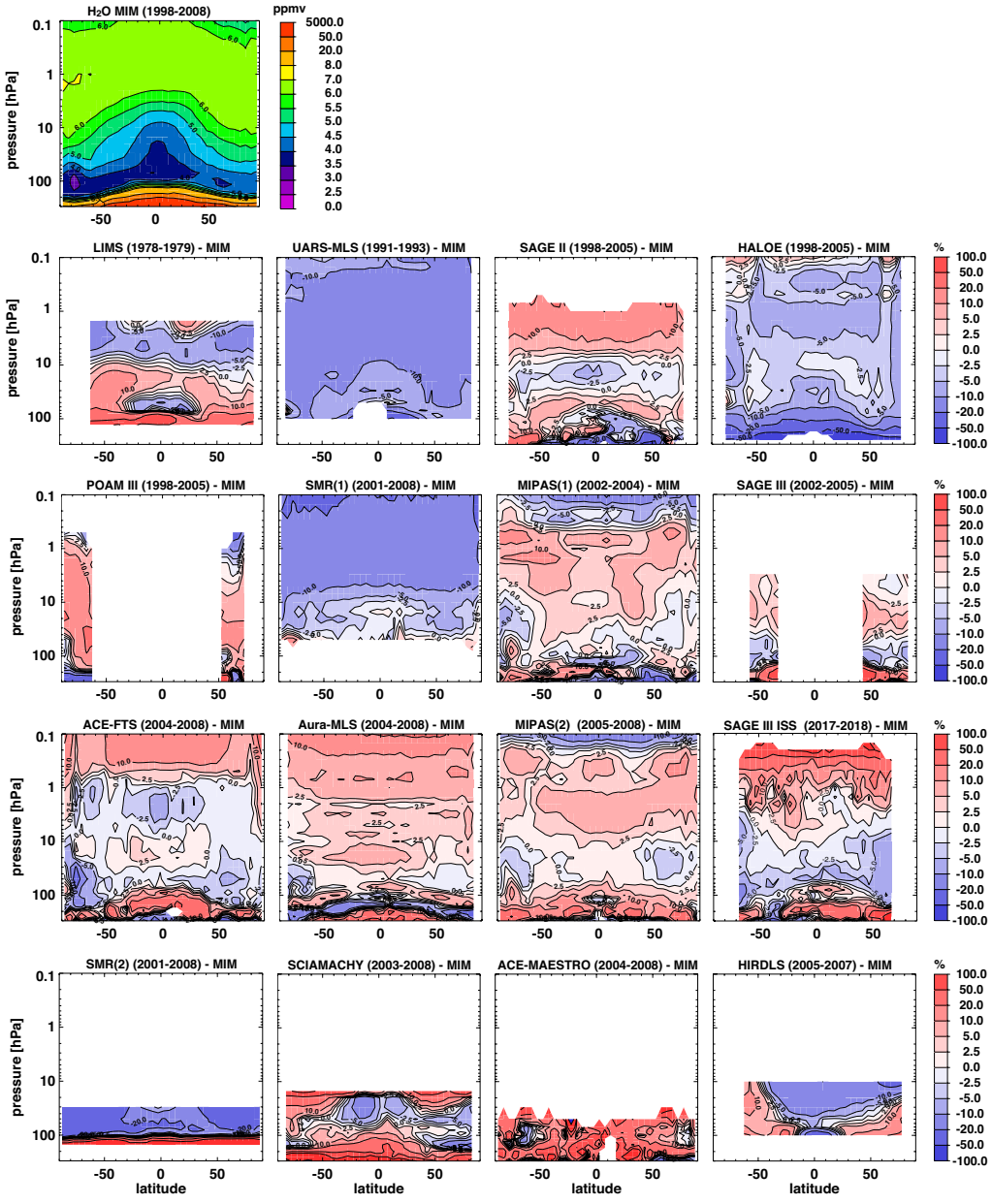

Figure 6. Relative difference cross sections with respect to the MIM (upper leftmost panel) for each individual instruments' water vapor distribution (update from Figure 5 in Hegglin et al. (2013)). Note that LIMS, UARS-MLS, ACE-MAESTRO, SMR(2), HIRDLS, and SAGE III/ISS are not included in the calculation of the MIM to allow for a more direct comparison with Hegglin et al. (2013).

https://doi.org/10.5194/essd-2020-342
Preprint. Discussion started: 21 November 2020

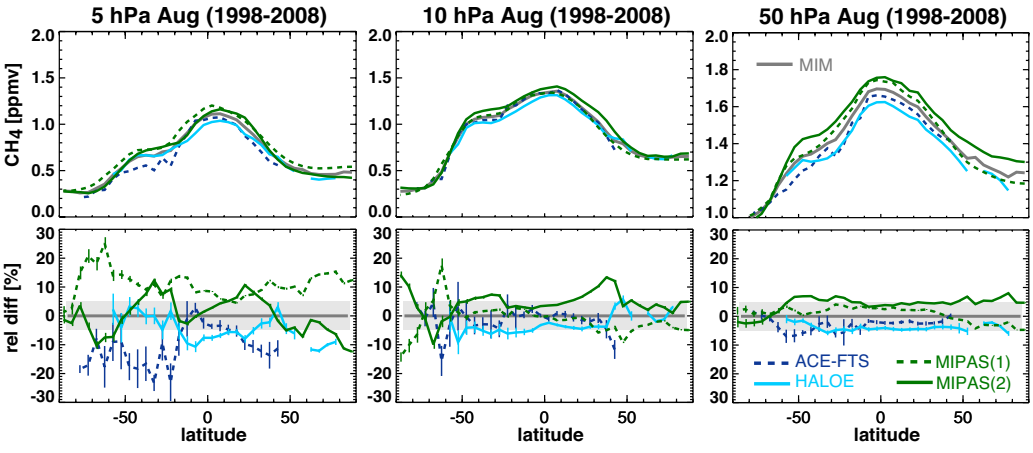

Figure 7. Meridional profiles of monthly zonal mean CH_4 at 5, 10, and 50 hPa and averaged over 1998-2008 are shown for the different instruments and the MIM (upper panels). Differences between the individual instruments and the MIM are shown in the lower panels.

https://doi.org/10.5194/essd-2020-342
Preprint. Discussion started: 21 November 2020

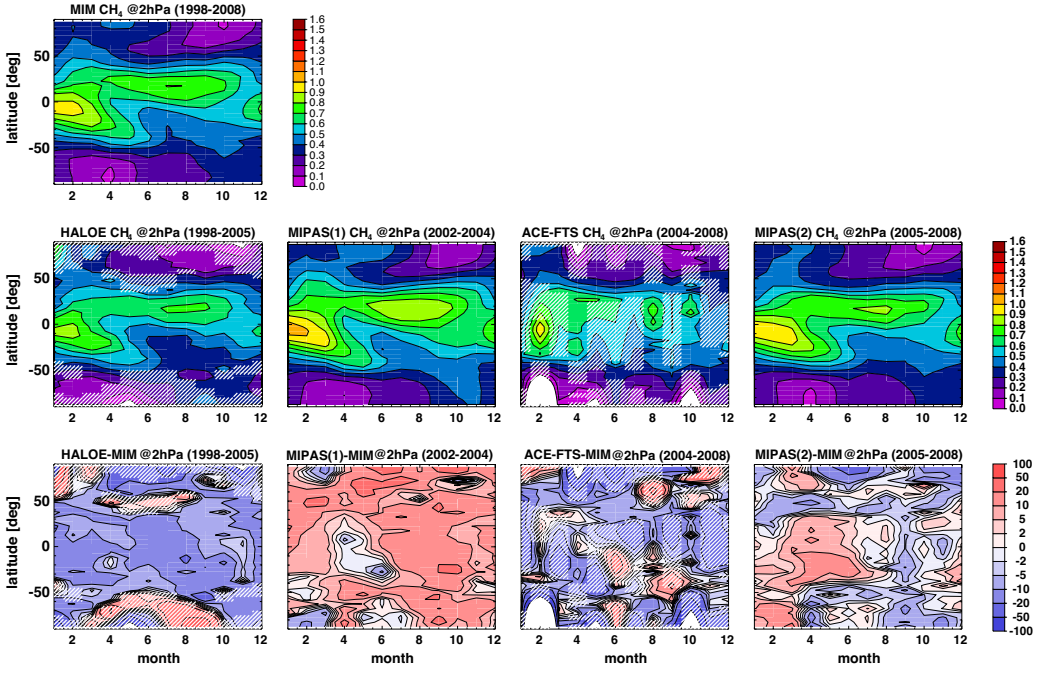

Figure 8. Latitude-time evolution of monthly zonal mean CH_4 at 2 hPa and averaged over 1998-2008. Shown are absolute values for the MIM (top panel) and the different instruments (middle row), and for the relative differences with respect to the MIM (lower row). Note that HALOE and ACE-FTS show linearly interpolated fields, with hatched regions indicating where no measurements are available.

https://doi.org/10.5194/essd-2020-342
Preprint. Discussion started: 21 November 2020

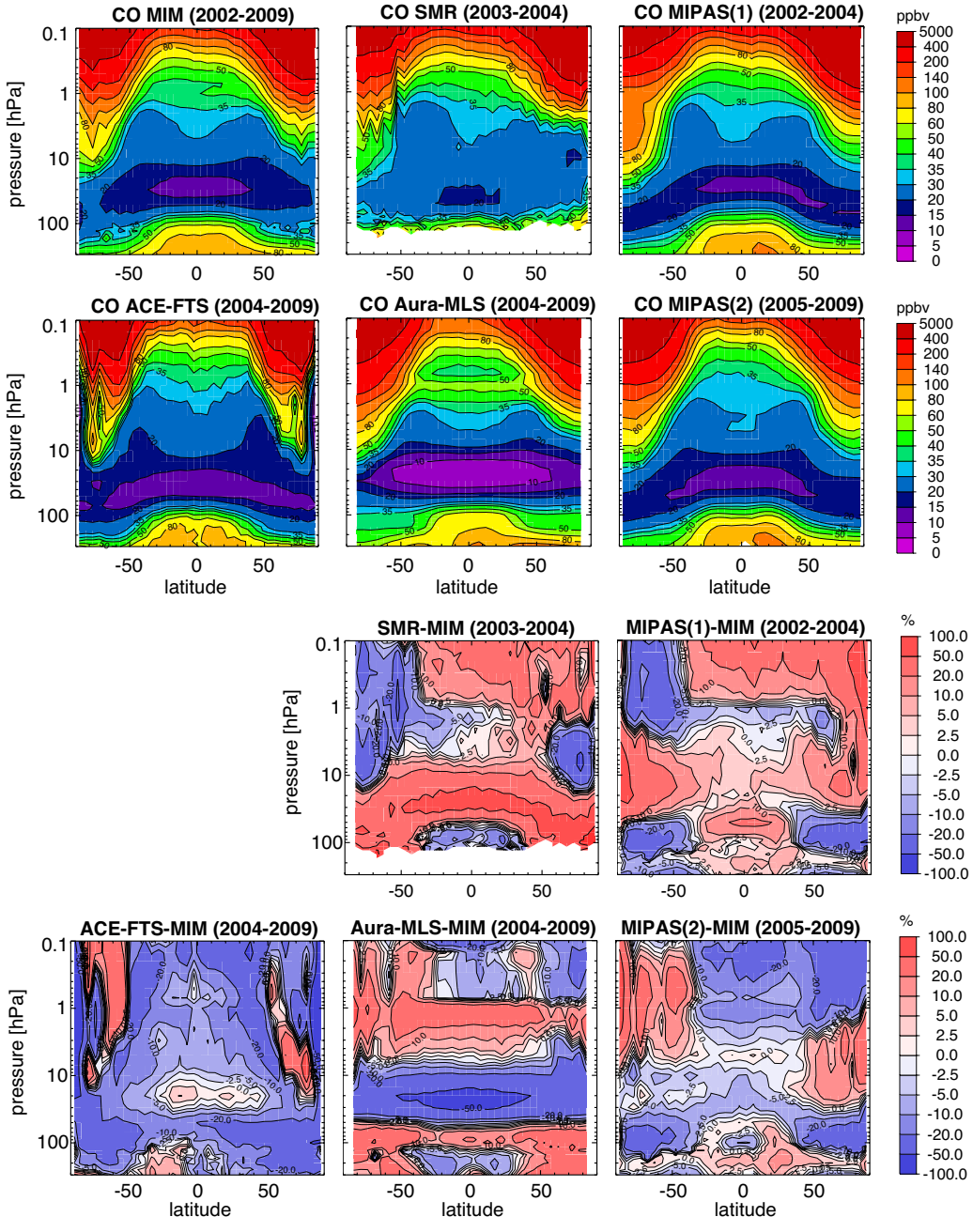

Figure 9. Annual zonal mean CO cross sections are shown for the MIM, SMR, MIPAS(1), ACE-FTS, MIPAS(2), and Aura-MLS averaged over 2002-2009 (upper half). Also shown are the relative differences for each instrument's climatology from the MIM (lower half).

https://doi.org/10.5194/essd-2020-342
Preprint. Discussion started: 21 November 2020

Open Access Earth System Science Data Discussions

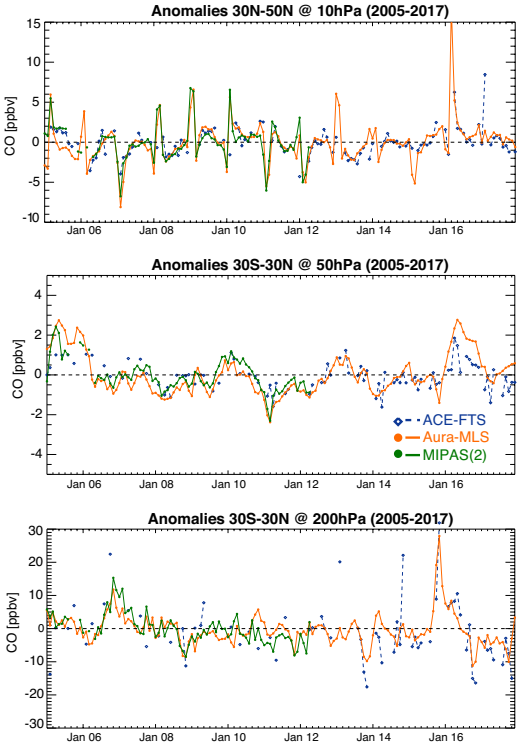

Figure 10. Deseasonalized CO anomalies from ACE-FTS, MIPAS(2), and Aura-MLS are shown for 30°N-50°N at 10 hPa (upper panel), and 50 hPa (middle panel) and 200 hPa (lower panel) for 30°S-30°N and the time period 2005-2017.

https://doi.org/10.5194/essd-2020-342
Preprint. Discussion started: 21 November 2020

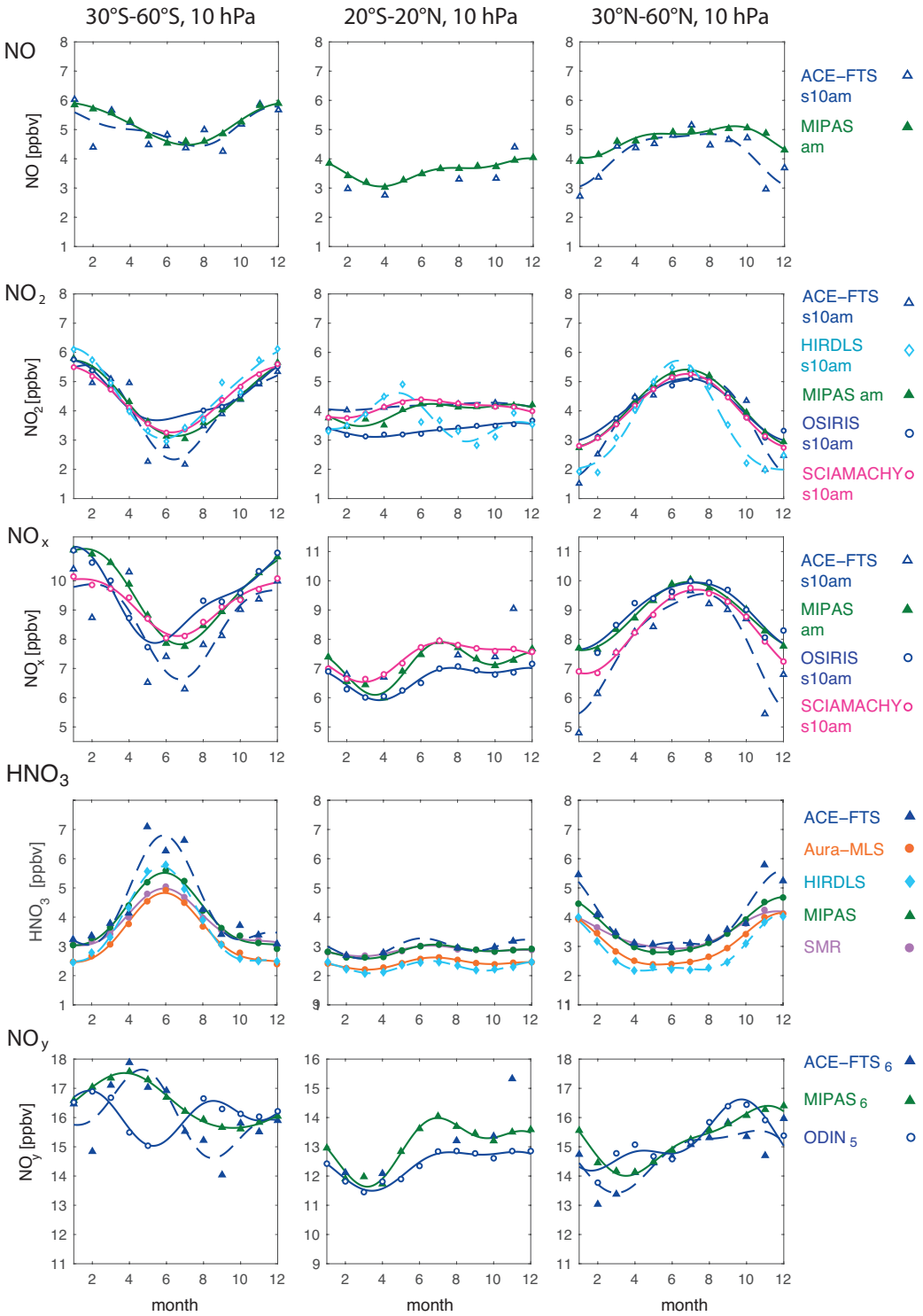

Figure 11. The seasonal cycle of NO, NO_2, NOx, HNO_3 and NO_y is displayed for the SH mid-latitudes (30°S-60°S, leftmost panels), the tropics (10 hPa 20°S-20°N, middle panels), and NH mid-latitudes (30°N-60°N, leftmost panels) at 10 hPa for the time period 2005-2010. Note, the NO, NO_2, and NOx seasonal cycles are based on 10 am climatologies.

https://doi.org/10.5194/essd-2020-342
Preprint. Discussion started: 21 November 2020

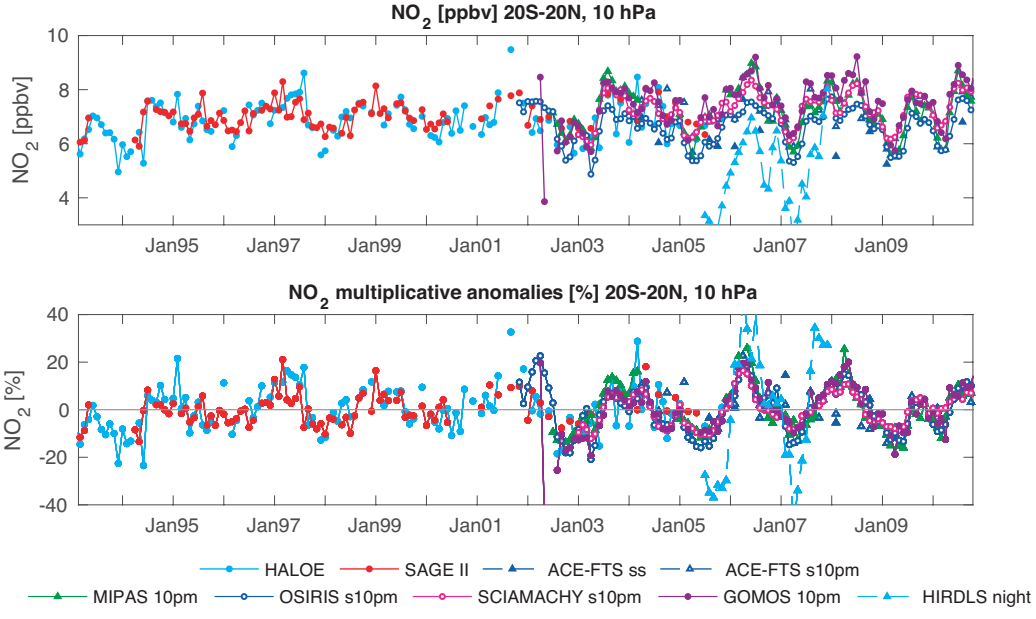

Figure 12. Time series of tropical NO_2 mean values (upper panels) and deseasonalized anomalies (lower panels) between 20°S-20°N at 10 hPa for 1993-2010. Data sets correspond to local sunset or to 10 pm LSTs as described in the text.

https://doi.org/10.5194/essd-2020-342
Preprint. Discussion started: 21 November 2020

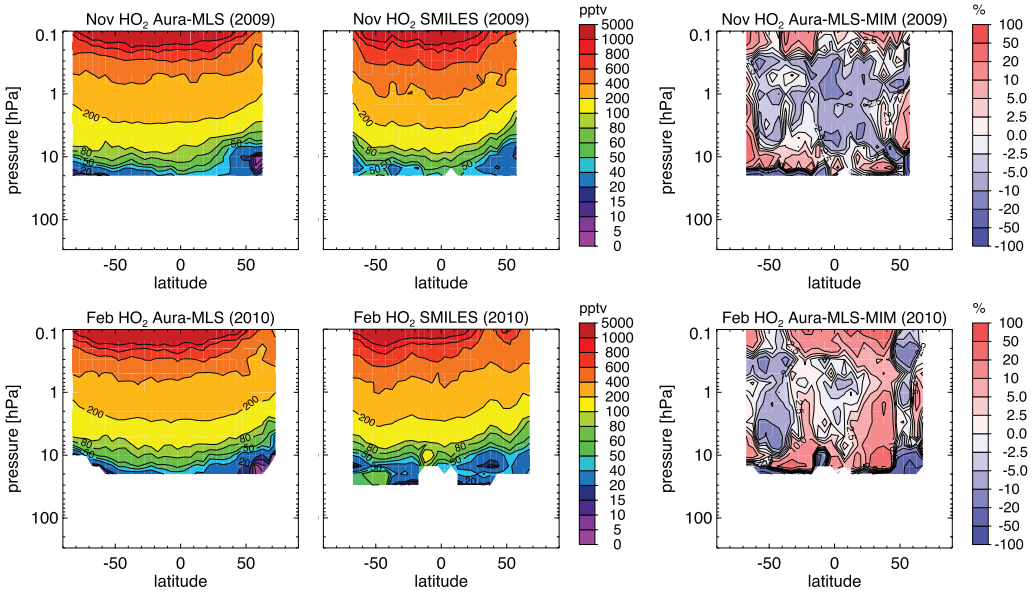

Figure 13. Monthly zonal mean HO_2 cross sections for Aura-MLS and SMILES daytime data (left two columns) and their differences from the MIM (right column) are shown for November 2009 (upper row) and February 2010 (lower row), respectively.

https://doi.org/10.5194/essd-2020-342
Preprint. Discussion started: 21 November 2020

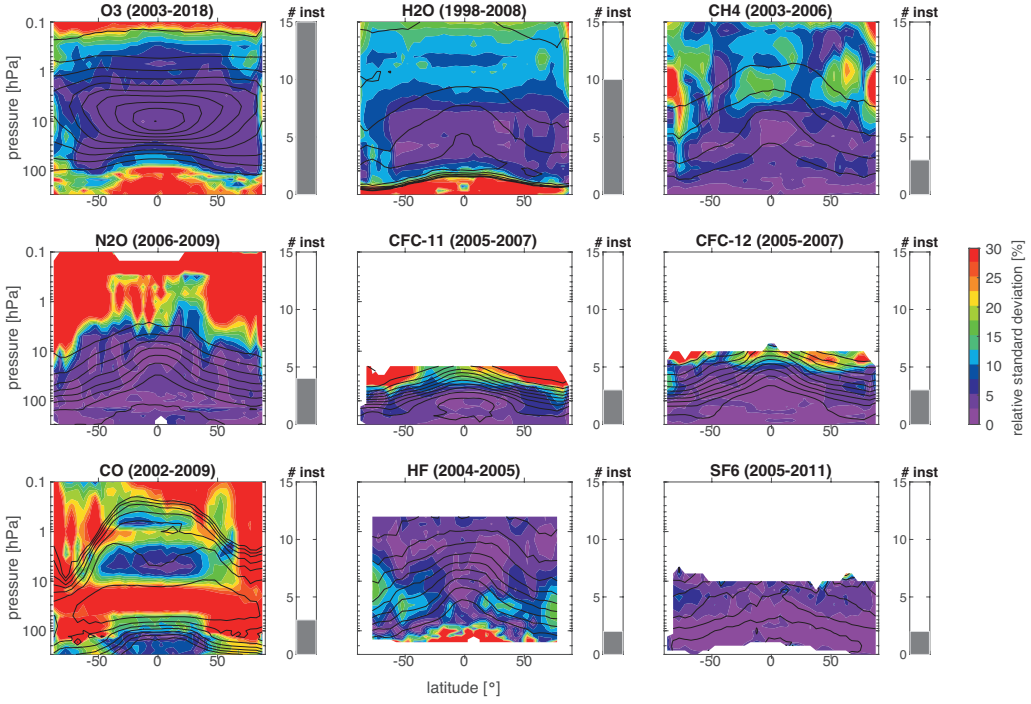

Figure 14. Synopsis of the uncertainty in the annual zonal mean state of the longer-lived species evaluated within the SPARC Data Initiative. The relative standard deviation over all instruments‘ multi-annual zonal mean datasets is presented for different chemical trace gas species (colour contours). The relative standard deviations are calculated by dividing the absolute standard deviations by the MIM. The black contour lines in each panel represent the MIM trace gas distribution for each species. The number of instruments included is given by the right-hand grey bar. Note that the time periods used depend on the availability of the instruments included in the assessment and hence differ from trace gas to trace gas.

https://doi.org/10.5194/essd-2020-342
Preprint. Discussion started: 21 November 2020

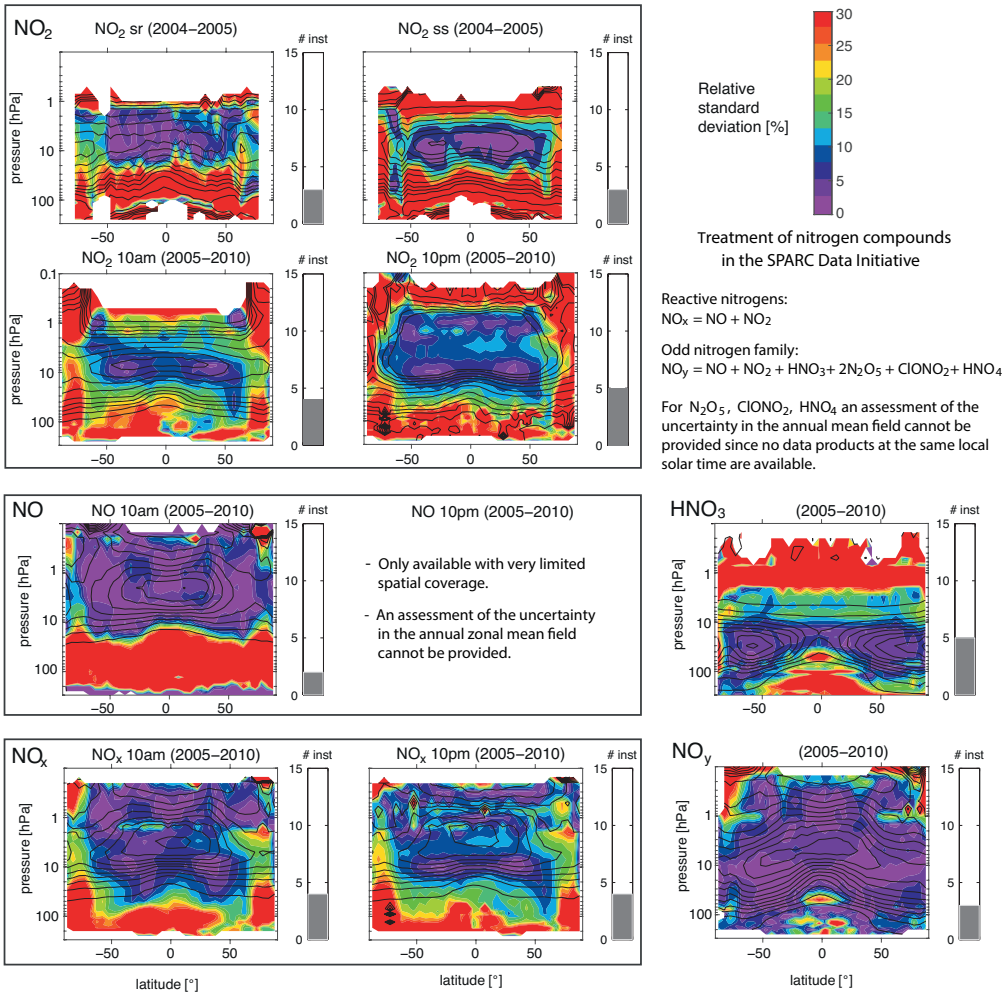

Figure 15. Same as Figure 14, but for nitrogen containing species. The assessment of the uncertainty in the annual mean state of NO, NO_x, and NO_2 is based on climatologies corresponding to 10am and 10pm, and for the latter also on climatologies corresponding to local sunrise (sr) and local sunset (ss). Note that some of the included climatologies have been derived by scaling the individual measurements with a chemical box model to 10am/10pm local solar time (LST). See SPARC (2017) for more detailed information.

https://doi.org/10.5194/essd-2020-342
Preprint. Discussion started: 21 November 2020

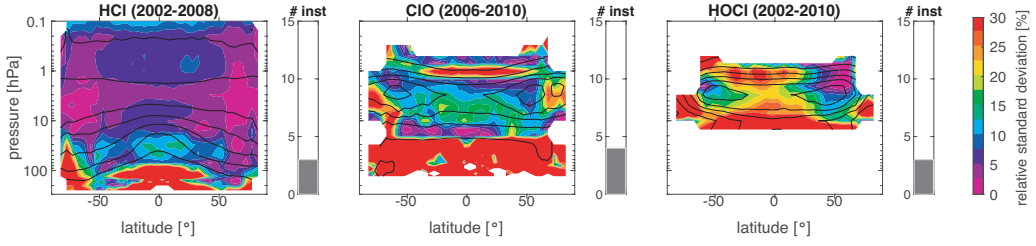

Figure 16. Same as Figure 14, but for chlorine-containing species. The assessment of the uncertainty in the annual mean state is based on ClO daytime and HOCl night-time climatologies. Note that for ClO, climatologies from SMR are included which have been derived by scaling the individual measurements with a chemical box model to 1:30pm LST. See SPARC (2017) for more detailed information.

https://doi.org/10.5194/essd-2020-342
Preprint. Discussion started: 21 November 2020

Table 1. Satellite instrument characteristics including satellite platform, observation period, spatial coverage, vertical range, vertical resolution, data density, local time (LT) at equator, LT of measurement, inclination, and instrument references. Note that the vertical range is generally species-dependent and the vertical resolution is often species- and altitude-dependent, see Tables A5-A12 for details.

Instrument Platform	**Obs. period**	**Spatial coverage**	**Vertical range**	**Vertical res.**	**Data density** [prof./day]	**LT at equator**	**LT of meas**	**Incl.**	**References**
LIMS Nimbus 7	11/1978 to 05/1979	64°S-84°N (daily)	cloud top-0.01 hPa 10-80 km	3.7 km	3000	a: 11:51 am d: 11:51 pm	a: 1 pm d: 11 pm	99.3°	Gille and Russell (1984)
SAGE I AEM-2	2/1979 to 11/1981	75°S-75°N (∼one month)	cloud top-55 km	1 km	30	N/A	sunrise sunset	56°	McCormick et al. (1989)
SAGE II ERBS	10/1984 to 08/2005	75°S-75°N (∼one month)	cloud top-70 km	1 km	30	N/A	sunrise sunset	57°	McCormick et al. (1989)
UARS-MLS UARS	10/1991 to 10/1999	80°S-80°N (∼two months)	100-0.01 hPa 17-80 km	3.5-5 km	1318	N/A	N/A	57°	Waters et al., 1993 Livesey et al. (2003)
HALOE UARS	10/1991 to 11/2005	75°S-75°N (∼one month)	250-0.002 hPa 10-90 km	2.5 km	30	N/A	sunrise sunset	57°	Russell et al., 1993
POAM II SPOT-3	10/1993 to 11/1996	88°S-63°S 55°N-71°N (one year)	15-50 km	1 km	28	a: 10:30 pm d: 10.30 am	N/A	98.7°	Glaccum et al. (1996)
POAM III SPOT-4	04/1998 to 12/2005	88°S-63°S 55°N-71°N (over one year)	5-60 km	1 km	28	a: 10:30 pm d: 10.30 am	N/A	98.7°	Lucke et al. (1999)
SMR Odin	07/2001 to present	82°S-82°N (daily)	100-0.001 hPa 15-120 km	2-6 km	600-975	a: 6:30 pm d: 6.30 am	a: 6:30 pm d: 6.30 am	97.8°	Murtagh et al. (2002)
OSIRIS Odin	10/2001 to present	82°S-82°N (daily, no winter)	10-60 km	2 km	300-975	a: 6:30 pm d: 6.30 am	a: 6:30 pm d: 6.30 am	97.8°	Murtagh et al. (2002)
SAGE III Meteor-3M	02/2002 to 12/2005	60°S-30°S 40°N-80°N (∼one month)	cloud top-100 km	1 km	30	a: 9:30 am d: 9.30 pm	sunrise sunset	99.6°	Thomason et al. (2010)

Open Access Earth System Science Data Discussions

Table 2. Table 1 continued.

Instrument Platform	Obs. period	Spatial coverage	Vertical range	Vertical res.	Data density	LT at equator	LT of meas	Incl.	References
GOMOS Envisat	04/2002 to 04/2012	90°S-90°N (daily, no summer poles for night meas.)	15-100 km	2-4 km	100-300 (night meas. only)	a: 10 pm d: 10 am	a: 10-12 pm d: 8-10.30 am	98.55°	Bertaux et al. (2010)
MIPAS Envisat	03/2002 to 04/2012	90°S-90°N (daily)	cloud top- 70 km	3.5-5 km 2.7-3.5 km	1000 1300	a: 10 pm d: 10 am	a: 10 pm d: 10 am	98.55°	Fischer et al. (2008)
SCIAMACHY ENVISAT	08/2002 to 04/2012	85°S-85°N (65° for winter hemisphere)	10-60 km	3-5 km	364-1456	a: 10 pm d: 10 am	d: 10 am	98.55°	Burrows et al. (1995)
ACE-FTS SCISAT-1	03/2004 to present	85°S-85°N (∼one season)	5-95 km	3-4 km	30	N/A	N/A	74°	Bernath et al. (2005)
ACE-MAESTRO SCISAT-1	03/2004 to present	85°S-85°N (∼one season)	5-60 km	2 km	30	N/A	N/A	74°	McElroy et al. (2007)
Aura-MLS Aura	07/2004 to present	82°S-82°N (daily)	316-0.002 hPa	3 km	3500	a: 1:43 pm d: 1:43 am	N/A	98.21°	Waters et al. (2006)
HIRDLS Aura	02/2005 to 03/2008	63°S-85°N (daily)	420-0.1 hPa 10-55 km	1 km	5600	a: 1:43 pm d: 1.43 am	N/A N/A	98.21°	Gille et al. (2008)
SMILES ISS	10/2009 to 04/2010	38°S-65°N (daily)	100-0.0005 hPa 16-96 km	3-5 km	1620	N/A	N/A	51.6°	Kikuchi et al. (2010)
Aura-TES Aura	07/2004 to present (2008/2009) (2010)	82°S-82°N (daily) (50°S-70°N) (30°S-50°N)	ground-10 hPa ground-32 km	6-7 km	3145 (2126) (1890)	a: 1:43 pm d: 1:43 am	a: 1:43 pm d: 1:43 am	98.21°	Beer et al. (2001) Beer (2006)
SAGE III ISS	06/2017 to present	75°S-75°N (∼one month)	cloud top- 100 km	0.75-1 km	30	N/A	sunrise sunset	51.6°	Wang et al. (in prep.)
OMPS-LP Suomi NPP	02/2012 to present	81.5°S-81.5°N	8-60 km	2-5 km	2000	a 1:30 pm d 1:30 am	1:30 pm	98.7°	Jaross et al. (2014)

https://doi.org/10.5194/essd-2020-342
Preprint. Discussion started: 21 November 2020

Open Access Earth System Science Data Discussions

https://doi.org/10.5194/essd-2020-342
Preprint. Discussion started: 21 November 2020

Open Access Earth System Science Data Discussions

Table 3. Terminology used to define agreement between instruments with respect to the multi-instrument mean (*MIM*).

Description	**deviation from MIM**
Excellent agreement	±2.5%
Very good agreement	±5%
Good agreement	±10%
Reasonably good agreement	±20%
Considerable disagreement	±50%
Large disagreement	±100%

https://doi.org/10.5194/essd-2020-342
Preprint. Discussion started: 21 November 2020

Open Access Earth System Science Data Discussions

Table 4. Definitions and abbreviations of different atmospheric regions as used in this study. Note, the full height range corresponds to about 9-65 km. Note that the abbreviations are often used in combination (e.g., UTLS or USLM).

Region	Abbreviation	Lower boundary	Upper boundary
Upper Troposphere	**UT**	300 hPa	tropopause
Lower Stratosphere	**LS**	tropopause	30 hPa
Middle Stratosphere	**MS**	30 hPa	5 hPa
Upper Stratosphere	**US**	5 hPa	1 hPa
Lower Mesosphere	**LM**	1	0.1 hPa

https://doi.org/10.5194/essd-2020-342
Preprint. Discussion started: 21 November 2020

Open Access Earth System Science Data Discussions

Appendix A

https://doi.org/10.5194/essd-2020-342
Preprint. Discussion started: 21 November 2020

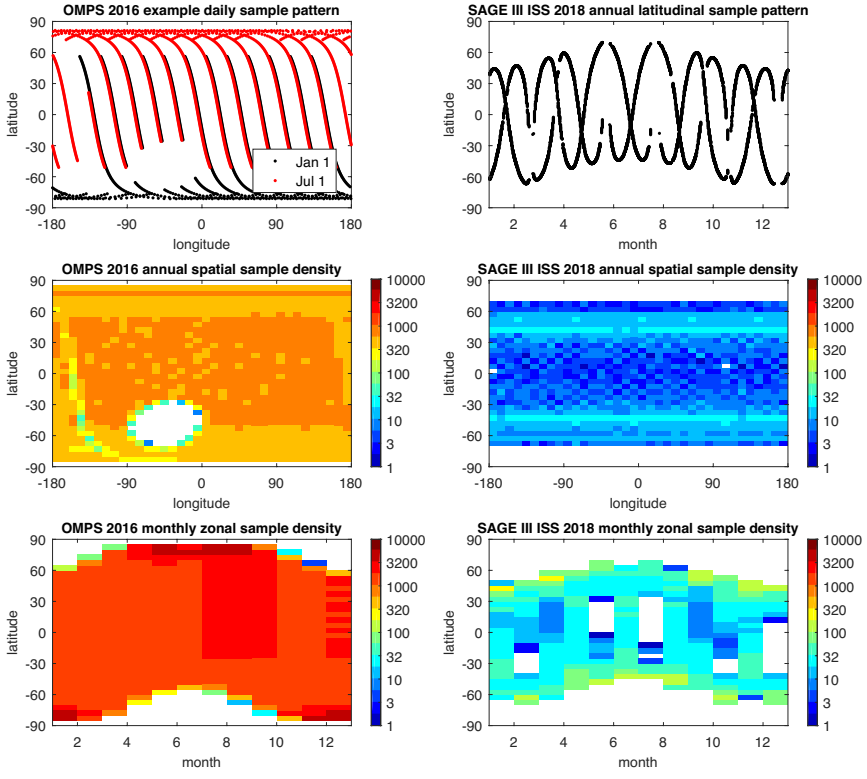

Figure A1. Sampling pattern (top) and resulting annual (middle) and monthly (bottom) sample density for OMPS-LP SUOMI (left) and SAGE III/ISS (right). Note that for OMPS-LP the daily and for SAGE the annual sampling pattern is shown. The OMPS sampling gap over South America results from a filter that removes measurements affected by the South Atlantic Anomaly, which causes increased noise in measured radiances from transient particle strikes to the instrument detector.

https://doi.org/10.5194/essd-2020-342
Preprint. Discussion started: 21 November 2020

Open Access Earth System Science Data Discussions

Table A1. Description of the content included in each of the SPARC Data Initiative monthly mean climatology files, here using N_2O as an example variable. Note, while much effort has been put into using consistent file format across the different instruments, some may still differ from the prescribed SPARC Data Initiative norm. Not-a-number values are filled in with '-999.0'. See also Figure 1 for an example.

Variable name	Long name	Variable type
time	time	1D
plev	pressure	1D
lat	latitude	1D
N2O	volume mixing ratio of N2O in air	Geo2D
N2O_NR	number of N2O measurements	Geo2D
N2O_STD	volume mixing ratio of N2O in air standard deviation	Geo2D
AVE_DOM	average day of month	Geo2D
AVE_LAT	average latitude	Geo2D
LST_MIN	minimum local solar time	Geo2D
LST_MAX	maximum local solar time	Geo2D
LST_MEAN	mean of local solar time	Geo2D

https://doi.org/10.5194/essd-2020-342
Preprint. Discussion started: 21 November 2020

Open Access Earth System Science Data Discussions

Table A2. Data versions used for the construction of the zonal monthly mean climatologies submitted to the SPARC Data Initiative assessment and as deposited in the Zenodo data archive (except for aerosol). Italics indicate data versions that have been updated since SPARC (2017). Bold italics indicates climatologies that have been added newly, i.e., were not part of SPARC (2017).

Instrument	O_3	H_2O	CH_4	N_2O	CCl_3F	CCl_2F_2	CO	HF	SF_6	NO	NO_2	NO_x	HNO_3
ACE-FTS	*v3.6*	*v3.6*	*v3.6*	*v3.6*	*v3.6*	*v3.6*	*v3.6*	*v3.6*	*v3.6*	*v3.6*	*v3.6*	*v3.6*	*v3.6*
Aura-MLS	*v4.2*	*v4.2*		*v4.2*			*v4.2*						*v4.2*
GOMOS	*v6.01*										*v6.01*		
HALOE	v19	v19	v19					v19		v19	v19	v19	
HIRDLS	*v7.0*	***v7.0***		***v7.0***	*v7.0*	*v7.0*					*v7.0*		*v7.0*
LIMS	v6.0	v6.0									v6.0		v6.0
ACE-MAESTRO	*v3.13*	***v31***											
MIPAS(1)	*v21*	*v20*	*v21*	*v21*	*v20*	*v20*	*v20*		*v20*	*v20*	*v20*	*v20*	*v22*
MIPAS(2)	*v224*	*v220*	*v224*	*v224*	*v220*	*v220*	*v220*		*v222*	v220	v220	v220	*v224*
OSIRIS	*v5.10*										v3.0	v3.0	
POAM II	v6.0										v6.0		
POAM III	v4.0	v4.0									v4.0		
SAGE I	v5.9												
SAGE II	*v7.0*	*v7.0*									*v7.0*		
SAGE III	v4.0	v4.0									v4.0		
SCIAMACHY	*v3-5*	*v4-2*									*v4-0*	*v4-0*	
SMILES	v2.1.5												v2.0.1
Odin/SMR(1)	*v3.1*	v2.1		v2.1			v2.1			v2.1			v2.0
Odin/SMR(2)		v2.0											
UARS-MLS	v5	v6											v6
IUP-OMPS	***v2-6***												
USask-OMPS	***v1.1.0***												
SAGE III/ISS	***v5.1***	***v5.1***											

https://doi.org/10.5194/essd-2020-342
Preprint. Discussion started: 21 November 2020

Open Access Earth System Science Data Discussions

Table A3. Table A1 continued. Note, Odin NO_y v3.0 is based on both OSIRIS and SMR data, hence has a double entry.

Instrument	HNO_4	N_2O_5	$ClONO_2$	NO_y	HCl	ClO	HOCl	BrO	OH	HO_2	CH_2O	CH_3CN	aerosol
ACE-FTS	*v3.6*	*v3.6*	*v3.6*	*v3.6*	*v3.6*						*v3.6*		
Aura-MLS					*v4.2*	v3.3	v3.3		v3.3	v3.3			
GOMOS													*v6.01*
AERGOM													*v1*
HALOE					v19								v19
HIRDLS		***v7.0***	***v7.0***										
MIPAS(1)	*v20*	*v21*	*v21*	*v22*		*v20*	*v20*				*v20*		
MIPAS(2)	*v220*	*v222*	*v222*	*v224*		*v220*							
OSIRIS				*v3.0*				v5					v5.7
POAM II													v6.0
POAM III													v4.0
SAGE II													v7.0
SAGE III/M3M													*[v4.0]*
SCIAMACHY								v4.1					*v1.4*
SMILES					v2.1.5	v2.0.1	v2.1.5	v2.0.1		v2.1.5		v2.0.1	
Odin/SMR				*v3.0*		v2.1				v2.1			
IUP-OMPS													
SAGE III/ISS													

https://doi.org/10.5194/essd-2020-342
Preprint. Discussion started: 21 November 2020

Open Access Earth System Science Data Discussions

Table A4. Instruments classified according to their observation geometry and wavelength categories. Only instruments that participated in the SPARC Data Initiative are listed.

	Microwave/Sub-mm **100 μm - 10 cm**	**Mid-IR** **2.5 - 20 μm**	**Near-IR** **1 - 2.5 μm**	**VIS/UV** **<1 μm**
Limb emission	UARS-MLS Aura-MLS Odin/SMR SMILES	LIMS MIPAS HIRDLS		
Solar occultation		HALOE ACE-FTS	POAM II/III SAGE I/II/III SAGE III/ISS	POAM II/III SAGE I/II/III ACE-MAESTRO SAGE III/ISS
Stellar or lunar occultation			 SAGE III/ISS	GOMOS SAGE III/ISS
Limb scattering			SCIAMACHY	SCIAMACHY OSIRIS OMPS-LP
Nadir emission		Aura-TES		

https://doi.org/10.5194/essd-2020-342
Preprint. Discussion started: 21 November 2020

Open Access Earth System Science Data Discussions

Table A5. Time period, vertical range, vertical resolution, references and other comments for O_3 measurements. Note, *tp* refers to tropopause in this table.

Instrument (version)	**Time Period**	**Vertical range**	**Vertical Resolution**	**References**	**Additional Comments**
LIMS (v6.0)	11/1978-05/1979	cloud top to 1 hPa	3.7 km	Remsberg et al. (submitted)	
SAGE I (v5.9)	10/1984-08/2005	cloud top to 50 km	1-2.5 km	McCormick et al. (1989)	data above 3 hPa excluded
SAGE II (v7.0)	10/1984-08/2005	cloud top to 70 km	1 km	Wang et al. (2002) Damadeo et al. (2013)	
UARS-MLS (v5)	10/1991-06/1997	18-45 km >45 km	3-4 km 5-8 km	Livesey et al. (2003)	
HALOE (v19)	10/1991-11/2005	up to 80 km	3.5 km	Grooss and Russell (2005)	data below tp excluded
SAGE III/M3M (v4.0)	05/2002-12/2005	cloud top to 70 km	1 km	Wang et al. (2006)	only solar products
POAM II (v6.0)	10/1993-11/1996	15-50 km	1 km	Lumpe et al. (1997) Roche et al. (1997)	
POAM III (v4.0)	04/1998-12/2005	5-60 km	1 km	Lumpe et al. (2006) Randall et al. (2003)	–
SMR (v3.1)	08/2001-present	170-0.3 hPa	3-4 km	Murtagh et al. (2018)	
OSIRIS (v5.10)	11/2001-present	tp to 59.5 km	2.2-3.5 km	Bourassa et al. (2018) Degenstein et al. (2009)	
GOMOS (ALGOM2s)	04/2002-04/2012	15-100 km	2-3 km	Sofieva et al. (2017)	
MIPAS MIPAS(1) (v21) MIPAS(2) (v224)	03/2002-04/2012 03/2002-03/2004 01/2005-04/2012	 6-68 km 6-70 km	 3.5-5.0 km 2.7-3.5 km	 Steck et al. (2007) Laeng et al. (2014)	Meas. mode switched in 2004 from high spectral to high vertical resolution
SCIAMACHY (v4)	09/2002-04/2012	11-25 km	3-5 km	Jia et al. (2015)	
ACE-FTS (v3.6)	03/2004-present	5-95 km	3-4 km	Sheese et al. (2017)	
ACE-MAESTRO (v3.13)	03/2004-present	5-60 km	1-2 km	Bognar et al. (2019)	
Aura-MLS (v4.2)	08/2004-present	261-0.02 hPa	2.5-5 km	Livesey et al. (2018) Hubert et al. (2015)	
HIRDLS (v7.0)	02/2005-03/2008	422-0.1 hPa	1 km	Gille and Gray (2012)	data degrade after 12/2007
IUP-OMPS (v2.6)	02/2012	8-60 km	2-5 km	Arosio et al. (2018)	
USask-OMPS (v1.1.0)	02/2012-present	tp to 58 km	1.5-2 km	Zawada et al. (2018)	
SAGE III/ISS (v5.1)	06/2017-present	cloud top to 70 km	0.75 km	Wang et al. (submitted)	

https://doi.org/10.5194/essd-2020-342
Preprint. Discussion started: 21 November 2020

Open Access Earth System Science Data Discussions

Table A6. Time period, vertical range, vertical resolution, references and other comments for H_2O measurements.

Instrument (version)	**Time Period**	**Vertical range**	**Vertical Resolution**	**References**	**Additional Comments**
LIMS (v6.0)	11/1978-05/1979	cloud top to 1 hPa	3.7 km	Remsberg et al. (2009)	–
SAGE II (v7.0)	10/1984-08/2005	cloud top to 50 km	1-2.5 km	Thomason et al. (2004) Damadeo et al. (2013)	data above 3 hPa excluded
UARS-MLS (v6)	10/1991-03/1993	18-50 km >50 km	3-4 km 5-7 km	Pumphrey (1999)	H_2O stops early, radiometer failure
HALOE (v19)	10/1991-11/2005	up to 80 km	3.5 km	Grooss and Russell (2005)	data below tp are excluded
SAGE III (v4.0)	05/2002-12/2005	cloud top to 50 km	1.5 km	Thomason et al. (2010)	only solar products used here
POAM III (v4.0)	04/1998-12/2005	5-45 km	1-2 km	Lumpe et al. (2006) Lucke et al. (1999)	–
SMR SMR(2) (v2-0) SMR(1) (v2-1)	07/2001-present	16-75 km 16-20 km 20-75 km	 3-4 km 3 km	 Urban (2008) Urban et al. (2007, 2012)	 544 GHz-band 489 GHz-band
MIPAS MIPAS(1) (V3o_H2O_21) MIPAS(2) (V5r_H2O_224)	03/2002-04/2012 03/2002-03/2004 01/2005-04/2012	cloud top to 70 km	 4-5 km 2-3.7 km	 Milz et al. (2005) Milz et al. (2009) von Clarmann et al. (2009)	Meas. mode switched in 2004 from high spectral to high vertical resolution
SCIAMACHY (v4.2)	09/2002-04/2012	11-25 km	3-5 km	Weigel et al. (2016)	 Weaver et al. (2019)
ACE-FTS (v3.6)	03/2004-present	5-101 km	3-4 km	Sheese et al. (2017) Lossow et al. (2019)	
ACE-MAESTRO (v31)	03/2004-present	5-20 km	1-2 km	Sioris et al. (2010, 2016) Lossow et al. (2019)	
Aura-MLS (v4.2)	08/2004-present	316-100 hPa 100-0.2 hPa < 0.1 hPa	2-3 km 3-4 km 6-11 km	Read et al. (2007) Lambert et al. (2007) Livesey et al. (2018)	
HIRDLS (v7.0)	02/2005-03/2008	100-10 hPa	1 km	Gille and Gray (2012)	values high below 100 hPa values low above 40 hPa Lossow et al. (2019)
SAGE III/ISS (v5.1)	06/2017-present	5-100 km	1.5 km	(first validation ongoing)	

https://doi.org/10.5194/essd-2020-342
Preprint. Discussion started: 21 November 2020

Open Access Earth System Science Data Discussions

Table A7. Time period, vertical range, vertical resolution, references and other comments for CH_4 measurements.

Instrument (version)	Time Period	Vertical range	Vertical Resolution	References	Additional Comments
HALOE (v19)	10/1991-11/2005	up to 80 km	3.5 km	Grooss and Russell (2005)	
MIPAS	03/2002-04/2012	cloud top-70 km		Glatthor et al. (2005), von Clarmann et al. (2009)	Change in spectral resolution in 2005
MIPAS-1 (v21)	03/2002-03/2004		4-5 km		
MIPAS-2 (v224)	01/2005-04/2012		2-3.7 km	Plieninger et al. (2016)	
ACE-FTS (v3.6)	03/2004-present	5-75 km	3-4 km	Plieninger et al. (2016) Olsen et al. (2016)	

https://doi.org/10.5194/essd-2020-342
Preprint. Discussion started: 21 November 2020

Open Access Earth System Science Data Discussions

Table A8. Time period, vertical range, vertical resolution, references and other comments for CO measurements.

Instrument (version)	Time Period	Vertical range	Vertical Resolution	References	Additional Comments
SMR (v2)	10/2003-09/2004	∼17-110 km	3-4 km	Dupuy et al. (2004)	
MIPAS	03/2002-04/2012		3.5-8 km	Funke et al. (2009)	Change in spectral resolution in 2005
MIPAS-1 (v20)	03/2002-03/2004	6-70 km			
MIPAS-2 (v220)	01/2005-04/2012	cloud top-70 km			
ACE-FTS (v3.6)	03/2004-present	5-110 km	3-4 km	Sheese et al. (2017)	
Aura-MLS (v4.2)	08/2004-present	215-0.1 hPa 0.1-0.005 hPa	4-5 km (UTLS) 6 km (above)	Livesey et al. (2018)	

Table A9. Time period, vertical range, vertical resolution, references and other comments for NO measurements.

Instrument	Time Period	Vertical range	Vertical Resolution	References	Additional Comments
HALOE v19	10/1991-11/2005	up to 140 km	3.5 km	Grooss and Russell (2005)	
ACE-FTS v3.6	03/2004-present	6-107 km	3-4 km	Sheese et al. (2016)	
SMR v2.1	10/2003-present	30-60 km 80-110 km	4-6 km 6-8 km	Sheese et al. (2013)	Only 1 day per month prior to 04/2007
MIPAS					
MIPAS v20	03/2002-03/2004	12-70 km	3.5-5 km	Funke et al., 2005b	Change in spectral resolution in 2005
MIPAS V220	01/2005-04/2012		2.5-6 km	Funke et al., 2014	

https://doi.org/10.5194/essd-2020-342
Preprint. Discussion started: 21 November 2020

Open Access Earth System Science Data Discussions

Table A10. Time period, vertical range, vertical resolution, references and other comments for NO_2 measurements.

Instrument	Time Period	Vertical range	Vertical Resolution	References	Additional Comments
LIMS v6.0	11/1978-05/1979	cloud top-50 km plus mesosphere for polar night	3.7 km	Remsberg et al. (2010)	
SAGE II v7.0	10/1984-08/2005	cloud top-50 km	1.5 km (<38 km) 5 km (>38 km)	Cunnold et al. (1991)	Only SS data used
HALOE v19	10/1991-11/2005	up to 50 km	2.5 km	Grooss and Russell (2005)	
POAM II v6.0	10/1993-11/1996	20-40 km	1.5-2.5 km	Lumpe et al. (2002) Randall et al. (2002)	
POAM III v4.0	04/1998-12/2005	20-40 km	1.5-2.5 km	Lumpe et al. (2002) Randall et al. (2002)	
OSIRIS v3-0	10/2001-present	13-45 km	2 km	Brohede et al. (2007)	
SAGE III v4.0	05/2002-12/2005	cloud top-50 km	1.5 km		Only SO data used
MIPAS					
MIPAS V20	03/2002-03/2004	12-50/70 km	3-6 km	Funke et al. (2005)	Change in spectral
MIPAS V220	01/2005-04/2012	for day/night	2.5-6 km	Funke et al. (2014)	resolution in 2005
GOMOS v6.01	03/2002-04/2012	20-50 km	4 km	Kyrölä et al. (2010)	
SCIAMACHY v4-0	09/2002-04/2012	9-48 km	3-5 km		
ACE-FTS v3.6	03/2004-present	7-52 km	3-4 km	Sheese et al. (2016)	
HIRDLS v7.0	01/2005-01/2008	20-50 km	1 km	Gille and Gray (2011) Belmont Rivas et al. (2014)	

https://doi.org/10.5194/essd-2020-342
Preprint. Discussion started: 21 November 2020

Open Access Earth System Science Data Discussions

Table A11. Time period, vertical range, vertical resolution, references and other comments for HNO_3 measurements.

Instrument	Time Period	Vertical range	Vertical Resolution	References	Additional Comments
LIMS v6.0	11/1978-05/1979	cloud top-50 km	3.7 km	Remsberg et al. (2010)	Original vertical resolution is 2 km but adjusted to make compatible with lower resolution LIMS products
UARS-MLS v6	10/1991-10/1999	100-4.6 hPa	5-10 km	Livesey et al. (2003)	Significant (1-3 ppbv) low bias <15 hPa and high bias <VMR peak.
SMR v2.0	07/2001-present	18-45 km	1.5-2 km	Urban et al. (2006) Urban et al. (2009)	Empirical scaling applied
MIPAS				Mengistu Tsidu et al. (2005)	
MIPAS V22	03/2002-03/2004	6 km (cloud top)	4-6 km	Wang et al. (2007)	Change in spectral
MIPAS V224	01/2005-04/2012	to 70 km	3-5 km	von Clarmann et al. (2009)	resolution in 2005
ACE-FTS v3.6	03/2004-present	5-62 km	3-4 km	Sheese et al. (2016)	
Aura-MLS v4.2	08/2004-present	215-1.5 hPa	3-5 km	Santee et al. (2007) Livesey et al. (2018) Fiorucci et al. (2013)	
HIRDLS v7.0	01/2005-01/2008	215 - 5.1 hPa	1 km	Gille and Gray (2012)	Latitude range 63°S-80°N
SMILES v2.0.1	10/2009-04/2010	18-45 km	3-4 km	Kreyling et al. (2013)	Bias due to problems in spectroscopic parameter and altitude shift.

https://doi.org/10.5194/essd-2020-342
Preprint. Discussion started: 21 November 2020

Open Access Earth System Science Data Discussions

Table A12. Time period, vertical range, vertical resolution, references and other comments for HO_2 measurements.

Instrument	Time Period	Vertical range	Vertical Resolution	References	Additional Comments
SMR v2	10/2003-10/2004	30-60 km (10-0.3 hPa)	3-4 km	Khosravi et al. (2013)	
Aura-MLS v3.3	07/2004-present	22-0.0046 hPa	4-10 km (UTLS)	Pickett et al. (2008) Khosravi et al. (2013)	Daytime climatology with night-time mean as background correction.
SMILES v2.0.1	10/2009-04/2010	26-95 km (20-0.001hPa)	4-5 km	Kreyling et al. (2013) Khosravi et al. (2013) Kuribayashi et al. (2013)	